

UC Irvine

UC Irvine Electronic Theses and Dissertations

Title

Palladium-Catalyzed Carbenylative Cross-Coupling and Carbenylative Amination Utilizing Vinylcarbenes

Permalink

<https://escholarship.org/uc/item/9c21b7jd>

Author

Agee, Christopher

Publication Date

2017

Peer reviewed|Thesis/dissertation

UNIVERSITY OF CALIFORNIA,
IRVINE

Palladium-Catalyzed Carbenylative Cross-Coupling and Carbenylative Amination
Utilizing Vinylcarbenes

THESIS

submitted in partial satisfaction of the requirements
for the degree of

MASTER OF SCIENCE

in Chemistry

by

Christopher Ronald Agee

Thesis Committee:
Professor David L. Van Vranken, Chair
Professor Christopher D. Vanderwal
Professor Andrej Luptak

2017

DEDICATION

To

My mother who I will never be able to repay
for twenty-eight years of unrelenting love and support

and to all my family and friends for all the encouragement, laughs and memories.

Also, Charlie,
nothing is better than coming home after a long day to a wagging tail and slobbery kisses

“Without change, something sleeps inside us, and seldom awakens.
The sleeper must awaken.”

-Frank Herbert

TABLE OF CONTENTS

	Page
LIST OF FIGURES	vii
LIST OF TABLES	xi
ACKNOWLEDGMENTS	xii
ABSTRACT OF THE THESIS	xiv
Chapter 1: Review of Palladium-Catalyzed Carbenylative Cross-Coupling, Carbenylative Aminations and Carbenylative Alkylations.	1
1.1 Introduction	1
1.2 The Three Components of Palladium-Catalyzed Carbenylative Cross-Coupling, Carbenylative Amination and Carbenylative Alkylation Reactions.	1
1.2.1 Electrophiles Used in Palladium-Catalyzed Carbenylative Processes	2
1.2.2 Carbene Sources and the Formation of Palladium-Carbene Intermediates from Diazo Compounds	3
1.2.3 Nucleophiles Used in Palladium-Catalyzed Carbenylative Processes	5
1.3 Palladium-Catalyzed Carbenylative Cross-Coupling Reactions with β -Hydride Elimination	6
1.4 Palladium-Catalyzed Carbenylative Cross-Coupling Reactions with Nucleophilic Trapping of Migratory Insertion Products	7
1.4.1 Carbenylative Cross-Coupling is Analogous to Carbonylative Cross-Coupling	7
1.4.2 Examples of Intermolecular Palladium-Catalyzed Carbenylative Cross-Coupling	8
1.4.2.1 Formation of Benzhydrys Through Intermolecular Carbenylative Cross-Coupling	8
1.4.2.2 Formation of Triarylmethanes with Hydride Nucleophiles Through Intermolecular Carbenylative Cross-Coupling	10
1.4.2.3 Intermolecular Palladium-Catalyzed Four-Component Tandem	11

Carbonylation and Carbenylative Cross-Coupling Utilizing an Acyl Migratory Insertion	
1.4.2.4 Mechanistic Evidence for an η^3 -Allylpalladium Intermediate When Using Vinyl Halides	12
1.4.3 Examples of Intramolecular Palladium-Catalyzed Carbenylative Cross-Coupling	13
1.4.3.1 Intramolecular Palladium-Catalyzed Carbenylative Cross-Coupling Reactions with Amine and Carbon Nucleophiles	13
1.4.3.2 Intramolecular Palladium-Catalyzed Carbenylative Cross-Coupling Reactions with Alkene Nucleophiles	14
1.4.3.3 Intramolecular Palladium-Catalyzed Four-Component Tandem Carbonylation and Carbenylative Cross-Coupling	15
1.5 Palladium-Catalyzed Carbenylative Amination and Alkylation Reactions	16
1.5.1 Background to Carbenylative Amination: Palladium-Catalyzed Hydroamination and Carboamination	16
1.5.1.1 Palladium-Catalyzed Hydroamination	16
1.5.1.2 Palladium-Catalyzed Carboamination	16
1.5.1.3 Comparison of Amination to Carbenylative Amination	17
1.5.2 Examples of Intermolecular Carbenylative Amination and Alkylation Reactions	17
1.5.3 Examples of Intramolecular Carbenylative Amination and Alkylation Reactions	19
1.5.4 Enantioselection in Palladium-Catalyzed Carbenylative Reactions	21
Chapter 2: Palladium-Catalyzed Carbenylative Cross-Coupling and Carbenylative Amination with Vinylcarbenes: Progress Towards Asymmetric Carbenylation	23
2.1 Introduction	23
2.2 Results and Discussion	26
2.2.1 Intercepting Symmetrical 1,3-Diphenylallyl, a Known Prochiral Intermediate	26

2.2.1.1 Introduction	26
2.2.1.2 Proposed Catalytic Cycle	27
2.2.1.3 Reaction Optimization	28
2.2.1.4 Asymmetric Induction Through Regioselective Control	30
2.2.2 Asymmetric Induction Through Enantiofacial Control in Unsymmetrical η^3 -Allylpalladium Systems – Installation of Prenyl Functional Groups	31
2.2.2.1 Intermolecular Carbenylation with Unsymmetrical η^3 -Allylpalladium Systems	31
2.2.2.2 Intramolecular Carbenylation with Unsymmetrical η^3 -Allylpalladium Systems	33
2.2.2.2.1 Formation of 5-member Isoindoline Systems with Amine Tethered Aryl Iodides and Prenyl Aldehyde <i>N</i> -Tosylhydrazones	33
2.2.2.2.2 Formation of 6-member Tetrahydroisoquinoline Systems with Amine Tethered Aryl Iodides and Prenyl Aldehyde <i>N</i> -Tosylhydrazones	40
2.3 Conclusion	43
2.4 Experimental	44
Chapter 3: Palladium-Catalyzed Carbenylative Cross-Coupling and Carbenylative Amination with Vinylcarbenes: Synthesis of <i>N</i> -Boc-Borrerine	54
3.1 Introduction	54
3.2 Results and Discussion	54
3.2.1 Initial Attempt to Synthesize 2-Iodo- <i>N</i> -methyltryptamine	54
3.2.2 Haloindole Sensitivity	55
3.2.3 Route to Stable Boc-Protected 2-Iodo- <i>N</i> -methyltryptamine	56
3.2.4 Synthesis of <i>N</i> -Boc-Borrerine Through Carbenylative Cross-Coupling	58
3.3 Conclusion	62

3.4 Experimental	62
REFERENCES	70
APPENDIX: NMR Spectra	77

LIST OF FIGURES

	Page	
Figure 1.1	Components Common to Palladium-Catalyzed Carbenylative Reactions	2
Figure 1.2	Synthesis of Diazo Compounds Through Diazo Transfer	4
Figure 1.3	Synthesis of <i>N</i> -Tosylhydrazones and Subsequent Generation of Diazo Compound through a Bamford-Stevens Reaction	4
Figure 1.4	Formation of Palladium-Carbene from Diazo Compounds	5
Figure 1.5	Formation of Polysubstituted Olefins Through Palladium-Catalyzed Carbenylative Cross-Coupling	6
Figure 1.6	Proposed Mechanism of Two-Component Palladium-Catalyzed Carbenylative Cross-Coupling	7
Figure 1.7	Heterocycle Formation Through Carbonylation	8
Figure 1.8	Palladium-Catalyzed Carbenylative Cross-Coupling Between Aryl Iodide, Trimethylsilyldiazomethane and Tributylphenyltin	8
Figure 1.9	Proposed Catalytic Cycle of Palladium-Catalyzed Carbenylative Cross-Coupling with Nucleophilic Trapping	9
Figure 1.10	Palladium-Catalyzed Carbenylative Cross-Coupling Between Aryl Bromide, Benzaldehyde <i>N</i> -Tosylhydrazone and Alkynylcopper	10
Figure 1.11	Palladium-Catalyzed Carbenylative Cross-Coupling Between Aryl Bromide, Diarylmethanone <i>N</i> -Tosylhydrazones and Ammonium Formate	11
Figure 1.12	Tandem Palladium-Catalyzed Carbonylation and Carbenylative Cross-Coupling	12
Figure 1.13	Nucleophilic Attack of η^3 -Allylpalladium vs. Reductive Elimination	12
Figure 1.14	Sterics Direct Nucleophilic Attack Indicating an η^3 -Allylpalladium Intermediate	13
Figure 1.15	Intramolecular Palladium-Catalyzed Carbenylative Cross-Coupling with Amine and Carbon Nucleophiles	14
Figure 1.16	Intramolecular Palladium-Catalyzed Carbenylative Cross-Coupling	15

with Alkene Nucleophiles

Figure 1.17	Intramolecular Palladium-Catalyzed Four-Component Tandem Carbonylation and Carbenylative Cross-Coupling	15
Figure 1.18	Palladium Catalyzed Hydroamination of Vinylarenes with Arylamines	16
Figure 1.19	Palladium Catalyzed Carboamination to Form Pyrrolidines	17
Figure 1.20	Comparison of Palladium-catalyzed Amination Reactions	17
Figure 1.21	Intermolecular Palladium-Catalyzed Carbenylation to form Vinylsilanes	18
Figure 1.22	Intermolecular Palladium-Catalyzed Carbenylative Amination Generating α,β -Unsaturated γ -Amino Esters	18
Figure 1.23	Intermolecular Palladium-Catalyzed Carbenylation with Alkylidene Precursors	19
Figure 1.24	Intramolecular Palladium-Catalyzed Carbenylation to Form Pyrrolidines, Piperidines and Cyclic Guanidines	20
Figure 1.25	Comparison of Palladium-Catalyzed Carbenylation Bond Formation	21
Figure 1.26	Reported Enantioselection in Palladium-Catalyzed Carbenylative Amination	22
Figure 2.1	Symmetrical and Non-Symmetrical Intermediates in Allylic Alkylations	24
Figure 2.2	β -hydride Elimination vs. Nucleophilic Trapping of Palladium-Carbene Insertion Intermediate	25
Figure 2.3	Natural Products Accessible Through Palladium-Catalyzed Cross-Coupling with Vinyl <i>N</i> -Tosylhydrazones	25
Figure 2.4	η^3 -Allylpalladium Intermediate Formation Through Carbenylative Insertion or Allylic Carbonate Ionization	26
Figure 2.5	Proposed Catalytic Cycle for Palladium-Catalyzed Carbenylative Cross-Coupling with Nucleophilic Trapping of η^3 -allylpalladium Intermediate	28
Figure 2.6	Chiral Ligands Screened	30

Figure 2.7	Intercepting a Known η^3 -1,3-Diphenylallylpalladium(II) Intermediate	31
Figure 2.8	Previous Nucleophilic Trapping of η^3 -Allylpalladium Intermediates Distal to the Carbene Carbon and Sources of Chirality	32
Figure 2.9	Determination of the Regioselectivity Preference for Sterics or Conjugation	33
Figure 2.10	Example of Regioselectivity in Allylic Alkylation	33
Figure 2.11	The Isoindoline Model System Proceeds Through an η^3 -Allylpalladium Intermediate That Has Been Shown to Generate Both Kinetic and Thermodynamic Allylic Alkylation	34
Figure 2.12	Sensitivity of Allylic Isoindoline Systems to Aerobic Decomposition	35
Figure 2.13	Initial Reaction Conditions for Intramolecular Vinylcarbene Insertion	36
Figure 2.14	Attempted Modification of Starting Materials and Isolation Techniques to Address	39
Figure 2.15	Liang's System and an Attempt to Apply it to My Model System	40
Figure 2.16	Synthesis of Tetrahydroisoquinoline Starting Material	40
Figure 2.17	Synthesis of 7- <i>O</i> -Methyl-Dehydrolophocerine	41
Figure 2.18	Suspected Side Products and Attempted Circumvention	42
Figure 2.19	Alkaloids Accessible Through Intramolecular Carbenylative Cross-Coupling	43
Figure 3.1	Carbenylative Cross-Coupling to Form Borrerine in Comparison to Pictet-Spengler	54
Figure 3.2	Synthetic Routes to Sensitive 2-Iodo- <i>N</i> -methyltryptamine	55
Figure 3.3	Sensitivities of 2-Haloindoles	56
Figure 3.4	Synthetic Route to Stable Substrate for Borrerine	57
Figure 3.5	Example of Palladium Chemistry Next to a Sterically Demanding Boc Group	58
Figure 3.6	Synthesis of <i>N</i> -Boc-Borrerine	60

Figure 3.7	Reaction Conditions with a Less Sterically Hindered Substrate	61
Figure 3.8	Ortho Substituents Have Been Shown to Dramatically Effect the Yield in Carbenylative Cross-Coupling Reactions	61

LIST OF TABLES

		Page
Table 2.1	Initial Palladium-Catalyzed Carbenylative Amination Reaction Optimization	28
Table 2.1	Results of Isoindoline Formation	37
Table 3.1	Base Effects on Bamford-Stevens <i>N</i> -Tosylhydrazone Decomposition	60

ACKNOWLEDGMENTS

I would like to thank Professor David Van Vranken for all of his help and support. He has a true love for chemistry and it is apparent every day with the amount of zeal and energy he brings to both the classroom and the lab. In the five years of undergraduate and graduate classes I have taken, he is my absolute favorite lecturer. Professor Van Vranken is somehow able to explain complex topics in ways that anyone can understand. He is also an inspiring mentor and PI. The moment that will always stand out the most to me was the day I came to him after doing poorly on a midterm in another professor's class. I met with the other professor initially (who I had a high regard for) expecting guidance, tips, or at least a few words of encouragement. I quickly realized teaching was not his priority. Completely demotivated and distraught I dragged my feet into Professor Van Vranken's office just to try and get pointers for studying and he instantly suggested we meet multiple times a week just so he could help me to go over problems and homework. Professor Van Vranken will do whatever he can in order to help people succeed.

I also need to thank my high school chemistry teacher, Joanne Overman, who instilled and nurtured my love of chemistry. Similar to Professor Van Vranken, Mrs. Overman has such a passion for chemistry and teaching and I am certain she is the reason why I have such a love for chemistry now. I will never forget the first day I walked into her classroom. She had what looked like a candle burning on the counter in front of her. She did not say a word until everyone was settled in their seats and then finally when everyone was quiet she opened her mouth...and ate the burning "candle". Her goal was to have us question our observations both in science and in life. Eventually she did spill the beans and let us know that the candle was just a simple potato. Her constant view altering demos and quirky energy always had me looking forward to her class. She was a real life Ms. Frizzle without the need for a magic school bus.

I also owe a great deal to my boss and professional mentor, Robert Orr. He has provided me with a job that I love both during my undergraduate career (as a budding intern) and in my graduate career. Even after knowing him for nine years, I find myself still constantly learning new things about chemistry, business and life from him. His understanding and willingness to let me take time off for school (or life) has been invaluable.

Additionally, I want to thank my friend and former lab mate Dr. Avinash Khanna for putting up with my shenanigans while in the DVV lab. He is reliable, eager to help and always down to talk chemistry over a few beers. My classmates Kim Le and Carlos Hernandez were vital in keeping me sane during our late nights and all nighters working on spec homework.

I would also like to thank the Medicinal Chemistry and Pharmacology (MCP) graduate gateway program for funding during my initial quarters at UCI. The staff and faculty associated with the MCP program are welcoming and supportive above and beyond what is expected. They were a valuable resource throughout my graduate career.

Finally, I would like to thank my thesis committee for offering their time, effort and support. Professor Chris Vanderwal was supportive of and helped facilitate my return to finish my degree. Even on short notice, Professor Andrej Luptak was kind enough to join my thesis committee. Professor Luptak truly took interest in and cared for all of the MCP students. I have never seen Professor Luptak without a smile on his face and it seems almost too easy for him to put smiles on others. This journey would not have been possible without all of these amazing people that I have encountered throughout my academic career.

ABSTRACT OF THE THESIS

Palladium-Catalyzed Carbenylative Cross-Coupling and Carbenylative Amination Utilizing Vinylcarbenes

By

Christopher Ronald Agee

Master of Science in Chemistry

University of California, Irvine, 2017

Professor David L. Van Vranken, Chair

This work focuses on the use of *N*-tosylhydrazones derived from α,β -unsaturated aldehydes – precursors to vinylcarbene ligands – in palladium-catalyzed carbenylative cross-coupling and carbenylative amination reactions. These carbenylative reactions were used to form η^3 -allylpalladium intermediates that generate stereogenic centers at the carbene center. An initial acyclic model system was used to intercept a well-known prochiral 1,3-diphenylallyl intermediate to probe the feasibility of enantioselectivity in a palladium-catalyzed carbenylative reaction as a proof of concept for asymmetric carbenylation. Following the proof of concept, the substrate scope was expanded to include aliphatic vinyl hydrazones in order to install prenyl functional groups. Conditions to form isoindolines and tetrahydroisoquinolines, present in many natural products, were developed by employing amine-tethered aryl iodides. The isoindoline model system established that kinetic 5-membered ring formation is preferred over thermodynamic 7-membered ring formation and that under our reaction conditions the cyclization is not reversible. Use of *N*-tosylhydrazones that generate unsymmetrical η^3 -allylpalladium intermediates that cannot racemize through η^3 - η^1 - η^3 isomerization provided evidence consistent with migratory insertion as the step responsible for enantioselection in the

catalytic cycle. Promising results are demonstrated indicating that selection of the right chiral ligand and reaction conditions could lead to high levels of enantioselection. Finally, formation of 6-membered ring systems proved challenging in comparison to 5-membered and acyclic systems but provided beneficial information about *N*-tosylhydrazone decomposition rates and reactivity effects seen from ortho-substitution on the aryl iodide. These results provide new insights into the mechanism of asymmetric palladium-catalyzed carbenylative cross-coupling and carbenylative amination and provide a foundation for future method development.

Chapter 1

Review of Palladium-Catalyzed Carbenylative Cross-Coupling, Carbenylative Aminations and Carbenylative Alkylations.

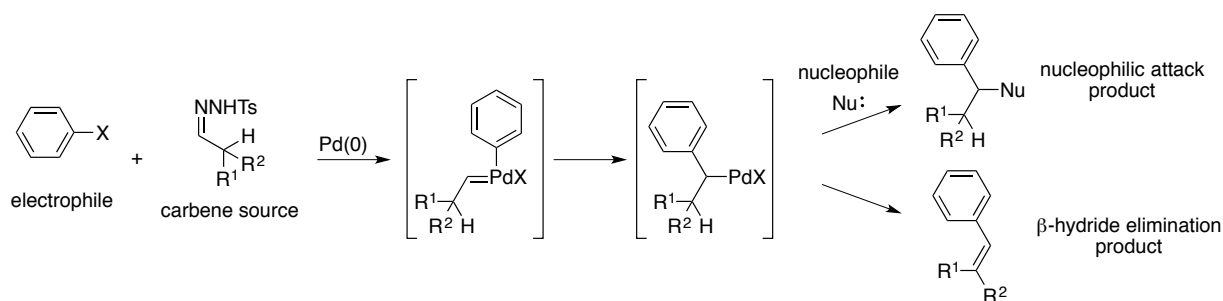
1.1 Introduction

Palladium catalysis has become a fundamental tool in organic synthesis allowing chemists to transform or stitch together complex organic molecules. Of particular note are the palladium-catalyzed cross-coupling reactions developed by Richard F. Heck, Ei-ichi Negishi and Akira Suzuki.¹ The reactions they developed led to their joint award of the Nobel Prize in chemistry in 2010.² These palladium-catalyzed carbon-carbon bond-forming reactions combine organic halides with organozinc reagents (Negishi coupling), boronic acids (Suzuki coupling) or alkenes (Heck coupling). Similar transformations can be carried out with other nucleophilic coupling partners for the organic halides: stannanes (Stille coupling), silanes (Hiyama coupling), Grignard reagents (Kumada coupling) alkynyl cuprates (Sonogashira coupling), and amines (Buchwald-Hartwig coupling). Within the past ten years there has been a rising interest in using a carbene source as a third coupling partner in palladium-catalyzed carbenylative cross-coupling processes.

1.2 The Three Components of Palladium-Catalyzed Carbenylative Cross-Coupling, Carbenylative Amination and Carbenylative Alkylation Reactions.

Components that are common to palladium-catalyzed carbenylative cross-coupling, carbenylative amination, and carbenylative alkylation are: an electrophile, a formal carbene source, and a nucleophile (Figure 1.1). When carbene sources or electrophiles are used that contain β -hydrido groups, a nucleophile is not required due to rapid β -hydride elimination.

Figure 1.1 Components Common to Palladium-Catalyzed Carbenylative Reactions



1.2.1 Electrophiles Used in Palladium-Catalyzed Carbenylative Processes

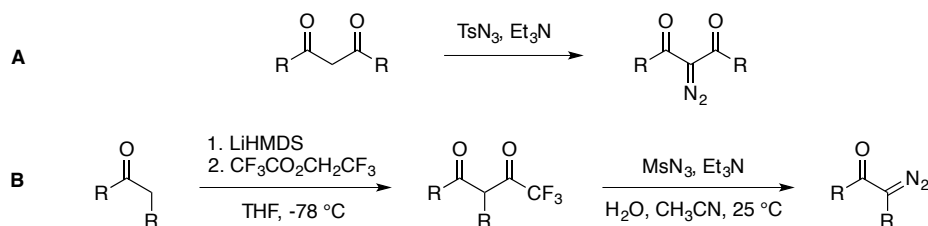
Electrophiles in palladium-catalyzed carbenylative reactions generally undergo oxidative addition, and the rate of the reaction follows the same trend seen in the rates of oxidative additions with palladium(0). Boronic acids^{3,4p,q} and azoles,^{4m,5} when combined with an oxidant, can also serve in a role equivalent to that of an electrophile. For reactions of vinyl halides, a substituent *syn* to the halide is important for reaction efficiency.⁶ Terminal *cis* vinyl halides perform better than *trans* vinyl halides and vinyl iodides produce higher yields than bromides.⁷ Aryl iodides are facile electrophiles whereas aryl bromides may require more electron rich palladium ligands (e.g. XPhos vs. PPh₃) in order to aid in the oxidative addition.⁸ Allylic bromides and chlorides, which go through highly studied η^3 -allylpalladium complexes,⁹ have been utilized. Allylic chlorides have been shown to outperform allylic bromides when the allylic halides are substituted.¹⁰ Both benzyl bromides and benzyl chlorides have been used and generate similar yields.^{11,12,13} The ability to use aryl triflates instead of aryl halides has been demonstrated allowing for simple reagent synthesis from phenol sources however, vinyl triflates fail to generate any of the desired carbene coupling products.^{7,14} Carbonates have also been used for carbenylative transformations and proceed through a palladium promoted decarboxylation.¹⁵

1.2.2 Carbene Sources and the Formation of Palladium-Carbene Intermediates from Diazo Compounds

The carbene source in palladium-catalyzed carbenylative reactions is generally a stabilized diazo compound or an arenesulfonylhydrazone that generates a diazo compound in situ. There are two classes of bench stable diazo compounds that have been used in palladium-catalyzed carbenylative reactions. The first class of bench stable diazo compounds are sterically stabilized silyl substituted diazomethanes. Trimethylsilyldiazomethane is the only silyl stabilized diazo compound utilized in reported palladium-catalyzed carbenylations. This is most likely due to trimethylsilyldiazomethane being the only commercially available silyldiazalkane.

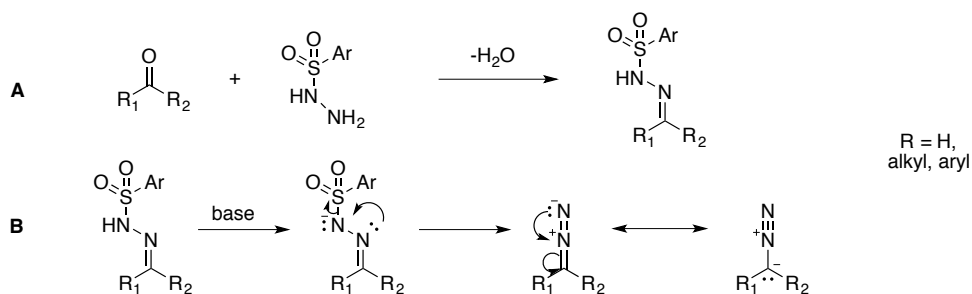
The second class of bench stable diazo compounds are stabilized by π -acceptor groups. α -Diazocarbonyl compounds are the most common carbene precursor with ethyl and *t*-butyl α -diazooacetate being commercially available. Various α -substituted α -diazocarbonyls can be easily synthesized through a diazo-transfer reaction. If a sufficiently acidic carbonyl is used, a simple one-step diazo-transfer can be carried out with a base such as triethylamine and a sulfonylazide diazo donor for instance *p*-acetamidobenzenesulfonyl azide or tosyl azide (Figure 1.2, A).¹⁶ If the carbonyl compound is not acidic enough, the substrate can be converted to a highly reactive 1,3-carbonyl through a Claisen condensation with ethyl formate and alkoxide base or through *C*-trifluoroacetylation of a lithium enolate with trifluoroethyl trifluoroacetate (Figure 1.2, B).¹⁶ The 1,3-carbonyl can then be subjected to standard diazo-transfer conditions resulting in α -diazocarbonyl formation and the release of the activating acyl or formyl group as the acylsulfonamide. Diaryldiazomethanes have also been used in palladium-catalyzed carbenylative reactions albeit with less prevalence than other stabilized diazo compounds.¹⁷

Figure 1.2 Synthesis of Diazo Compounds Through Diazo Transfer



Arenesulfonylhydrazones are used to generate unstable diazo carbene precursors *in situ*, are readily accessible and provide several benefits over stabilized diazo compounds. The most commonly used type of arenesulfonylhydrazone in palladium-catalyzed carbonylations are *N*-tosylhydrazones. Both ketones and aldehydes can be used to quickly generate *N*-tosylhydrazones in high yields by treatment with *N*-tosylhydrazine in a suitable solvent (Figure 1.3, A).¹⁸ Formation of the desired unstable diazo carbene precursor from the bench stable *N*-tosylhydrazone is carried out *in situ* through a base-promoted Bamford-Stevens reaction (Figure 1.3, B).¹⁹

Figure 1.3 Synthesis of *N*-Tosylhydrazones and Subsequent Generation of Diazo Compound through a Bamford-Stevens Reaction

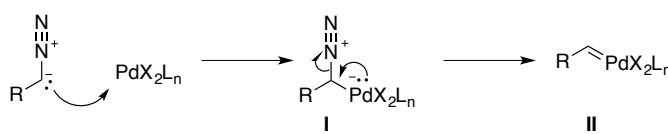


The use of *N*-tosylhydrazones as diazo precursors in palladium-catalyzed carbene reactions provides several benefits over stabilized diazo compounds. Since any aldehyde or ketone can be readily transformed into an *N*-tosylhydrazone, they provide facile access to a large range of carbene donors. Furthermore, metallated *N*-tosylhydrazones are much less prone to

dimerization than their diazo counterparts.^{11,20} *N*-tosylhydrazones slowly generate diazo compounds in low concentration in situ eliminating the need to use syringe pumps.²¹ The safety profile of *N*-tosylhydrazones is also improved compared to trimethylsilyldiazomethane and α -diazocarbonyls with decreased toxicity and reduced explosive potential.²¹ Other less common carbene precursors for metal-catalyzed reactions include diazirines,²² tethered alkynes,²³ Fischer carbenes,²⁴ chloroform,²⁵ and *N*-sulfonyl-1,2,3-triazoles.²⁶

Formation of the palladium-carbene is believed to proceed by addition of the anionic carbon center of the diazo compound to palladium(II) to form palladate intermediate **I**, which then goes on to release N₂ forming the reactive palladium-carbene species **II** (Figure 1.4).

Figure 1.4 Formation of Palladium-Carbene from Diazo Compounds



1.2.3 Nucleophiles Used in Palladium-Catalyzed Carbenylative Processes

There are two common types of nucleophiles seen in palladium-catalyzed carbenylative reactions: amines and stabilized enolates. Less frequently used nucleophiles include: stannanes,¹¹ tethered alkenes,^{27,28} hydrides,^{29,30} organocopper compounds,³¹ and sulfonates³². In intermolecular reactions a high concentration of nucleophile, achieved with excess reagent, is typically needed when using *N*-tosylhydrazones in order to outcompete the nucleophilic *N*-tosylhydrazone anions. In contrast, with intramolecular reactions the nucleophile has a high effective concentration because it is tethered to the electrophile.³³

Amine nucleophiles that are used in palladium-catalyzed carbenylative reactions fall into four categories: alkylamines, anilines, azoles and protected amines. Alkylamines are the most common amine nucleophiles used, as they are the most nucleophilic and tend to give the highest

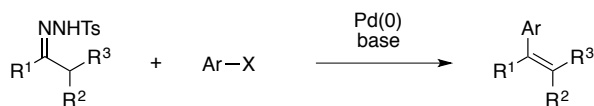
yields. Secondary amines outperform primary amines possibly due to their increased nucleophilicity.⁷ Anilines are ineffective nucleophiles in carbenylative reactions,³⁴ but arylalkylamines can be used to generate high yields.³⁵ Sulfonamide nucleophiles work poorly in palladium-catalyzed carbenylative reactions.³⁴

1,3-Dicarbonyls and related compounds such as malonates, beta-ketoesters and malonitriles when used in combination with bases are useful in generating carbon-carbon bonds in carbenylative processes. Typical bases used include sodium hydride and potassium, sodium and lithium tert-butoxides. With simple 1,3-dicarbonyl compounds, the poor solubility of the metal-enolate can make it difficult to achieve a sufficiently high concentration of nucleophile to outcompete the nucleophilic diazo compound.⁶

1.3 Palladium-Catalyzed Carbenylative Cross-Coupling Reactions with β -Hydride Elimination

Palladium-catalyzed carbenylative cross-coupling reactions involving β -hydride elimination can be used to form polysubstituted olefins (Figure 1.5).³ⁿ The reactions utilize *N*-tosylhydrazones or stabilized diazo compounds as the carbene source and aryl-, benzyl- or allyl-halides or pseudo halides as the electrophile.⁴ Surprisingly, there have been no reports of two-component couplings with vinyl halides.

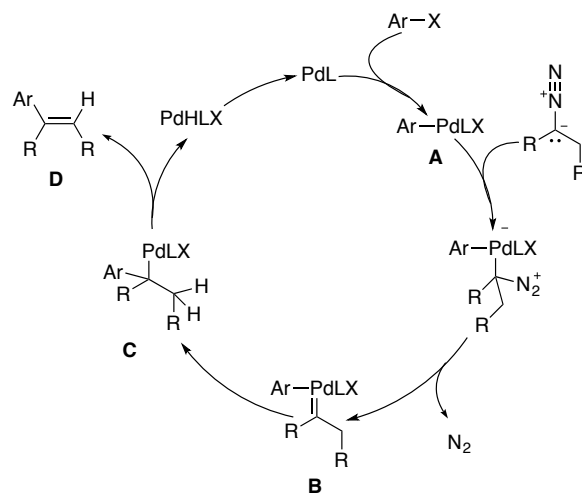
Figure 1.5 Formation of Polysubstituted Olefins Through Palladium-Catalyzed Carbenylative Cross-Coupling



The proposed mechanism is shown in Figure 1.6. Palladium(0) oxidatively adds to the aryl halide to form intermediate **A**. Addition of the diazo compound and loss of nitrogen gas leads to palladium(II)carbene intermediate **B**. Migratory insertion of the aryl group into the

carbene generates intermediate **C**. Finally, β -hydride elimination from the alkylpalladium(II) intermediate **C** forms the olefin product **D** while regenerating the palladium(0) catalyst.

Figure 1.6 Proposed Mechanism of Two-Component Palladium-Catalyzed Carbenylative Cross-Coupling



In these reactions, the carbene precursors serve as an equivalent of a vinylmetal (e.g. vinylboronic acid, vinylstannane, etc.) or alkene. Although this methodology provides an alternate synthetic route to polysubstituted olefins, there isn't an obvious advantage to utilizing this cross-coupling of diazo compounds over the better-known cross-coupling reactions of, for example, alkenes (Heck), vinylboronates (Suzuki), or related compounds.

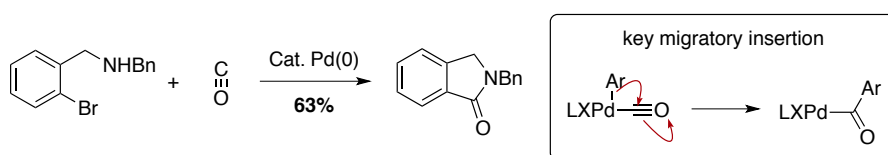
1.4 Palladium-Catalyzed Carbenylative Cross-Coupling Reactions with Nucleophilic Trapping of Migratory Insertion Products

1.4.1 Carbenylative Cross-Coupling is Analogous to Carbonylative Cross-Coupling

Palladium-catalyzed carbenylative cross-coupling reactions are directly analogous to a broad range of palladium-catalyzed carbonylative cross-coupling reactions. Carbonylative cross-coupling of aryl, vinyl, or benzyl halides or triflates has been performed with numerous nucleophiles: alkoxides, amines and hydrides as well as organoborane, organoaluminum,

organosilane, organoantimony and organozinc compounds.³⁶ Trapping of the migratory insertion products allows for formation of both new carbon-carbon and new carbon-heteroatom bonds. For example, palladium-catalyzed carbonylative cross-couplings have been used to generate lactams from aryl halides containing an ortho tethered nitrogen group (Figure 1.7).³⁷ This carbonylative cyclization provides access to five-, six-, and seven-membered ring lactams. While carbonylative cross-couplings are powerful, they do not create new stereogenic centers.

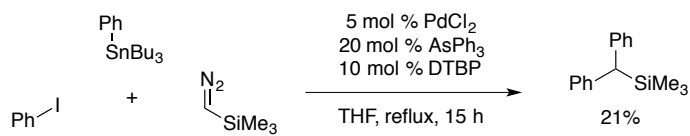
Figure 1.7 Heterocycle Formation Through Carbonylation



1.4.2 Examples of Intermolecular Palladium-Catalyzed Carbonylative Cross-Coupling

1.4.2.1 Formation of Benzhydryls Through Intermolecular Carbonylative Cross-Coupling

Figure 1.8 Palladium-Catalyzed Carbonylative Cross-Coupling Between Aryl Iodide, Trimethylsilyldiazomethane and Tributylphenyltin

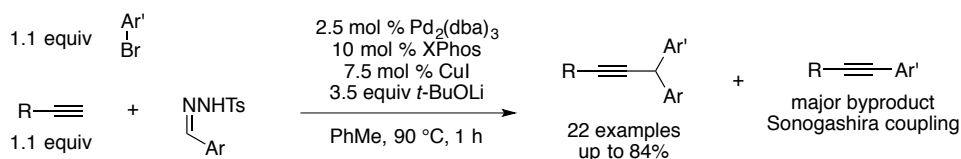


In 2001 Van Vranken and co-workers reported the first example of a palladium-catalyzed carbonylative process: carbonylative cross-coupling of an aryl iodide and an arylstannane. They used aryl halides, trimethylsilyldiazomethane and tris(*n*-butyl)phenylstannane to generate benzhydrylsilanes (Figure 1.8).¹¹ The catalytic cycle (Figure 1.9) is proposed to go through an initial oxidative addition of palladium into the aryl halide forming intermediate **I**. Trimethylsilyldiazomethane then attacks intermediate **I** to form a zwitterionic palladate intermediate **II** which then extrudes nitrogen gas to generate palladium-carbene intermediate **III**. Migratory insertion forms intermediate **IV**, which undergoes transmetalation with the

it was an important proof of concept for migratory insertion into palladium-carbene intermediates.

Expanding on the use of organometallics as nucleophiles in palladium-catalyzed carbenylative cross-couplings, Wang and co-workers engaged alkynylcopper species, generated in-situ, with aryl halides and *N*-tosylhydrazones to form benzhydryl acetylenes (Figure 1.10).³¹ The Sonogashira coupling product was the major byproduct seen and was theorized to occur due to slow palladium-carbene formation from the low concentrations of diazo substrates generated in situ. Slow addition of alkyne via syringe pump failed to limit the undesired Sonogashira coupling. Switching from an aryl iodide to an aryl bromide to slow down the oxidative addition step helped to reduce the Sonogashira product and increase the yield. Attempts to follow the trend using the aryl chloride failed to generate any desired product.

Figure 1.10 Palladium-Catalyzed Carbenylative Cross-Coupling Between Aryl Bromide, Benzaldehyde *N*-Tosylhydrazone and Alkynylcopper

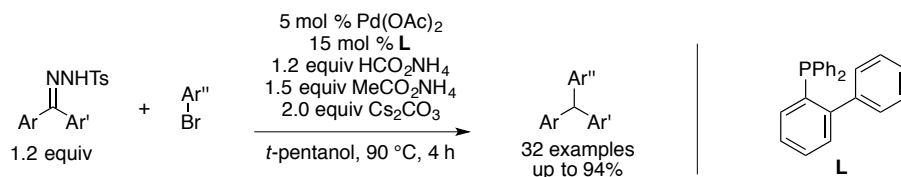


1.4.2.2 Formation of Triarylmethanes with Hydride Nucleophiles Through Intermolecular Carbenylative Cross-Coupling

Wang and co-workers have developed a palladium-catalyzed carbenylative cross-coupling route using benzophenone *N*-tosylhydrazones, aryl bromides and a hydride nucleophile to form triarylmethanes (Figure 1.11).³⁰ Ammonium formate was employed as a mild hydride source, which forms a hydridopalladium(II) intermediate in situ. Attempts to use other hydride sources such as triethylsilane and isopropanol failed to provide more than trace product. The major side reaction was found to be direct reduction of the aryl halide, which was inhibited by

the addition of ammonium acetate. The authors postulate that the ammonium acetate additive acts in a manner similar to the common-ion effect.

Figure 1.11 Palladium-Catalyzed Carbenylative Cross-Coupling Between Aryl Bromide, Diarylmethanone *N*-Tosylhydrazones and Ammonium Formate

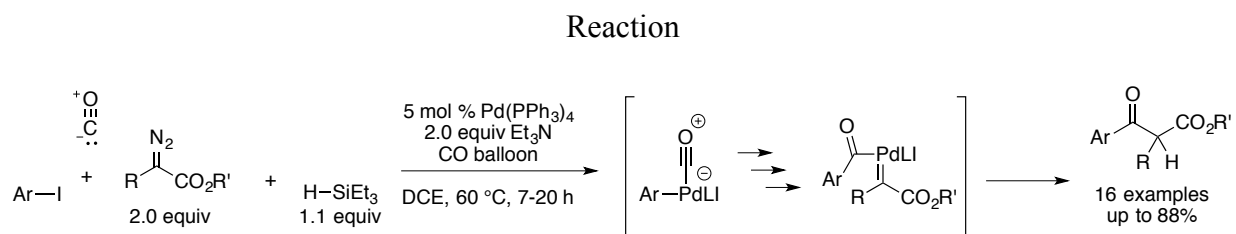


1.4.2.3 Intermolecular Palladium-Catalyzed Four-Component Tandem Carbonylation and Carbenylative Cross-Coupling Utilizing an Acyl Migratory Insertion

In palladium-catalyzed carbenylative transformations, the migratory insertion step typically involves aryl, benzyl, vinyl or allyl groups derived from their respective halides. A palladium-catalyzed four-component tandem carbonylation/carbenylative cross-coupling reaction between an aryl iodide, α -diazocarbonyls or *N*-tosylhydrazones, carbon monoxide and triethylsilane has provided the first example of an acyl migratory insertion into a palladium-carbene (Figure 1.12).²⁹ The reaction is proposed to proceed through an oxidative addition of palladium(0) to the aryl iodide followed by insertion of carbon monoxide generating an acylpalladium(II) intermediate. Next, the acylpalladium(II) intermediate is thought to form an acylpalladium(II) carbene intermediate by reacting with the diazo compound, which can then undergo a migration of the acyl group onto the carbene carbon. Finally, transmetalation with triethylsilane followed by reductive elimination yields the ketone in competition with β -hydride elimination to produce the enone. When using α -diazocarbonyls, β -hydride elimination side reactions are not observed. The use of *N*-tosylhydrazones does lead to the formation of β -hydride elimination products however two sets of optimized reaction conditions were developed that could provide either the β -hydride elimination product or the transmetalation/reductive

elimination product.

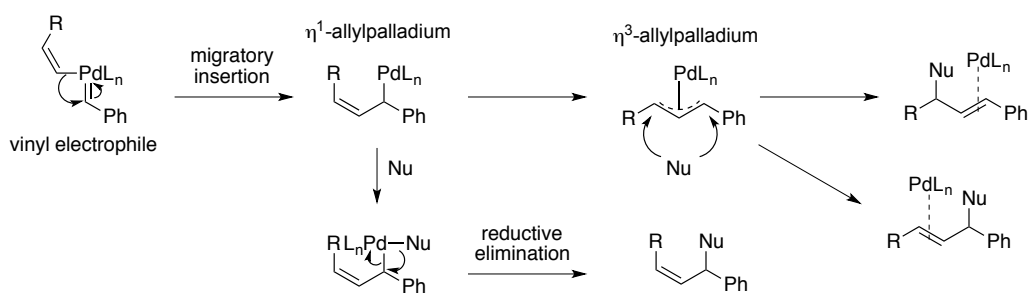
Figure 1.12 Tandem Palladium-Catalyzed Carbonylation and Carbenylative Cross-Coupling



1.4.2.4 Mechanistic Evidence for an η^3 -Allylpalladium Intermediate When Using Vinyl Halides

Of the reactions discussed so far, either no nucleophile is used (reaction proceeds through β -hydride elimination) or a reductive elimination step is involved. When vinyl halides are used the reaction is believed to involve nucleophilic attack of an η^3 -allylpalladium intermediate which forms after the migratory insertion step (Figure 1.13). If an η^3 -allylpalladium intermediate was not involved there would be only one possible isomer.

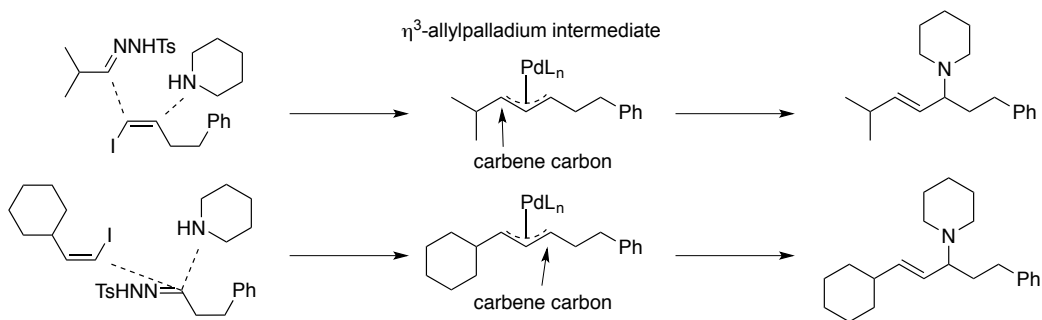
Figure 1.13 Nucleophilic Attack of η^3 -Allylpalladium vs. Reductive Elimination



It is well known that sterics can be used to direct the site of nucleophilic attack on η^3 -allylpalladium intermediates.³⁸ In the case of palladium-catalyzed carbenylation the nucleophile can attack the carbene carbon of the η^3 -allylpalladium intermediate (cross-coupling) or attack distal to the carbene carbon (amination/alkylation). Van Vranken and co-workers demonstrated that carbenylation with vinyl halides involves an η^3 -allylpalladium intermediate by showing that

intermolecular nucleophilic attack will occur at the least hindered side of the substrate regardless of whether the vinyl iodide or the *N*-tosylhydrazone is substituted with a bulky group (Figure 1.14).³³

Figure 1.14 Sterics Direct Nucleophilic Attack Indicating an η^3 -Allylpalladium Intermediate



1.4.3 Examples of Intramolecular Palladium-Catalyzed Carbenylative Cross-Coupling

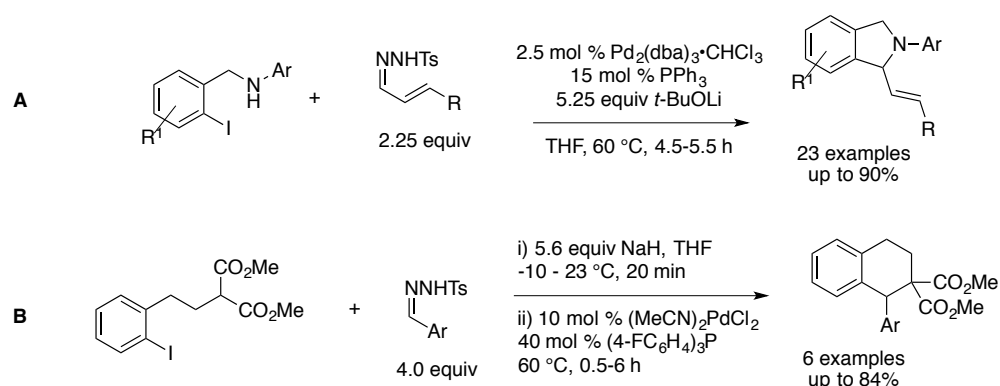
1.4.3.1 Intramolecular Palladium-Catalyzed Carbenylative Cross-Coupling Reactions with Amine and Carbon Nucleophiles

Intramolecular palladium-catalyzed carbenylative cross-coupling reactions utilize electrophiles with tethered nucleophiles to generate five- and six-membered rings. During the course of my research, Liang and co-workers published a paper on palladium-catalyzed carbenylative cross-coupling to form *N*-aniline isoindolines from *N*-(2-iodobenzyl)anilines and α,β -unsaturated *N*-tosylhydrazones (Figure 1.15, A).³⁵ Although Liang's system is similar to some of the systems presented in this thesis, there are several aspects that were not addressed: *N*-anilines were the only nucleophile used, the cited applications for isoindolines with bioactivity did not contain *N*-arylisindoline, *N*-aryl groups are difficult to remove; *p*-methoxyphenylamine can be deprotected, but the radical conditions required³⁹ are not compatible with vinylisoindolines and no examples of 6-member ring formation or asymmetric induction were reported.

Similarly, tethered carbon nucleophiles have produced 1-arylidanes and 1-aryltetralines

from dimethyl (2-iodobenzyl) malonate or dimethyl 2-(2-iodophenethyl)malonate and aryl *N*-tosylhydrazones (Figure 1.15, B).⁴⁰ While optimizing the reaction, it was found that using sodium hydride to form both the enolate and *N*-tosylhydrazone salt provided the best results in contrast to carbonate and tert-butoxide salts typically seen in palladium-catalyzed carbenylation reactions.

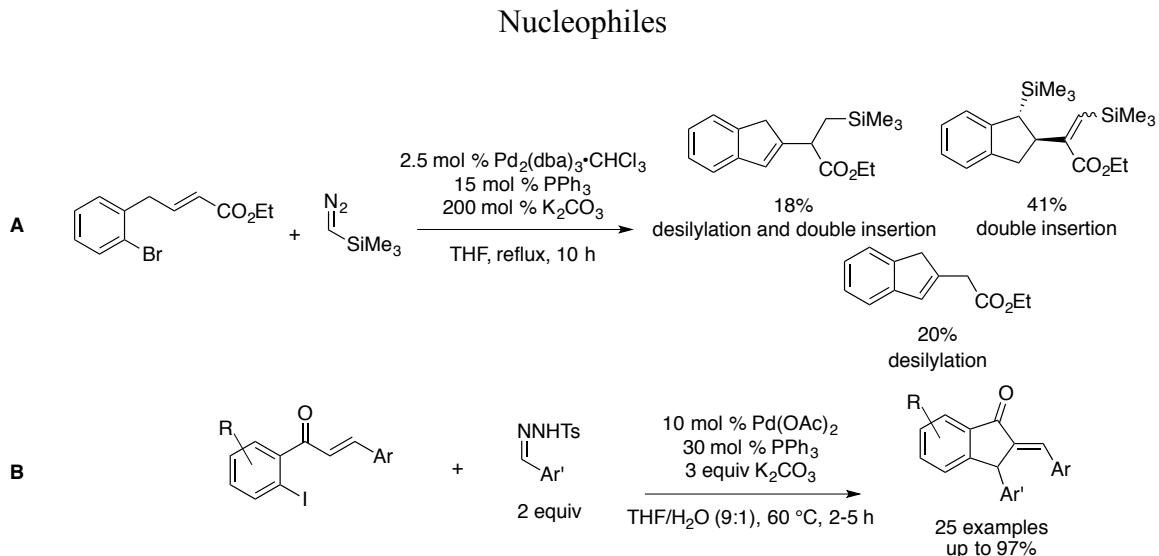
Figure 1.15 Intramolecular Palladium-Catalyzed Carbenylative Cross-Coupling with Amine and Carbon Nucleophiles



1.4.3.2 Intramolecular Palladium-Catalyzed Carbenylative Cross-Coupling Reactions with Alkene Nucleophiles

Palladium-catalyzed carbenylative cross-coupling with alkene nucleophiles is analogous to the Heck reaction. The first attempt to use tethered alkenes as a nucleophile led to poor results from carbene over insertion and protodesilylation, both due to the use of trimethylsilyldiazomethane as the carbene source (Figure 1.16, A).²⁷ Subsequent use of tethered alkenes with aryl *N*-tosylhydrazones as the carbene source produced high yields of the desired intramolecular carbenylative Heck products (Figure 1.16, B).²⁸

Figure 1.16 Intramolecular Palladium-Catalyzed Carbenylative Cross-Coupling with Alkene



1.4.3.3 Intramolecular Palladium-Catalyzed Four-Component Tandem Carbonylation and Carbenylative Cross-Coupling

Tandem palladium-catalyzed carbonylation/carbenylative cross-coupling provides a novel method to generate cyclic α,α -disubstituted α -amino esters in modest yields (Figure 1.17).³⁴ The reaction is believed to go through palladium-catalyzed insertion of aryl iodide into carbon monoxide followed by palladium-carbene formation, migratory insertion of the acyl group into the palladium-carbene and finally nucleophilic attack by the tethered amine.

Figure 1.17 Intramolecular Palladium-Catalyzed Four-Component Tandem Carbonylation and

Carbenylative Cross-Coupling



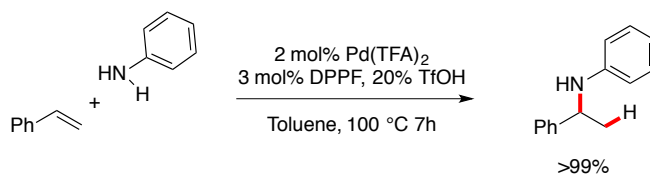
1.5 Palladium-Catalyzed Carbenylative Amination and Alkylation Reactions

1.5.1 Background to Carbenylative Amination: Palladium-Catalyzed Hydroamination and Carboamination

1.5.1.1 Palladium-Catalyzed Hydroamination

The development of palladium-catalyzed amination reactions has generated powerful transformations that chemists can use to piece together amines through non-traditional C-N bond forming reactions. Hydroamination allows for the addition of N-H from a nucleophilic amine across an alkene generating new C-N and C-H bonds in the process.⁴¹ In 2000 Hartwig and Kawatsura reported an efficient palladium-catalyzed hydroamination reaction involving anilines and vinylarenes with the use of an acid co-catalyst (Figure 1.18).⁴²

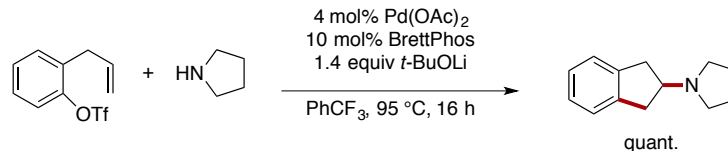
Figure 1.18 Palladium Catalyzed Hydroamination of Vinylarenes with Arylamines



1.5.1.2 Palladium-Catalyzed Carboamination

Di-functionalization of alkenes allows for more complexity to be added to molecules in a single step, compared to hydroamination. In 2004 Wolfe and Ney demonstrated the first catalytic insertion of an alkene into a [Pd(Ar)(NR₂)] complex.⁴³ The use of tethered alkenes afforded pyrrolidine carboamination products containing both new C-N and C-C bonds. Further expansion of substrates and optimization of reaction conditions has led to a powerful way to generate pyrrolidines as well as nitrogen substituted carbocycles in high yield (Figure 1.19).^{44,45}

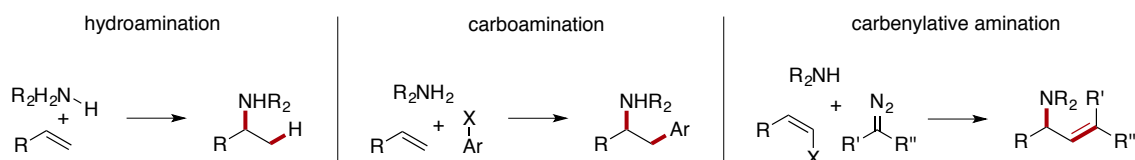
Figure 1.19 Palladium Catalyzed Carboamination to Form Pyrrolidines



1.5.1.3 Comparison of Amination to Carbenylative Amination

The Van Vranken group developed the first palladium-catalyzed carbenylative amination and alkylation reactions.^{7,6} In these reactions palladium-carbenes insert into vinyl halides leading to η^3 -allylpalladium intermediates that can be efficiently trapped with carbon or nitrogen nucleophiles. In the case of carbenylative amination, the reaction efficiently generates allyl amines with new C-N and C-C bonds formed across the vinyl halide. While mechanistically different, the bonds formed in this fashion are analogous to the bonds formed in palladium-catalyzed hydroamination and carboamination (Figure 1.20).

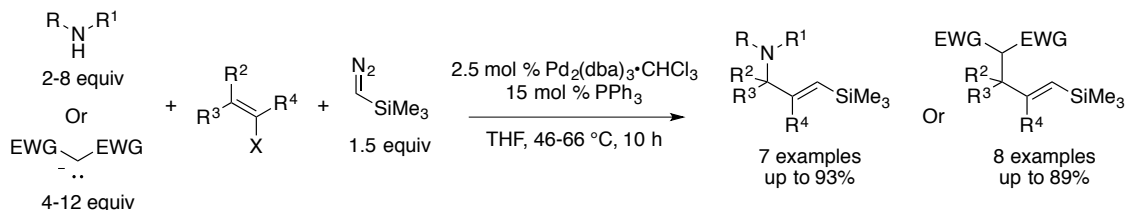
Figure 1.20 Comparison of Palladium-catalyzed Amination Reactions



1.5.2 Examples of Intermolecular Carbenylative Amination and Alkylation Reactions

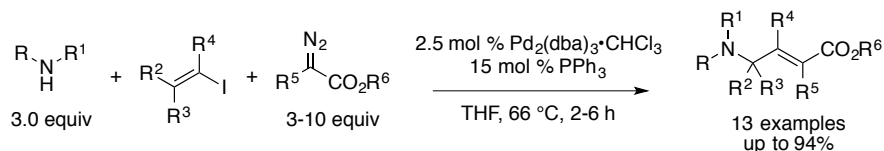
In 2007 Van Vranken and co-workers reported the first example of an intermolecular palladium-catalyzed carbenylative amination of vinyl halides with trimethylsilyldiazomethane and alkyl amines to form vinylsilanes (Figure 1.21).⁷ Following on the success of trapping carbene insertion intermediates with amine nucleophiles a set of reaction conditions were optimized replacing amine nucleophiles with carbon nucleophiles.⁶ The vinylsilanes formed are useful intermediates for stereospecific electrophilic substitution reactions or can be transformed into terminal alkenes through protodesilylation.

Figure 1.21 Intermolecular Palladium-Catalyzed Carbenylation to form Vinylsilanes



Subsequent work led to the use of α -diazoesters instead of trimethylsilyldiazomethane as a carbene source alongside amine nucleophiles in order to generate α,β -unsaturated γ -amino esters (Figure 1.22).⁴⁶ Slow addition of the diazo compound is required to prevent inactivation of the palladium catalyst and to inhibit reactions with the enoate products, which were shown to be sensitive to α -diazoesters.

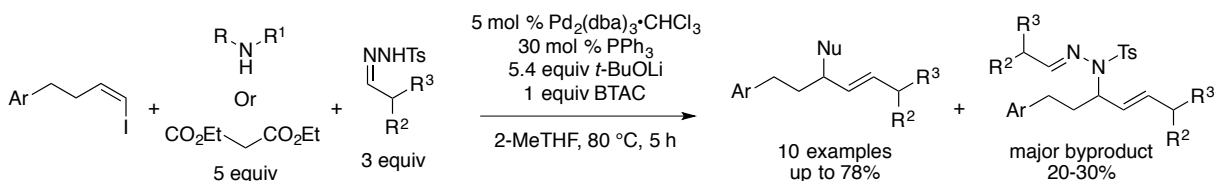
Figure 1.22 Intermolecular Palladium-Catalyzed Carbenylative Amination Generating α,β -Unsaturated γ -Amino Esters



Additional expansion of this methodology has led to conditions suitable for intermolecular carbenylative amination and alkylation with alkylidene precursors (Figure 1.23).³³ Typically alkylidene carbene precursors with α -hydrogens are seen in palladium-catalyzed carbenylative cross-coupling reactions where β -hydride elimination occurs following insertion (*vide supra*). Van Vranken and co-workers demonstrated that the use of vinyl iodides allowed nucleophilic trapping to outcompete β -hydride elimination. The nucleophiles can outcompete due to the vinyl iodides generating η^3 -allylpalladium intermediates, which resist β -hydride elimination. However, under the optimized reaction conditions, lithiated sulfonylhydrazone competes with the desired nucleophile to attack the η^3 -allylpalladium intermediate, which leads

to 20-30% of undesired byproduct.

Figure 1.23 Intermolecular Palladium-Catalyzed Carbenylation with Alkylidene Precursors



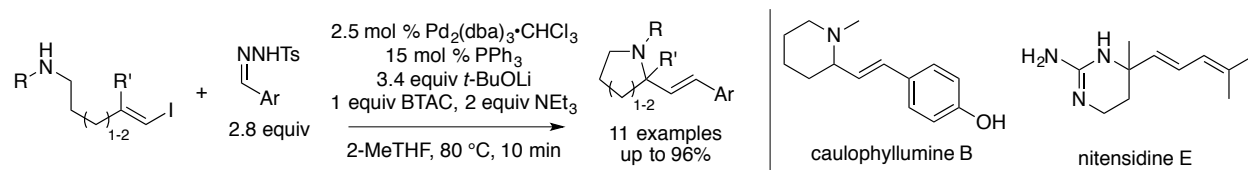
1.5.3 Examples of Intramolecular Carbenylative Amination and Alkylation Reactions

In intramolecular palladium-catalyzed carbenylative amination and alkylation reactions the nucleophile is tethered to the electrophilic component. These reactions have been used to generate cyclopentanes and 5- or 6-membered heterocyclic amines. Due to the speed with which intramolecular nucleophilic attack occurs, compared to intermolecular attack, competition with other nucleophiles such as lithiated sulfonylhydrazone is not observed. Another benefit of using tethered nucleophiles is reagent efficiency; typical intermolecular palladium-catalyzed carbenylative reactions require a large excess of nucleophile, up to twelve equivalents, while intramolecular use one.

Van Vranken and co-workers reported the first intramolecular palladium-catalyzed carbenylative amination reaction using amine-tethered vinyl iodides and aryl or cinnamyl *N*-tosylhydrazones to generate pyrrolidine and piperidine products (Figure 1.24).⁴⁷ Utilizing this new reactivity they were able to synthesize the natural product caulophyllumine B through carbenylative amination (70%) followed by nucleophilic deprotection of the methyl ether (68%). The work in this thesis was extended by a coworker in the synthesis of the cyclic guanidine alkaloid natural product nitensidine E.⁴⁸ After optimization of reaction conditions for the tethered protected guanidine vinyl iodide and vinyl *N*-tosylhydrazone starting material, the nitensidine E trifluoroacetic acid salt was obtained through palladium-catalyzed carbenylative amination

(76%) and *N*-Boc deprotection (58%).

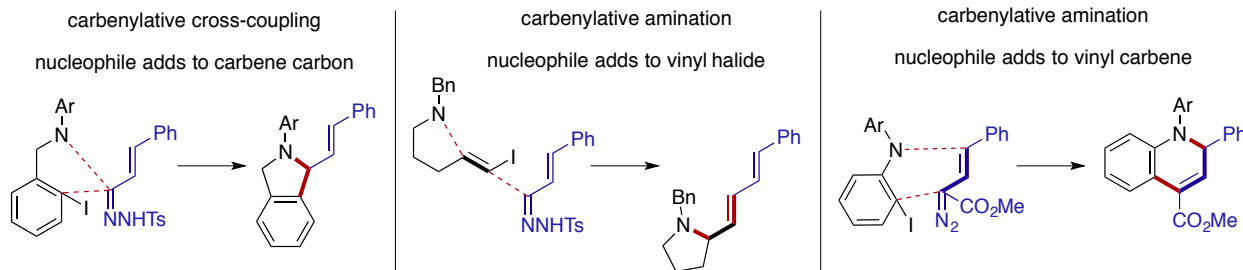
Figure 1.24 Intramolecular Palladium-Catalyzed Carbenylation to Form Pyrrolidines,
Piperidines and Cyclic Guanidines



In order to use aliphatic precursors for intramolecular carbenylations it was found that *N*-trisyldiazones had to be employed instead of *N*-tosylhydrazones to generate the palladium alkylidene intermediates.³³ Initial attempts to use aliphatic *N*-tosylhydrazones led to dimerization and unreacted starting material. The lack of activity seen with *N*-tosylhydrazones was postulated to be due to poor solubility of the lithiated form, which limits concentration. In the reaction conditions, lithiated *N*-trisyldiazones, which are known to be more reactive than the corresponding *N*-tosylhydrazones,⁴⁹ were found to be more soluble and led to product formation.

Substrate design by Liang and co-workers led to an intramolecular palladium-catalyzed carbenylation that provides novel connectivity utilizing aryl vinyl diazoacetates and *N*-substituted-2-iodoanilines.³⁴ In palladium-catalyzed cross-couplings both the nucleophile and electrophile form bonds to the carbene carbon whereas palladium-catalyzed carbenylative amination typically results in the nucleophile and carbene adding across a vinyl halide (Figure 1.25). The substrates that Liang and co-workers utilize result in a 1,3-addition across the arylvinyl diazoacetate (Figure 1.25) instead of the cross-coupling product due to unfavorable 4-membered ring formation.

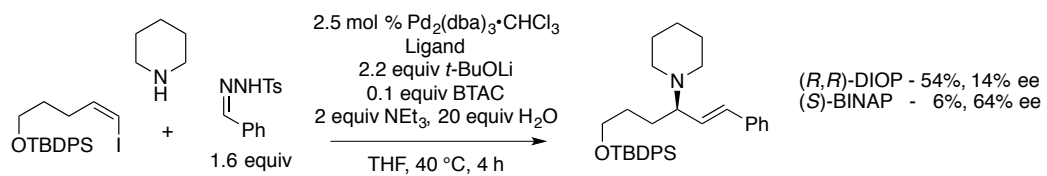
Figure 1.25 Comparison of Palladium-Catalyzed Carbenylation Bond Formation



1.5.4 Enantioselection in Palladium-Catalyzed Carbenylative Reactions

The migratory insertion of a group into the palladium-carbene intermediate typically generates a new chiral center. In the case of reactions involving β -hydride elimination, the newly formed stereochemistry is erased by the β -hydride elimination. Surprisingly, there has been only one published example of using chiral ligands in palladium-catalyzed carbenylative reactions to control enantioselectivity during the migratory insertion step (Figure 1.26).⁴⁷ Yields tended to be lower with the chiral bidentate ligands tested compared to triphenylphosphine. Using a (*Z*)-vinyl iodide generated higher enantiomeric excess (ee) than an (*E*)-vinyl iodide indicating that *cis*-substitution may contribute to enantioselection, however the (*E*)-vinyl iodide had a tethered nucleophile so a direct comparison cannot be made. The use of (*S*)-BINAP greatly slowed down the reaction and had a dramatic affect on yield, 6%, but provided a modest 64% ee. Due to the observation that fast reactions and high yields were inversely correlated with ee it was speculated that two catalytic species, a slow chiral palladium complex and a fast achiral palladium complex were in competition. Because the reaction was optimized for triphenylphosphine, an achiral, monodentate ligand, the authors believe that ligand screening and reaction optimization could lead to both high yields and ees.

Figure 1.26 Reported Enantioselection in Palladium-Catalyzed Carbenylative Amination



Chapter 2

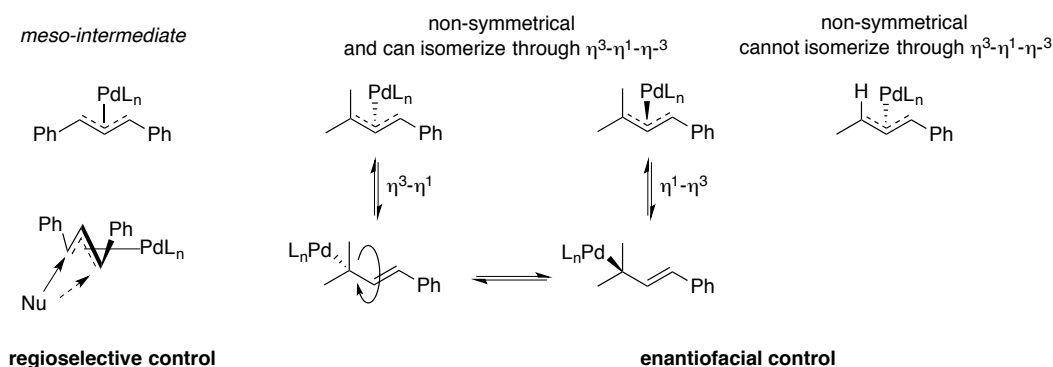
Palladium-Catalyzed Carbenylative Cross-Coupling and Carbenylative Amination with Vinylcarbenes: Progress Towards Asymmetric Carbenylation.

2.1 Introduction

Asymmetric palladium-catalyzed allylic alkylations reactions have been mechanistically studied in detail and extensively used in total synthesis over the past forty years.⁹ Within the class of palladium-catalyzed asymmetric allylic alkylations there are two types of η^3 -allylpalladium intermediates, symmetrical *meso*-intermediates and non-symmetrical, both of which differ in how stereocontrol is achieved (Figure 2.1). In symmetrical *meso*-intermediates, the chiral palladium species provides regioselective control through steric interactions, which direct the site of nucleophilic attack. In non-symmetrical systems, enantiofacial control generates the enantioselectivity due to the chiral palladium species preferring one face of the olefin to the other. If the substrate has two identical groups on one side, the η^3 -allylpalladium intermediate can undergo an η^3 - η^1 - η^3 isomerization (Figure 2.1) leading to a loss in stereochemical information. In the case of allylic alkylation, this isomerization can erase stereochemistry generated from enantiotopic olefin face coordination or enantiotopic ionization; however, enantiotopic olefin face coordination and enantiotopic ionization are outside of the scope of this work. η^3 -Allylpalladium intermediates formed through carbenylative processes can also lose stereochemical information generated from the migratory insertion step through η^3 - η^1 - η^3 isomerization. Substrates that do not contain two identical substitutions on the same side of the η^3 -allylpalladium system can still isomerize by enantioface exchange resulting from addition of palladium(II) to an η^1 -allylpalladium(II) intermediate; but the isomerization can be inhibited by using reactive allylic substrates, low palladium concentrations, bidentate ligands and halide ions.

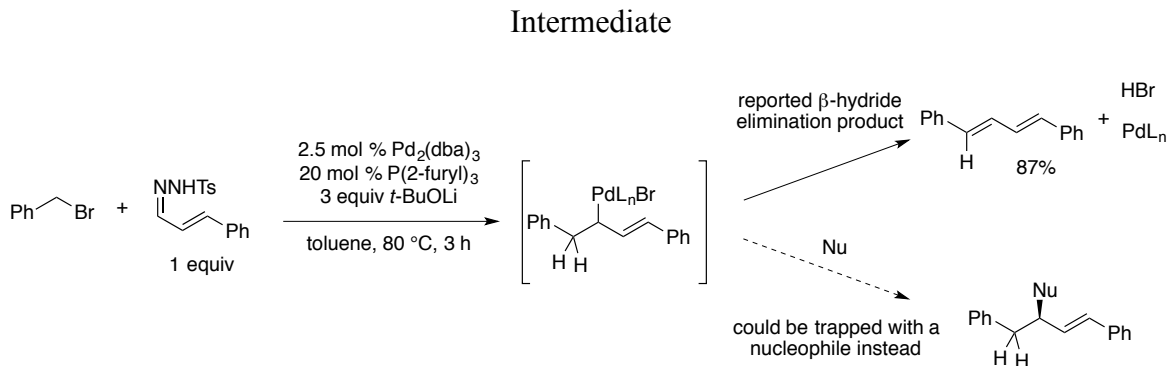
Employing α,β -unsaturated *N*-tosylhydrazones in palladium-catalyzed carbenylative cross-coupling and carbenylative amination reactions would provide access to these well studied symmetrical and non-symmetrical η^3 -allylpalladium intermediates. Demonstrating asymmetric induction through a carbenylative process that intercepts a well-known prochiral intermediate is an important first-step proof of concept.

Figure 2.1 Symmetrical and Non-Symmetrical Intermediates in Allylic Alkylations



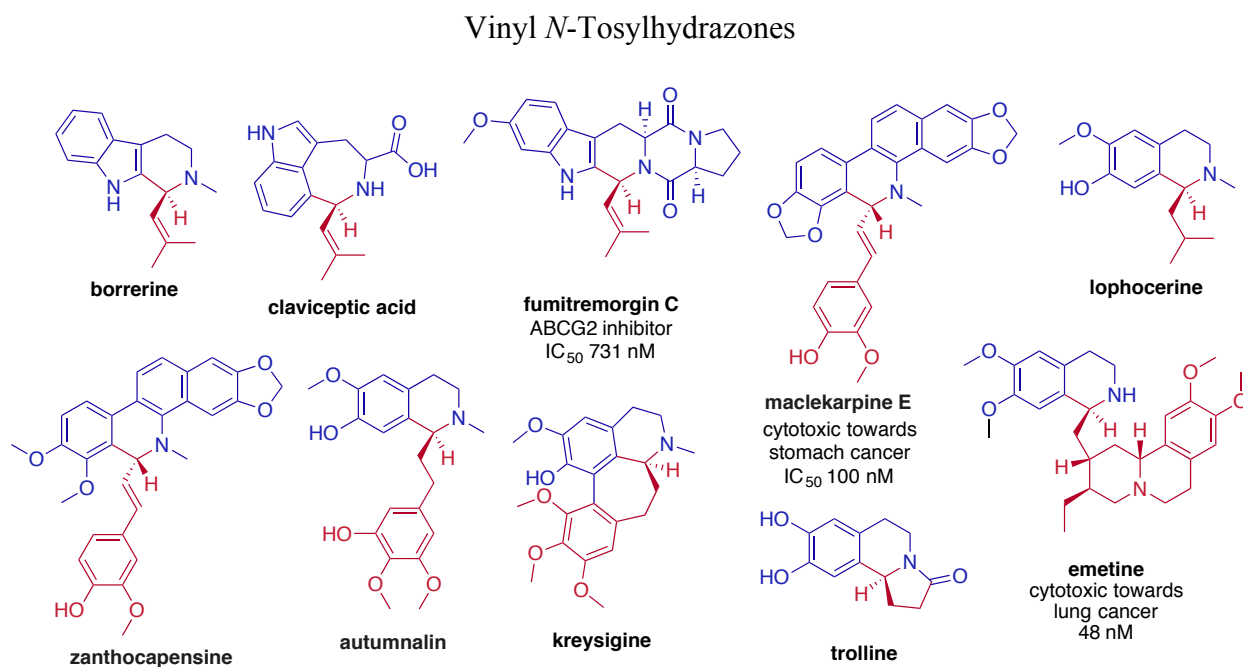
The growing interest in use of a carbene source as a coupling partner in palladium-catalyzed carbenylative cross-coupling and carbenylative amination reactions has led to the development of reactions and conditions to form a diverse range of useful products.⁵⁰ The advent of using *N*-tosylhydrazones to generate unstabilized diazo compounds in situ allowed for vinyl groups to be introduced through the carbene component. Wang and co-workers first reported the use of an α,β -unsaturated *N*-tosylhydrazone in a two-component palladium-catalyzed carbenylative coupling reaction between cinnamaldehyde-*N*-tosylhydrazone and benzyl bromide.⁵¹ The reaction forms a diene through β -hydride elimination of a palladium-vinylcarbene migratory insertion intermediate (Figure 2.2). Greater utility could be obtained from vinyl carbenes by trapping the migratory insertion intermediate with a nucleophile rather than β -hydride elimination.

Figure 2.2 β -hydride Elimination vs. Nucleophilic Trapping of Palladium-Carbene Insertion



Use of a tethered amine nucleophile in palladium-catalyzed carbenylative cross-coupling of aryl halides (mapped in blue) with α,β -unsaturated *N*-tosylhydrazones (mapped in red) would provide access to numerous natural products (Figure 2.3). Additionally, nucleophilic trapping of the insertion intermediate can preserve the chiral center that is typically formed during the migratory insertion step allowing for the possibility of asymmetric induction.

Figure 2.3 Natural Products Accessible Through Palladium-Catalyzed Cross-Coupling with



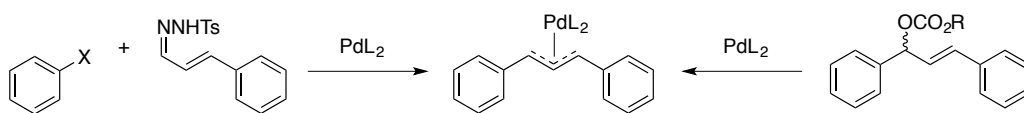
This work focuses on the use of *N*-tosylhydrazones derived from α,β -unsaturated aldehydes – precursors to vinylcarbenes – in palladium-catalyzed carbenylative cross-coupling and carbenylative amination reactions. These carbenylative reactions will be used to form η^3 -allylpalladium intermediates that generate stereogenic centers at the carbene center. An initial acyclic model system of iodobenzene, cinnamaldehyde-*N*-tosylhydrazone and piperidine was used to intercept a well-known prochiral 1,3-diphenylallyl intermediate to probe the feasibility of enantioselectivity in a palladium-catalyzed carbenylative reaction as a proof of concept for asymmetric carbenylation. Following the proof of concept, the substrate scope was expanded to include aliphatic vinyl hydrazones in order to install prenyl functional groups. Finally, cyclic systems to form isoindolines and tetrahydroisoquinolines, which could be mapped onto natural products, were developed by employing amine tethered aryl iodides.

2.2 Results and Discussion

2.2.1 Intercepting Symmetrical 1,3-Diphenylallyl, a Known Prochiral Intermediate

2.2.1.1 Introduction

Figure 2.4 η^3 -Allylpalladium Intermediate Formation Through Carbenylative Insertion or Allylic Carbonate Ionization



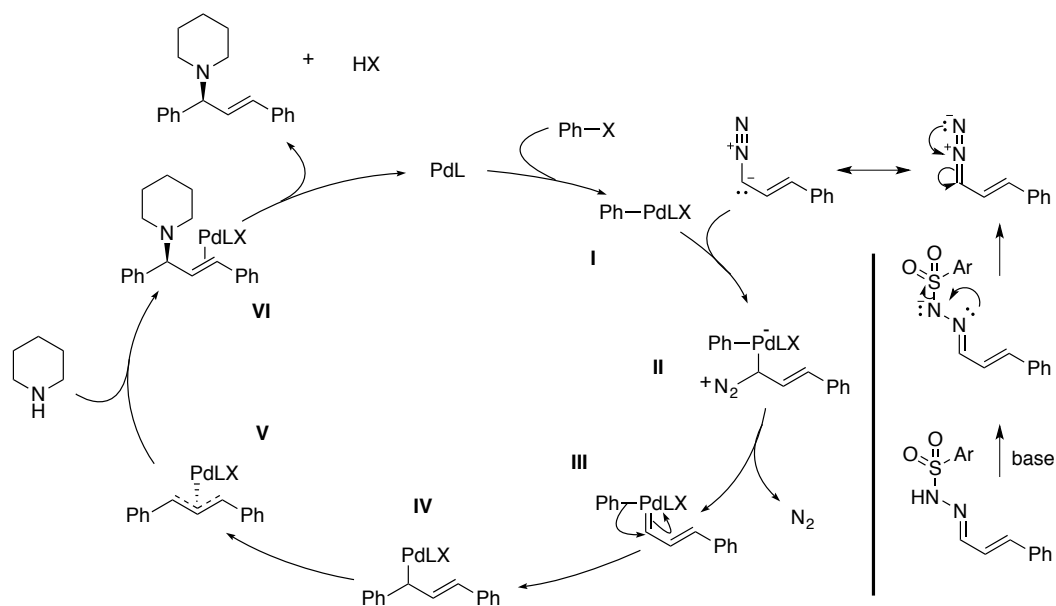
The enantioselective palladium-catalyzed allylic alkylation and amination of symmetrical 1,3-diphenylallyl systems has been studied extensively.⁹ The *meso* η^3 -1,3-diphenylallyl intermediates give rise to enantioselectivity through regioselective addition to the η^3 -allylpalladium species. The same η^3 -1,3-diphenylallyl intermediates can be accessed through carbenylative insertion (Figure 2.4) in order to demonstrate that the η^3 -diphenylallyl palladium

intermediates generated through carbenylative insertion can generate equivalent enantiomeric excesses (ees) as those generated from ionization of allylic carbonates. As long as the chiral ligands are bound to palladium during the nucleophilic attack, the reaction should generate products with ees that are comparable to values reported for allylic amination with allylic carbonate starting materials. While it is possible that the ees obtained are generated during the migratory insertion, rather than the nucleophilic attack, this system will not provide insight into the source of enantioselectivity, but that topic will be explored later on (*vide infra*). While there are more examples for generating high ees using carbon nucleophiles over amine nucleophiles in these systems, the use of amines is applicable to the work reported herein. As proof of concept, a carbenylative amination was used to access a well-known η^3 -1,3-diphenylallylpalladium from *N*-tosylhydrazone **2** and iodobenzene followed by nucleophilic trapping with piperidine to afford a chiral product.

2.2.1.2 Proposed Catalytic Cycle

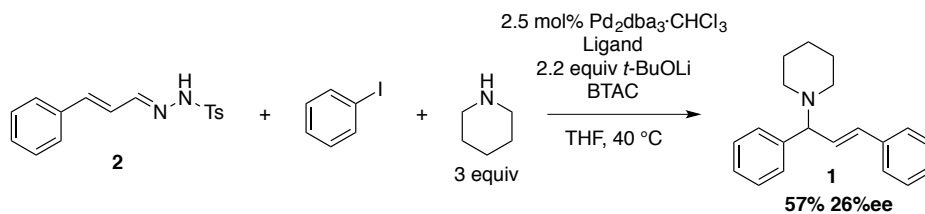
The catalytic cycle (Figure 2.5) is proposed to go through an initial oxidative addition of palladium into the aryl halide forming arylpalladium(II) intermediate **I**. A vinyl diazo compound generated in situ through a Bamford-Stevens reaction then attacks arylpalladium(II) intermediate **I** to form a zwitterionic palladate intermediate **II** which then extrudes nitrogen gas to generate vinylpalladium carbene intermediate **III**. Migratory insertion forms η^1 -allylpalladium(II) intermediate **IV**, which goes from η^1 to η^3 forming η^3 -allylpalladium(II) intermediate **V**. Nucleophilic attack of η^3 -allylpalladium(II) intermediate **V** leads to allylic amine **VI**, which dissociates from palladium to regenerate the catalyst.

Figure 2.5 Proposed Catalytic Cycle for Palladium-Catalyzed Carbenylative Cross-Coupling with Nucleophilic Trapping of η^3 -allylpalladium Intermediate



2.2.1.3 Reaction Optimization

Table 2.1 Initial Palladium-Catalyzed Carbenylative Amination Reaction Optimization



Entry	equiv 2	equiv PhI	Ligand	BTAC	Time	Yield (%)
1	1.1	1	15 mol% PPh ₃	100 mol%	7 h	32%
2	1.1	1	15 mol% PPh ₃	10 mol%	7 h	32%
3	1	1	7.5 mol% (<i>R,R</i>)-DIOP	100 mol%	4.5 h	47% ^a
4	1	2	7.5 mol% (<i>R,R</i>)-DIOP	100 mol%	4.5 h	57%
5	1	2	7.5 mol% (<i>R,R</i>)-DIOP	10 mol%	10 h	59% ^a
6	1	2	5.0 mol% (<i>R,R</i>)-DIOP	100 mol%	10 h	33% ^a
7	1	2	15 mol% (<i>R,R</i>)-DIOP	100 mol%	21 h	51%
8	1	2	7.5 mol% (<i>S</i>)-BINAP(S)	100 mol%	10 h	<5%

^aNMR yield based on internal standard

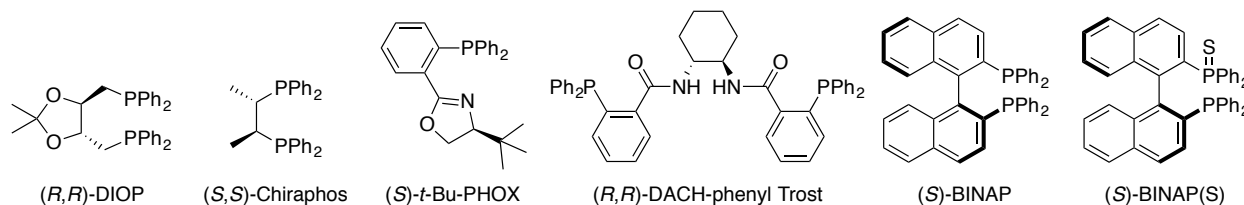
Starting from conditions that had previously been used for arylhydrazones, a set of reaction conditions was screened for the palladium-catalyzed carbenylative amination between

iodobenzene, piperidine and cinnamaldehyde *N*-tosylhydrazone **2**. Initial reaction optimization revealed that the bidentate ligand (*R,R*)-DIOP (Figure 2.6) provided an increase in yield from 32% to 47% compared to triphenylphosphine (Table 2.1, entries 1 and 3). Benzyltriethylammonium chloride (BTAC) was added as a phase-transfer catalyst to solubilize the lithiated *N*-tosylhydrazone salts that form during the reaction. When changing from 100 mol% BTAC to 10 mol% BTAC with triphenylphosphine as a ligand there was no difference in yield or catalyst turnover rate (Table 2.1, entry 1 and 2). When using (*R,R*)-DIOP as a ligand, changing the BTAC concentration from 100 mol% to 10 mol% also had no effect on the yield, however there was a marked decrease in the rate of catalyst turnover as seen by the increase in reaction time from 4.5 h to 10 h (Table 2.1, entry 4 and 5). Iodobenzene could not be monitored by TLC due to its volatility. To ensure that the aryl iodide was not being depleted, the *N*-tosylhydrazone was utilized as the limiting reagent. Increasing the amount of iodobenzene from 1 to 2 equivalents led to an increase in yield from 47% to 57% (Table 2.1, entry 3 and 4). To address concerns of over- or under-ligation of palladium, ligand concentrations were varied. Lowering the amount of ligand to 5 mol % showed a marked decrease in yield while increasing the amount of ligand to 15 mol % did little to affect the yield but quadrupled the reaction time, probably due to over-ligation of the palladium (Table 2.1, entry 4, 6 and 7). In order to deprotonate the *N*-tosylhydrazone and quench the hydroiodic acid formed in the reaction 2.2 equivalents of lithium *t*-butoxide was added. An attempt to use conditions developed by Barluenga and co-workers (XPhos, dioxanes, 70 °C) for two-component carbenylative coupling reactions that proceed through β -hydride elimination⁴ⁿ rather than nucleophilic trapping, failed to generate any product. The reaction conditions developed for the 1,3-diphenylallyl system were sufficient to obtain the necessary ees in this proof of concept system and were not optimized

further.

2.2.1.4 Asymmetric Induction Through Regioselective Control

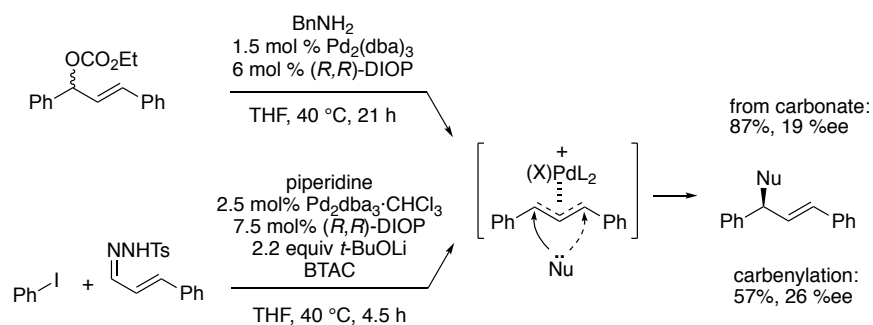
Figure 2.6 Chiral Ligands Screened



A report by Faller and co-workers employed the use of the mono-sulfide (*S*)-BINAP(*S*) (Figure 2.6) as a ligand for allylic amination which generated high ees with various amine nucleophiles.⁵² Hoping that (*S*)-BINAP(*S*) would also work well for our reaction, we synthesized the P=S bond of (*S*)-BINAP(*S*) by addition of elemental sulfur to (*S*)-BINAP followed by separation of bis-phosphine starting material, mono-sulfide and bis-sulfide. Unfortunately, (*S*)-BINAP(*S*) performed poorly in the carbenylative process yielding <5% product, insufficient to purify and determine ee. Utilizing carbenylative amination conditions published by a co-worker,⁴⁷ an additional attempt was made to use (*S*)-BINAP(*S*), unfortunately no product was detected. Complexes of (*S*)-BINAP and (*R,R*)-DACH-phenyl Trost ligand also failed to engage in the carbenylation reaction. Finally, optimized conditions for a 5-membered intramolecular reaction, *vide infra*, failed to generate product with (*S,S*)-chiraphos or (*S*)-*t*-Bu-PHOX. We were able to obtain sufficient material using (*R,R*)-DIOP to determine an ee. Hayashi has reported that under conditions similar to our current reaction an ee of 19% was obtained using benzylamine as a nucleophile and (*R,R*)-DIOP as a chiral ligand (Figure 2.7).⁵³ Previous studies have shown that benzylamine works poorly in carbenylative coupling but utilizing piperidine instead of benzylamine, we obtained an ee of 26% (Table 2.1, entry 4), comparable to Hayashi's result but perhaps higher due to the increased steric demands of a secondary amine nucleophile. Having

shown that palladium-catalyzed carbenylative insertions produce comparable ees when intercepting known η^3 -1,3-diphenylallylpalladium intermediates, we were ready to expand substrate scope.

Figure 2.7 Intercepting a Known η^3 -1,3-Diphenylallylpalladium(II) Intermediate

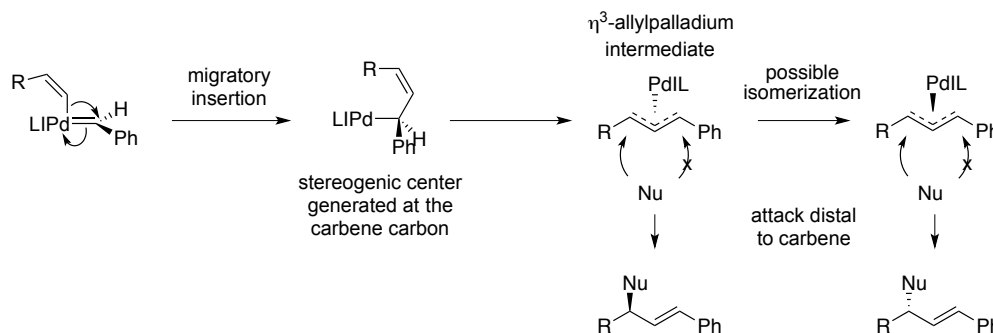


2.2.2 Asymmetric Induction Through Enantiofacial Control in Unsymmetrical η^3 -Allylpalladium Systems – Installation of Prenyl Functional Groups

2.2.2.1 Intermolecular Carbenylation with Unsymmetrical η^3 -Allylpalladium Systems

Next, we wanted to exploit palladium-catalyzed carbenylative cross-coupling with unsymmetrical η^3 -allylpalladium intermediates, which formed new stereogenic centers at the carbene carbon. In previous non-asymmetric examples of palladium-catalyzed carbenylative reactions that intercepted η^3 -allylpalladium intermediates the nucleophiles were designed to attack the η^3 -allylpalladium intermediate at a site distal from the original carbene center which obscured the carbene center as the potential origin of chirality (Figure 2.8).⁴⁶ There are two possible mechanistic sources of asymmetric induction in these reactions, migratory insertion and/or isomerization of the palladium species to a preferred face before nucleophilic trapping (Figure 2.8).

Figure 2.8 Previous Nucleophilic Trapping of η^3 -Allylpalladium Intermediates Distal to the Carbene Carbon and Sources of Chirality



We set out to determine if there is a steric or electronic preference for nucleophilic attack when a non-symmetrical η^3 -allylpalladium intermediate such as **3** is encountered (Figure 2.9). Regioselectivity can be difficult to predict for alkylation of differentially substituted η^3 -allylpalladium intermediates. For example, palladium-catalyzed allylic alkylation with differentially substituted η^3 -allylpalladium intermediates generated conjugated product with 1-methyl-3-phenylallyl and non-conjugated product with 1-*t*-butyl-3-phenylallyl (Figure 2.10).⁵⁴ Since the available data was insufficient to predict the outcome for the system in Figure 2.9, *N*-tosylhydrazone **4** was synthesized from the corresponding β -methylcrotonaldehyde and *p*-toluenesulfonylhydrazine and used in a carbenylative amination. Electronic preferences would favor nucleophilic attack at the tertiary carbon center of the η^3 -allylpalladium intermediate **A** in order to preserve conjugation with the aromatic ring as well as place the palladium, which has an affinity for π -bonds, next to the aromatic ring. Sterics on the other hand would favor attack next to the phenyl ring at the secondary carbon as opposed to the tertiary carbon with two methyl groups. Because it is desired to set the stereocenter at the carbene-carbon, it would be ideal for the sterics to govern the regioselectivity of the reaction. The choice of using *p*-iodoanisole over

iodobenzene was simply for ease of reaction monitoring by TLC. After performing the reaction it was found that the electronic preference is indeed the major factor for determining the regioselectivity producing the achiral conjugated product **5** with a 29% yield; none of the chiral non-conjugated product was observed in the product mixture. The selectivity we found in this intermolecular system was not desirable for our development of an asymmetric palladium-catalyzed carbenylative cross-coupling reaction with nucleophilic attack at the carbene carbon.

Figure 2.9 Determination of the Regioselectivity Preference for Sterics or Conjugation

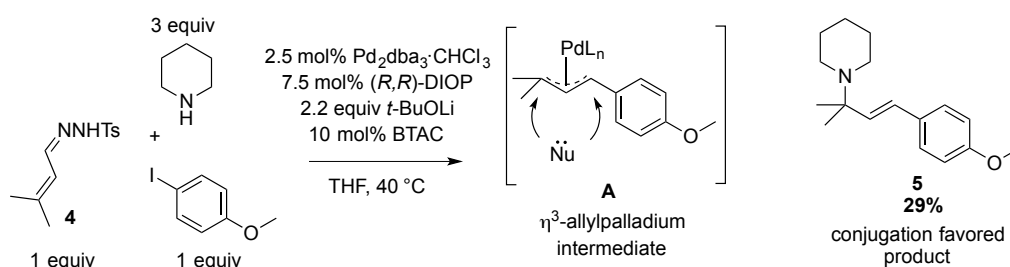
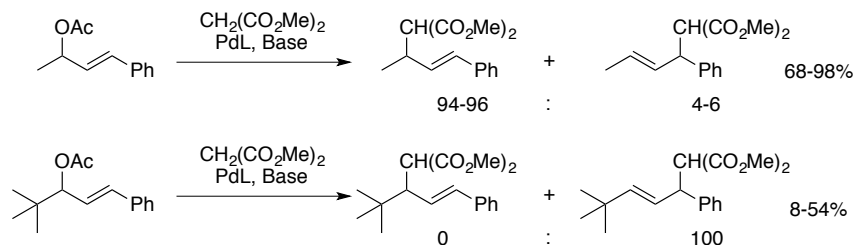


Figure 2.10 Example of Regioselectivity in Allylic Alkylation



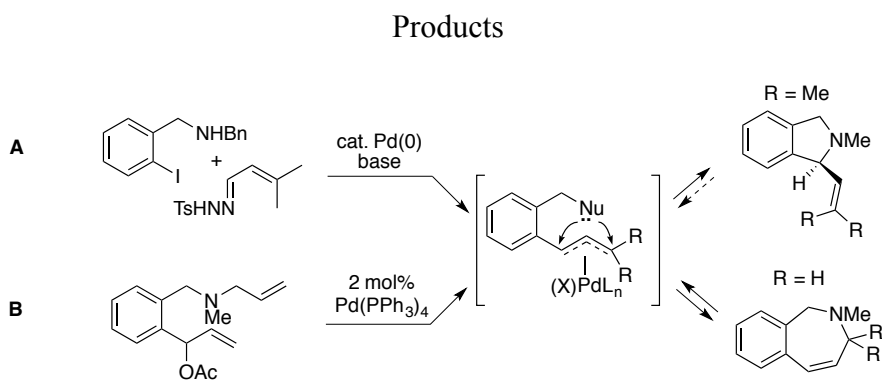
2.2.2.2 Intramolecular Carbenylation with Unsymmetrical η^3 -Allylpalladium Systems

2.2.2.2.1 Formation of 5-member Isoindoline Systems with Amine Tethered Aryl Iodides and Prenyl Aldehyde *N*-Tosylhydrazones

In order to control the site of nucleophilic attack after carbene insertion, a model system was designed using a tether to constrain the nucleophile to add kinetically to the end of the η^3 -allyl derived from the carbene center, generating a chiral non-conjugated product (Figure 2.11, A). This system does have the potential to form both 5- and 7-membered rings, which could be

detrimental to the desired product yield. Grellier and Pfeffer published work on intramolecular palladium-catalyzed allylic amination on a similar isoindoline system and it was found that the reaction yielded a mixture of both the 5- and 7-membered products (Figure 2.11, B).⁵⁵ It was hypothesized, the kinetic 5-membered isoindoline formed and over time isomerization occurred to generate the thermodynamic 7-membered ring product. To confirm the hypothesis Grellier and Pfeffer subjected the pure 5-membered isoindoline product to the reaction conditions and after 9.5 hours 66% had converted to the 7-membered product and after 48 hours 96% was converted. These findings by Grellier and Pfeffer have important mechanistic implications for our model system. Fortuitously only the 5-membered isoindoline was observed in our system. Due to the fact that we do not observe any thermodynamic 7-membered products we can infer that under our reaction conditions, ring opening of the product does not occur, and therefore isomerization and decreases or increases in ee is not possible following nucleophilic cyclization.

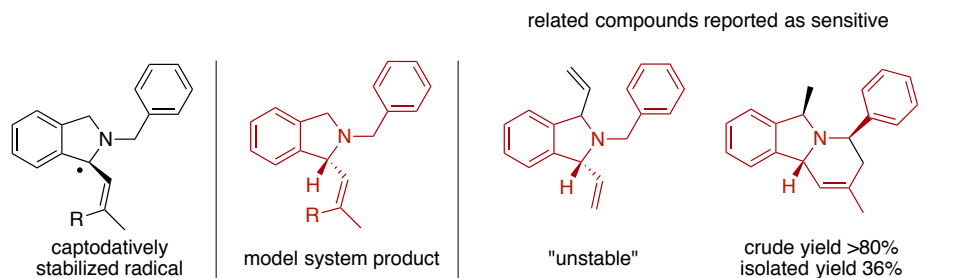
Figure 2.11 The Isoindoline Model System Proceeds Through an η^3 -Allylpalladium Intermediate That Has Been Shown to Generate Both Kinetic and Thermodynamic Allylic Alkylation



An unanticipated characteristic of the initial model system (Table 2.2) was that the isoindoline product **6** was highly sensitive to molecular oxygen and radical decomposition, which lead to rapid decomposition within minutes if left exposed to air, particularly when dissolved in chlorinated solvents such as $CDCl_3$. The sensitivity to autoxidation is most likely

due to potential for benzylic autoxidation via a captodatively stabilized radical (Figure 2.12). Similar compounds that have been reported in literature (Figure 2.12) are also reported to be highly sensitive.^{56,57}

Figure 2.12 Sensitivity of Allylic Isoindoline Systems to Aerobic Decomposition

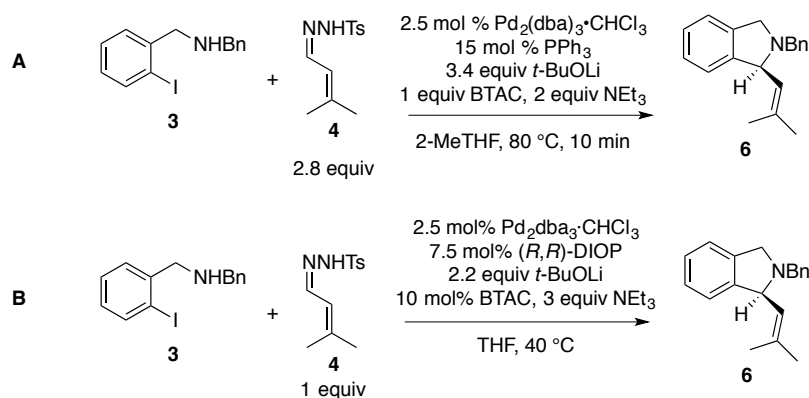


To minimize decomposition of isoindoline **6**, the crude reaction mixtures were passed through a plug of silica instead of an aqueous workup to minimize exposure to air, but isolated yields were variable and much lower than crude yields obtained by ¹H NMR against an internal standard. Benzene-*d*₆ was used instead of CDCl₃ for NMR spectroscopy and was compatible with a chiral salt method for determination of enantioselection.⁵² An additional aspect that made handling and purification of product **6** challenging was the compound's basic, yet highly hydrophobic properties. Flash column chromatography had to be performed in 99:1 hexane/Et₂O to provide any separation and any attempt to add a TEA modifier to reduce streaking of the amine in product **6** would result in inferior separation due to increased polarity in the mobile phase.

Two sets of conditions were initially tested for the formation of isoindolines through palladium-catalyzed carbenylative cross-coupling. The first set of conditions was developed by a co-worker for carbenylative amination of amine tethered vinyl iodides and aryl hydrazones (Figure 2.13, A)⁴⁷ and the second set of conditions were the optimized conditions from the 1,3-diphenylallyl system (Table 2.1, entry 5) replacing piperidine with TEA and reducing the amount

of aryl iodide **3** which can be monitored by TLC in this system (Figure 2.13, B). Yields for these initial reactions were not obtained due to the compound instability, which was not known at the time. Both conditions produced product by crude NMR however the milder 1,3-diphenylallyl conditions produced a much cleaner reaction with a more promising crude NMR. Once it was apparent there was product stability issues the reaction was repeated with the mild conditions and a NMR yield of 27% was obtained. Increasing the temperature to 50 °C improved the yield to 42% by NMR. Finally, removal of TEA and the addition of an extra equivalent of hydrazone **4** and *t*-BuOLi produced a 68% yield by NMR (Table 2.2, entry 1). From this point it was clear this system was not ideal due to the sensitive nature of the products so instead of further optimization it was decided to test asymmetric induction and then move onto a system with more utility.

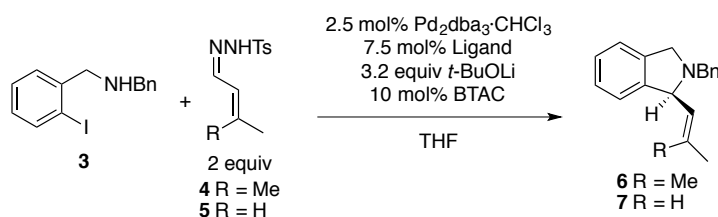
Figure 2.13 Initial Reaction Conditions for Intramolecular Vinylcarbene Insertion



(*R,R*)-DIOP provided the highest yield but it only generated 3% ee (Table 2.2, entry 1). Switching to (*S*)-BINAP greatly increased reaction time and significantly lowered yield but slightly increased ee to 11% (Table 2.2, entry 2). Encouragingly, (*S,S*)-chiraphos provided product with 30% ee (Table 2.2, entry 4). A comparison of (*S,S*)-chiraphos at room temperature, 50 °C and 70 °C demonstrated a noticeable effect on yield and ee (Table 2.2, entries 3,4 and 5). The room temperature reaction was sluggish, producing a 6% yield after 7 days and decomposed

before an ee could be determined. Using a higher temperature, 70 °C, resulted in a 51% yield and 43% ee, an 11% and 13% increase over 50 °C respectively. Unfortunately data was not obtained for (*S,S*)-chiraphos at 50 °C in MeTHF, instead of THF, and therefore the increase in yield and ee seen at 70 °C could also be due in part or in whole to the change in solvent. More importantly though, these results suggest that the right ligand and reaction conditions will be able to control the absolute stereochemistry in palladium-catalyzed carbenylative cross-coupling reactions.

Table 2.2 Results of Isoindoline Formation



Entry	Hydrazone	Ligand	Time	Temperature	NMR Yield	Isolated Yield	%ee
1	4	(<i>R,R</i>)-DIOP	5 h	50 °C	68%	43%	3%
2	4	(<i>S</i>)-BINAP	12 h	50 °C	15%	15%	11% ^c
3	4	(<i>S,S</i>)-chiraphos	7 d	r.t. ^{a,b}	6%	n.d.	n.d.
4	4	(<i>S,S</i>)-chiraphos	12 h	50 °C	40%	37%	30%
5	4	(<i>S,S</i>)-chiraphos	4 h	70 °C ^a	51%	29%	43%
6	5	(<i>S,S</i>)-chiraphos	19 h	50 °C	n.d.	24%	27%
7	5	(<i>R,R</i>)-DIOP	34 h	50 °C ^b	n.d.	11%	4%

^a Reaction was carried out in MeTHF

^b An extra equiv of *t*-BuOLi and hydrazone was added

^c Conservative approximation due to excessive decomposition in chiral shift NMR sample

Because hydrazone **4** has a symmetric gem-dimethyl functional group we can not tell whether $\eta^3\text{-}\eta^1\text{-}\eta^3$ -isomerization of the allylpalladium intermediate is erasing the stereochemistry initially set by the carbene insertion step. In order to eliminate the possibility of isomerization of palladium between enantiopic faces of the allyl fragment, *N*-tosylhydrazone **5** (Table 2.2), which generates an η^3 -allylpalladium intermediate that can not isomerize through an $\eta^3\text{-}\eta^1\text{-}\eta^3$ mechanism, was synthesized from crotonaldehyde and *p*-toluenesulfonylhydrazide. With *N*-tosylhydrazone **5** the (*S,S*)-chiraphos ligand appears to out-perform the (*R,R*)-DIOP ligand in

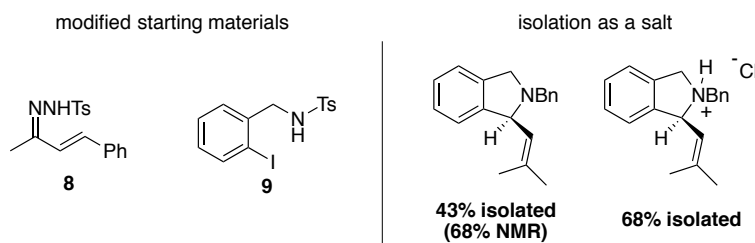
catalyst turnover and overall amount of product generated based on reaction monitoring by TLC (Table 2.2, entries 6 and 7). This is a reverse in ligand reactivity compared to the reaction involving hydrazone **4** (Table 2.2, entries 1 and 4). Although the reaction involving the (*S,S*)-chiraphos ligand was mostly product by TLC, it was found that isoindoline product **7**, with only a single methyl substitution, was actually more sensitive to decomposition in comparison to isoindoline product **6**, which contained a gem-dimethyl substitution. With (*S,S*)-chiraphos, hydrazones **4** and **5** afforded products with comparable yields and ees (27-29%) consistent with carbene insertion as the origin of enantioselection for both substrates (Table 2.2, entries 4 and 6).

The extraordinary air sensitivity of the *N*-benzyl-2-vinylindoline products led us to vary the carbene precursor and nucleophile in the model reaction. In an attempt to generate products without the sensitive benzylic hydrogen atom, ketohydrazone **8** (Figure 2.14) was synthesized and employed in the carbenylation reaction. However, the ketone hydrazone failed to engage in carbenylation under the reaction conditions probably due to a competitive cyclization of the *N*-tosylhydrazone anion to a pyrazole, which has been reported.⁵⁸ Attempting to lower the radical susceptibility of the product by using a sulfonamide **9** (Figure 2.14) also failed to generate any isoindoline product under the reaction conditions. The failure of sulfonamide **9** to generate insertion product may be due to formation of a stable palladacycle.⁵⁹ Eventually, we found that addition of the radical inhibitor (BHT) during the workup and use of the solvent toluene prior to column chromatography of the *N*-benzyl-2-vinylindoline **6** minimized decomposition. Addition of ethereal-HCl to the column fractions allowed the isoindoline to be isolated as a stable HCl salt. Formation of the salt allows for isolation of product without resorting to NMR to calculate a reaction yield (Figure 2.14). Unfortunately, the HCl salt of indoline **6** exists as a mixture of diastereomers that exhibit broadened peaks by ¹H NMR and the dissolved salt is still sensitive to

decomposition.

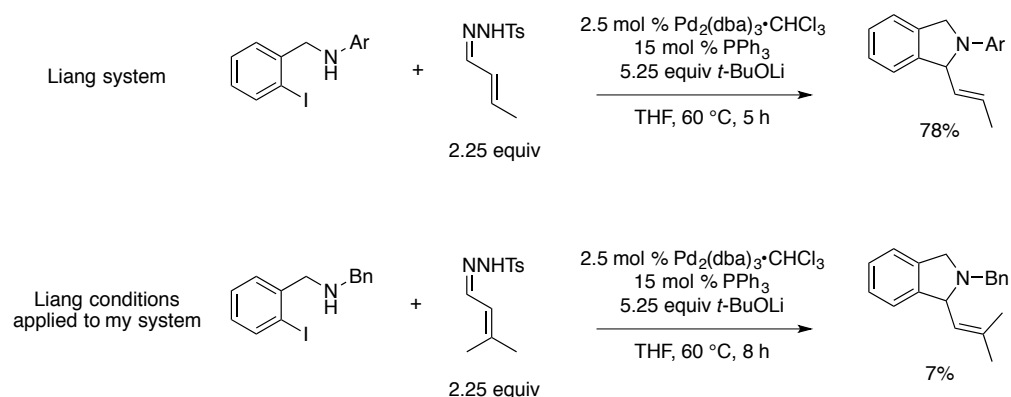
Figure 2.14 Attempted Modification of Starting Materials and Isolation Techniques to Address

Product Decomposition



As previously mentioned, during the course of my research, Liang and co-workers published a paper on palladium-catalyzed carbenylative cross-coupling to form *N*-aniline isoindolines (*vide supra*).³⁵ Due to the similarity between Liang's system and my own it was pertinent to test the robustness of Liang's reaction conditions in my model system (Figure 2.15). With care to minimize decomposition I was only able to obtain a yield of 7% (NMR) with a tethered dialkylamine. It is clear that Liang's methodology cannot be directly applied to non *N*-aniline nucleophiles. Additionally, Liang's system utilizing vinyl hydrazones is shown to only generate 5-membered rings through an intramolecular nucleophilic attack and there are no examples provided for intermolecular nucleophiles or 6-membered ring formation. Furthermore, no attempt is made to control the newly formed stereocenter. My demonstration of intermolecular nucleophilic attack, the ability to control the stereochemistry of carbenylative insertion (*vide supra*), and formation of 6-membered ring systems (*vide infra*) distinguishes my methodology.

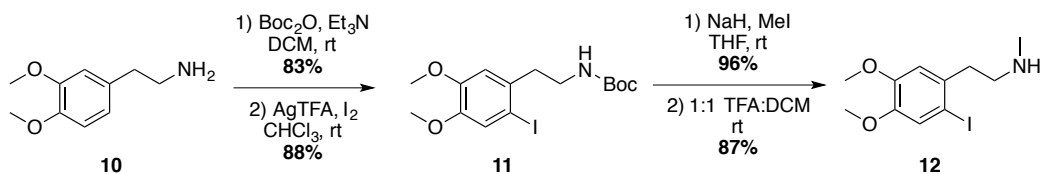
Figure 2.15 Liang's System and an Attempt to Apply it to My Model System



2.2.2.2.2 Formation of 6-member Tetrahydroisoquinoline Systems with Amine Tethered Aryl Iodides and Prenyl Aldehyde *N*-Tosylhydrazones

After demonstrating the potential for asymmetric induction in a sensitive 5-membered isoindoline system we moved on to formation of 6-membered tetrahydroisoquinolines. Tetrahydroisoquinolines are a common synthetic scaffold found frequently in natural products (Figure 2.3). Boc protection of 3,4-dimethoxyphenethylamine **10** followed by iodination with silver trifluoroacetate forms aryl iodide **11** in 88% yield (Figure 2.16). Attempted LAH reduction of Boc protected amine **11** to phenethyl-*N*-methylamine **12** led to deiodination. An alternative route of *N*-methylation of carbamate **11** followed by removal of the Boc group successfully generated aryl iodide **12** in an 87% yield.

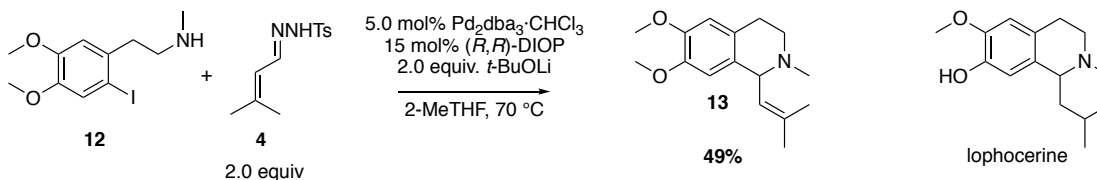
Figure 2.16 Synthesis of Tetrahydroisoquinoline Starting Material



Initially, substrate **12** was subjected to the optimized conditions for substrate **25** (Figure 3.4) *vide infra* (15% yield Boc-borrerine) and generated a chromatographically inseparable mixture of approximately 70% product and 30% of two unknown but structurally similar side

products equating to an approximate 30% yield of 7-*O*-methyl-dehydrolophocerine **13**. To ensure that the inseparable side products were not due to radical decomposition as seen with the isoindoline system, a sample of tetrahydroisoquinoline **13** was analyzed by NMR after storage for a week and no change was seen between the ratio of product and impurity peaks. Although the resulting product couldn't be fully purified, the system was still explored to gain insight into formation of 6-membered ring systems through carbenylation. Using the optimized conditions for the 5-membered cyclization to form isoindolines (Table 2.2, entry 1) without BTAC led to an approximate 40% yield, and slightly outperformed the reaction with BTAC. Increasing the temperature to 70 °C led to rapid decomposition of hydrazone **4** with little change to the aryl iodide starting material. Screening of various bases (*t*-BuOLi, *t*-BuONa, *t*-BuOK, Hünig's and DBU), amounts of base (1-3.2 equivalents) and reaction temperatures (50-110 °C, Dioxanes used instead of MeTHF for high temperatures) in order to try and match the rate of diazo formation with the rate of product formation did little to increase the yields. Switching from bidentate (*R,R*)-DIOP to monodentate PPh₃ led to a decrease in yield. Finally, increasing the catalyst loading from 5 mol% palladium to 10 mol% palladium provided an approximate 49% yield which is only a marginal improvement in comparison to 5 mol% (Figure 2.17).

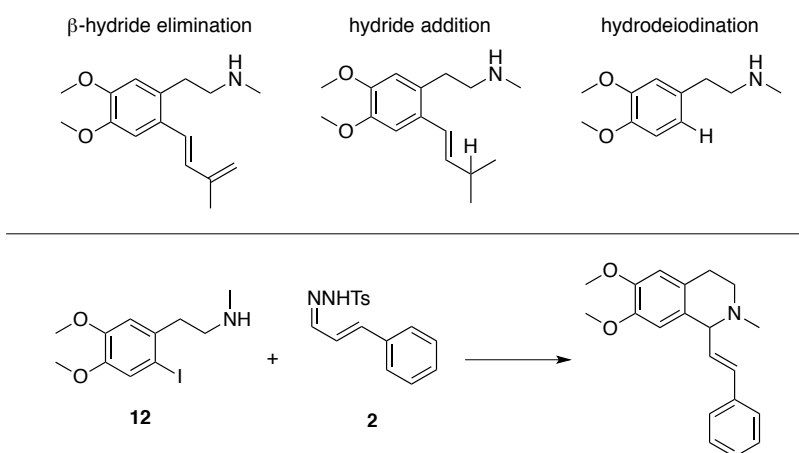
Figure 2.17 Synthesis of 7-*O*-Methyl-Dehydrolophocerine



Based on mass spectrometry and *R_f* data, several of the main side reactions are believed to stem from β-hydride elimination and hydridopalladium species (Figure 2.18). If the nucleophilic cyclization with the η³-allylpalladium intermediate is slow, β-hydride elimination

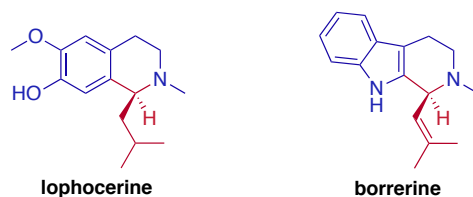
could occur leading to diene formation. Alternatively, if there is a proton source, the η^3 -allylpalladium intermediate could pick up a hydride and reductively eliminate leading to a hydride addition product. Having sources of palladium hydride in the reaction would also lead to hydrodeiodination of the starting materials. To eliminate the possibility for β -hydride elimination from the η^3 -allylpalladium intermediate and reduce the possible palladium hydride sources, cinnamyl hydrazone **2**, which contains no β -hydrogens, was used (Figure 2.18). The use of a hydrazone without β -hydrogens appeared to curb hydrodeiodination as there was still aryl iodide **12** present at the end of the reaction following consumption of two batches of hydrazone. Unfortunately, cinnamyl hydrazone **2** failed to effectively engage in the reaction generating a minimal amount of product.

Figure 2.18 Suspected Side Products and Attempted Circumvention



Having developed adequate insight and experience with 6-membered ring formation in this tetrahydroisoquinoline model system, which provides access to the skeleton of natural products such as lophocerine, we moved on to a more challenging application towards the synthesis of the natural product borrerine (Figure 2.19).

Figure 2.19 Alkaloids Accessible Through Intramolecular Carbenylative Cross-Coupling



2.3 Conclusion

In conclusion, we have demonstrated that *N*-tosylhydrazones derived from α,β -unsaturated aldehydes – precursors to vinylcarbenes – can be successfully employed in both intermolecular and intramolecular palladium-catalyzed carbenylative cross-coupling and carbenylative amination reactions with aryl iodides to form η^3 -allylpalladium intermediates that generate stereogenic centers at the carbene center. By intercepting known 1,3-diphenylallylpalladium intermediates through carbenylative insertion, we were able to produce ees that are comparable to palladium-catalyzed allylic alkylations. With an isoindoline model system we established that kinetic 5-membered ring formation is preferred over thermodynamic 7-membered ring formation and that under our reaction conditions the cyclization is not reversible. Evidence was given for chirality being set during migratory insertion and promising ees were achieved indicating that selection of the right chiral ligand and reaction conditions could lead to high ees. Furthermore, the scope of the reaction was expanded to include 6-member cyclization to generate tetrahydroisoquinolines, which map onto natural products. Though the 6-membered cyclizations proved much more challenging than intermolecular or 5-member cyclization we believe that the reaction could be sufficiently optimized through removal of hydride sources, speeding up the sluggish cyclization and tuning the rate of diazo formation. These results are an important proof of concept for asymmetric palladium-catalyzed carbenylative amination and carbenylative cross-coupling in both inter- and intramolecular

systems. The development of palladium-catalyzed carbenylative cross-coupling and carbenylative amination reactions with α,β -unsaturated *N*-tosylhydrazones and amine nucleophiles presented in this thesis set the stage for further palladium-catalyzed vinyl carbene insertion reactions.^{35,47,48,60}

2.4 Experimental

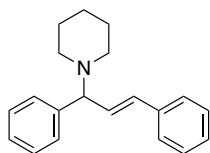
General. NMR spectral data were recorded using either a Bruker 500 or 600 MHz spectrometer. The NMR data are reported as follows: chemical shift in ppm from an internal tetramethylsilane standard on the δ scale, multiplicity (br = broad, app = apparent, s = singlet, d = doublet, t = triplet, q = quartet, and m = multiplet), coupling constants (Hz), and integration. If the tetramethylsilane signal could not be referenced the residual proton found in the NMR solvent was used (¹HNMR CDCl₃: δ 7.26 (CHCl₃), C₆D₆: δ 7.16 (C₆D₅H); ¹³CNMR CDCl₃: δ 77.16 (CHCl₃), C₆D₆: δ 128.06 (C₆D₅H)). Analytical thin layer chromatography was performed using EM Reagents 0.25 mm silica gel 60-F plates. When triethylamine was used as a co-eluent for thin layer chromatography, the plates were briefly pre-soaked in the eluent and allowed to dry for a few minutes before spotting with analyte. All reactions were carried out under an atmosphere of nitrogen in glassware that had been flame-dried under a stream of nitrogen or in glassware that had been flame-dried under vacuum. Unless otherwise noted, all reagents were commercially obtained and, where appropriate, purified prior to use. (*S*)-BINAP(S),⁶¹ **2**,⁶² **3**,⁶³ **9**,⁶⁴ and **11**⁶⁵ were synthesized according to reported literature procedures. (*S*)-BINAP(S),⁶⁶ **2**,⁶² **3**,⁶³ **9**,⁶⁷ and **11**⁶⁵ had spectroscopic data consistent with published values.

Determination of Enantiomeric Excess

Enantiomeric excess (%ee) was determined for compounds **1**, **6**, and **7** by ¹H NMR using a chiral shift reagent.^{52,68} To purified product (**1**, **6**, or **7**) 1.0 equiv of (*R*)-(+)-MTPA or (*S*)-(-)-MTPA

was added and the mixture was dissolved in C₆D₆. The resulting solution of diastereomeric salts were then analyzed by NMR spectroscopy. Spectra were acquired at elevated temperature (308 K when using the 500 MHz spectrometer and 318 K with the 600 MHz spectrometer) to improve resolution between diagnostic diastereomeric peaks. A diagnostic signal corresponding to the methine proton adjacent nitrogen was used for comparison of integrals. In order to increase the accuracy and reproducibility of integration, both diastereomeric protons were integrated as one integral and software peak deconvolution was used to determine the individual peak contributions. The ratio between the two peak areas was then used to calculate a %ee.

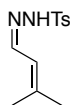
(*E*)-1-(1,3-Diphenylallyl)piperidine, 1.



A 5 mL round-bottom flask was charged with (*R,R*)-DIOP (3.8 mg, 0.0076 mmol, 7.6 mol%), Pd₂dba₃•CHCl₃ (2.6 mg, 0.0025 mmol, 2.5 mol%) and THF (0.2 mL). The mixture was stirred under nitrogen for approximately 20 minutes until a clear orange solution was obtained. A separate 5 mL round-bottom flask was charged with *N*-tosylhydrazone **2** (30.5 mg, 0.102 mmol, 100 mol%), iodobenzene (22.4 μL, 0.201 mmol, 197 mol%), *t*-BuOLi (17.9 mg, 0.224 mmol, 220 mol%), BTAC (22.4 mg, 0.0983 mmol, 96.4 mol%) and piperidine (29.6 μL, 0.300 mmol, 294 mol%). The catalyst solution was transferred by syringe into the flask containing **2**; an additional 0.8 mL of THF was used to ensure complete transfer. The reaction mixture was placed into an oil bath at 40 °C and monitored by TLC. After 5 h the reaction was diluted with 1% (w/v) NaOH_(aq) and extracted with EtOAc (3×), washed with brine, dried over MgSO₄ then concentrated *in vacuo* to obtain a yellow oil (34.9 mg). The crude material was further purified by flash column chromatography using hexanes/EtOAc/AcOH (70:27:3) followed by

hexanes/EtOAc (70:30) and finally hexanes/EtOAc/TEA (70:27:3) to obtain allylamine **1** as a yellow oil (16.0 mg, 0.0577 mmol, 57%). $R_f = 0.44$ (70:30 hexanes/EtOAc) $^1\text{H NMR}$ (600 MHz, C_6D_6) δ 7.50 (d, $J = 7.6$ Hz, 2H), 7.23 (t, $J = 7.5$ Hz, 2H), 7.18 (d, $J = 7.5$ Hz, 2H), 7.10 (t, $J = 7.3$ Hz, 1H), 7.07 (t, $J = 7.4$ Hz, 2H), 7.02 (appt, $J = 7.2$ Hz, 1H), 6.49 (d, $J = 15.8$ Hz, 1H), 6.40 (dd, $J = 15.8, 8.6$ Hz, 1H), 3.80 (d, $J = 8.5$ Hz, 1H), 2.48 (bs, 2H), 2.36 (bs, 2H), 1.52 (bs, 4H), 1.32 (bs, 2H); $^{13}\text{C NMR}$ (150 MHz, CDCl_3) δ 141.7, 137.1, 131.61, 131.53, 128.65, 128.63, 128.33, 127.56, 127.31, 126.5, 74.7, 52.6, 25.9, 24.6; MS (ESI) m/z calcd for $\text{C}_{20}\text{H}_{23}\text{NH}$ ($\text{M} + \text{H}$) $^+$ 278.2, found 277.7.

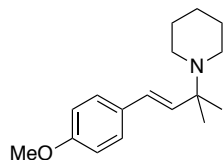
4-Methyl-*N'*-(3-methylbut-2-en-1-ylidene)benzenesulfonohydrazide, **4**.⁶²



A 100 mL round-bottom flask was charged with *p*-toluenesulfonyl hydrazide (15.4 g, 82.7 mmol, 100 mol%) and MeOH (40 mL). The heterogeneous mixture was stirred vigorously at 40 °C and 3-methyl-2-butenal (7.96 mL, 82.5 mmol, 100 mol%) was added by syringe. The reaction turned clear yellow upon addition. The flask was removed from the oil bath and placed in a -20 °C freezer. After 3 h, a white precipitate had formed. The precipitate was collected by vacuum filtration followed by washing with cold MeOH. The product was recrystallized from hot EtOH, filtered and washed with cold EtOH to obtain an off-white solid. The solid was dissolved in DCM and transferred to a tared recovery flask. Concentration *in vacuo* provided *N*-tosylhydrazone **4** (8.36 g, 33.1 mmol, 40%) of off-white solid. $R_f = 0.33$ (70:30 hexanes/EtOAc) $^1\text{H NMR}$ (600 MHz, CDCl_3) δ 7.82 (d, $J = 8.3$ Hz, 2H), 7.73 (bs, 1H), 7.70 (d, $J = 9.7$ Hz, 1H), 7.31 (d, $J = 8.0$ Hz, 2H), 5.92 (dm, $J = 9.7$ Hz, 1H), 2.42 (s, 3H), 1.83 (s, 3H), 1.79 (s, 3H); $^{13}\text{C NMR}$ (150 MHz, CDCl_3) δ 147.9, 146.1, 144.1, 135.4, 129.7, 127.9, 121.3, 26.5, 21.6, 18.8; IR (thin film) 3053, 2985, 2684, 2305, 1644 cm^{-1} ; HRMS (ESI) m/z calcd for $\text{C}_{12}\text{H}_{16}\text{N}_2\text{O}_2\text{SNa}$ ($\text{M} +$

Na)⁺ 275.0830, found 275.0833.

(E)-1-(4-(4-Methoxyphenyl)-2-methylbut-3-en-2-yl)piperidine, 5.



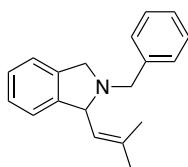
A 5 mL round bottom flask was charged with (*R,R*)-DIOP (7.4 mg, 0.015 mmol, 7.4 mol%), Pd₂dba₃•CHCl₃ (5.4 mg, 0.0052 mmol, 2.5 mol%) and THF (1.0 mL). The mixture was stirred under nitrogen for approximately 20 minutes until a clear orange solution was obtained. A separate 5 mL round-bottom flask was charged with *N*-tosylhydrazone **4** (50.2 mg, 0.199 mmol, 100 mol%), 4-iodoanisole (46.5 mg, 0.199 mmol, 100 mol%), *t*-BuOLi (34.8 mg, 0.435 mmol, 219 mol%), BTAC (4.8 mg, 0.021 mmol, 11 mol%) and piperidine (60 μL, 0.61 mmol, 310 mol%). The catalyst solution was transferred by syringe into the flask containing **4**; an additional 1.0 mL of THF was used to ensure complete transfer. The reaction mixture was placed into an oil bath at 40 °C and monitored by TLC. After 4 h the reaction was diluted with 1% (w/v) NaOH_(aq) and extracted with EtOAc (3×), washed with brine, dried over MgSO₄ then concentrated *in vacuo* to obtain a yellow oil (97.5 mg). The crude material was further purified by flash column chromatography using hexanes/EtOAc (70:30) followed by hexanes/EtOAc/TEA (67:30:3) to obtain allylamine **5** as a yellow oil (14.9 mg, 0.0574 mmol, 29%). *R*_f = 0.13 (94:5:1 hexanes/EtOAc/TEA) ¹H NMR (600 MHz, CDCl₃) δ 7.32 (d, *J* = 8.7 Hz, 2H), 6.84 (d, *J* = 8.7 Hz, 2H), 6.30 (d, *J* = 16.4 Hz, 1H), 6.17 (d, *J* = 16.3 Hz, 1H), 3.80 (s, 3H), 2.54 (bs, 4H), 1.58 (quintet, *J* = 5.4 Hz, 4H), 1.41 (bs, 2H) 1.22 (s, 6H); ¹³C NMR (125 MHz, CDCl₃) δ 159.0, 130.3, 127.4, 126.9, 114.1, 55.3, 47.5, 26.6, 24.8, 23.0; by HMQC it is apparent that one of the alkene carbons is in the baseline of the spectrum at approximately 136 ppm. The quaternary carbon alpha to nitrogen is believed to also be in the baseline around 59 ppm; IR (thin film)

2931, 1607, 1551, 1512, 1247 cm^{-1} ; HRMS (ESI) m/z calcd for $\text{C}_{17}\text{H}_{25}\text{NOH}$ ($\text{M} + \text{H}$)⁺ 260.2014, found 260.2007.

General procedure to form isoindoline through carbenylative cross-coupling

A round bottom flask containing a magnetic stir bar, $\text{Pd}_2(\text{dba})_3 \cdot \text{CHCl}_3$ (2.5 mol%), and bidentate ligand (7.5 mol%) was placed under nitrogen and charged with 200 μL THF. The mixture was stirred at 50 $^\circ\text{C}$ until a clear orange solution was obtained (approximately 5 min). A separate round bottom flask, containing a magnetic stir bar, was charged with aryl iodide **3** (0.165 mmol, 100 mol%), *N*-tosylhydrazone (0.330 mmol, 200 mol%), *t*-BuOLi (0.528 mmol, 320 mol%) and BTAC (0.0165 mmol, 10 mol%) under nitrogen. The catalyst solution was transferred by syringe into the flask containing aryl iodide; an additional 0.8 mL of THF was used to ensure complete transfer. The reaction mixture was placed into an oil bath at 50 $^\circ\text{C}$ and monitored by TLC. Once finished by TLC the reaction was passed through a plug of silica using EtOAc and concentrated *in vacuo*. Further purification by flash column chromatography using the designated solvent system afforded isoindole product.

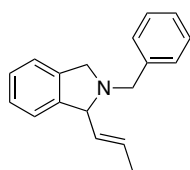
2-Benzyl-1-(2-methylprop-1-en-1-yl)isoindoline, **6**.



Isoindoline **6** was synthesized according to the general procedure for isoindoline formation using $\text{Pd}_2\text{dba}_3 \cdot \text{CHCl}_3$ (4.0 mg, 0.0039 mmol, 2.4 mol%), (*S,S*)-chiraphos (5.3 mg, 0.012 mmol, 7.8 mol%), **3** (51.5 mg, 0.159 mmol, 100 mol%) and *N*-tosylhydrazone **4** (81.4 mg, 0.323 mmol, 203 mol%). The product was purified by flash chromatography (95:5 hexanes/ethyl ether) to obtain isoindoline **6** as a yellow oil, approximately 95% pure by ^1H NMR (15.3 mg, 0.0581 mmol, 37%). $R_f = 0.82$ (70:30 hexanes/EtOAc) ^1H NMR (500 MHz, C_6D_6) δ 7.41 (d, $J = 7.6$ Hz, 2H),

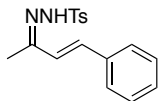
7.22 (t, $J = 7.5$ Hz, 2H), 7.15–7.06 (m, 4H), 6.93 (d, $J = 7.1$ Hz, 1H), 5.49 (d, $J = 8.9$ Hz, 1H), 4.51 (d, $J = 8.8$ Hz, 1H), 4.19 (d, $J = 13.1$, Hz 1H), 4.00 (d, $J = 12.6$ Hz, 1H), 3.37 (d, $J = 12.5$ Hz, 1H), 3.37 (d, $J = 13.2$ Hz, 1H), 1.68 (s, 3H) 1.65 (s, 3H); ^{13}C NMR (125 MHz, C_6D_6) δ 144.1, 140.5, 140.4, 135.6, 129.1, 128.5, 127.2, 127.1, 126.89, 126.88, 122.8, 122.5, 67.4, 58.0, 57.7, 26.0, 18.2; IR (thin film) 2388, 2279, 1618, 1453 cm^{-1} ; HRMS (ESI) m/z calcd for $\text{C}_{19}\text{H}_{21}\text{NH}$ ($\text{M} + \text{H}$) $^+$ 264.1752, found 264.1754.

(*E*)-2-Benzyl-1-(prop-1-en-1-yl)isoindoline, 7.



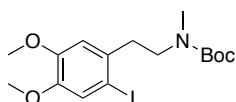
Isoindoline **7** was synthesized according to the general procedure for isoindoline formation using $\text{Pd}_2\text{dba}_3 \cdot \text{CHCl}_3$ (4.9 mg, 0.0047 mmol, 2.5 mol%), (*S,S*)-chiraphos (6.0 mg, 0.014 mmol, 7.4 mol%), **3** (61.1 mg, 0.189 mmol, 100 mol%) and *N*-tosylhydrazone **5** (92.0 mg, 0.386 mmol, 204 mol%). The product was purified by flash chromatography (97:3 hexanes/EtOAc) to obtain isoindoline **7** as a yellow oil, approximately 95% pure by ^1H NMR (11.5 mg, 0.0581 mmol, 24%). $R_f = 0.83$ (70:30 hexanes/EtOAc); ^1H NMR (500 MHz, C_6D_6) δ 7.40 (d, $J = 7.6$ Hz, 2H), 7.22 (t, $J = 7.5$ Hz, 2H), 7.13–7.05 (m, 4H), 6.92 (d, $J = 7.2$ Hz, 1H), 5.69–5.58 (m, 2H), 4.22 (d, $J = 13.2$ Hz, 1H), 4.15 (bs, 1H), 3.99 (d, $J = 12.7$ Hz, 1H), 3.38 (dd, $J = 12.9, 2.5$ Hz 1H), 3.34 (d, $J = 13.2$ Hz, 1H), 1.60 (d, $J = 4.8$ Hz, 3H); ^{13}C NMR (150 MHz, C_6D_6) δ 143.7, 140.4, 140.1, 132.8, 129.3, 129.0, 128.6, 128.3, 127.3, 127.1, 126.9, 123.0, 122.5, 72.5, 57.7, 57.6, 17.9; IR (thin film) 2293, 2253, 1636, 1443 cm^{-1} ; HRMS (ESI) m/z calcd for $\text{C}_{18}\text{H}_{19}\text{NH}$ ($\text{M} + \text{H}$) $^+$ 250.1596, found 250.1591.

4-Methyl-*N'*-((2*E*,3*E*)-4-phenylbut-3-en-2-ylidene)benzenesulfonylhydrazide, **8**.



A 100 mL round-bottom flask was charged with *p*-toluenesulfonyl hydrazide (2.55 g, 13.7 mmol, 100 mol%) and MeOH (20 mL). The mixture was stirred vigorously at 40 °C followed by addition of *trans*-4-phenyl-3-buten-2-one (2.00 g, 13.7 mmol, 100 mol%). The reaction turned clear yellow and solids slowly began to precipitate. After one hour an additional batch of *p*-toluenesulfonyl hydrazide (0.0558 g, 0.300 mmol, 2.2 mol%) was added and allowed to react for an additional hour. The reaction was filtered, rinsed with cold MeOH and dried *in vacuo* to obtain solid *N*-tosylhydrazone **8** (4.00 g, 12.7 mmol, 93%). $R_f = 0.13$ (70:30 hexanes/EtOAc); ^1H NMR (500 MHz, CDCl_3) δ 7.90 (d, $J = 8.2$ Hz, 2H), 7.84 (s, 1H), 7.43 (d, $J = 7.4$ Hz, 2H), 7.35–7.32 (m, 4H), 7.28 (d, $J = 7.1$ Hz, 1H), 6.83 (s, 2H), 2.42 (s, 3H), 1.99 (s, 3H) 1.62 (s, 1H); ^{13}C NMR (125 MHz, CDCl_3) δ 153.2, 144.2, 136.0, 135.3, 134.0, 129.7, 128.8, 128.7, 128.4, 128.0, 127.0, 21.6, 11.3; MS (ESI) m/z calcd for $\text{C}_{17}\text{H}_{18}\text{N}_2\text{O}_2\text{SH}$ ($\text{M} + \text{H}$) $^+$ 315.1, found 315.1.

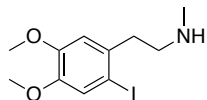
tert-Butyl (2-iodo-4,5-dimethoxyphenethyl)(methyl)carbamate, **S1**.



A 100 mL pear-shaped flask was charged with aryl iodide **11** (1.52 g, 3.73 mmol, 100 mol%), sodium hydride (60%) (304 mg, 7.60 mmol, 204 mol%) and THF (15 mL). While stirring, methyl iodide (0.70 mL, 11.2 mmol, 300 mol%) was added by syringe. After 9 hours the reaction was quenched by slow addition of H_2O , diluted with brine and extracted with Et_2O (3 \times). The organic layer was dried over MgSO_4 and concentrated *in vacuo* to give 1.66 g of yellow oil. Further purification by flash column chromatography using pentane/EtOAc (85:15) provided *N*-Boc-aryl iodide **S1** as a clear oil (1.51 g, 3.58 mmol, 96%) $R_f = 0.26$ (80:20 pentane/EtOAc)

Rotamers due to the *N*-Boc group were observed by NMR leading to broad peaks. ¹H NMR (600 MHz, 434 K, C₆D₆) δ 7.19 (s, 1H), 6.65 (bs, 1H), 3.44 (s, 3H), 3.39 (bs, 2H), 3.30 (s, 3H), 2.87 (bs, 2H), 2.71 (s, 3H), 1.44 (s, 9H); MS (ESI) *m/z* calcd for C₁₆H₂₄INO₄Na (M + Na)⁺ 444.1, found 443.8.

2-(2-Iodo-4,5-dimethoxyphenyl)-*N*-methylethan-1-amine, **12**.



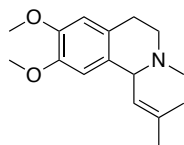
A 200 mL pear-shaped flask was charged with *N*-Boc-aryl iodide **S1** (1.49 g, 3.54 mmol) and DCM (5 mL). While stirring, TFA/DCM (50:50, 17.5 mL) was added by syringe. After 40 minutes the reaction was diluted with toluene and concentrated *in vacuo* (3×). 1 M NaOH_(aq) was added to the salt and the solution was extracted with EtOAc (2x). The combined organic layer was washed with brine, dried over anhydrous K₂CO₃ and concentrated *in vacuo* to provide 1.24 g of yellow oil. Flash column chromatography using toluene/MeOH/TEA (90:5:5) provided aryl iodide **12** as a yellow oil that solidified over several days (987.5 mg, 3.07 mmol, 87%). *R_f* = 0.20 (90:5:5 toluene/MeOH/TEA); ¹H NMR (600 MHz, C₆D₆) δ 7.17 (s, 1H), 6.59 (s, 1H), 3.32 (s, 3H), 3.19 (s, 3H), 2.84 (t, *J* = 7.2 Hz, 2H), 2.72 (t, *J* = 7.3 Hz, 2H), 2.26 (s, 3H) 0.65 (bs, 1H); ¹³C NMR (125 MHz, CDCl₃) δ 150.4, 149.2, 135.7, 122.6, 113.8, 88.6, 55.51, 55.49, 52.7, 41.1, 36.6.

General procedure for the carbenylative coupling to form 7-*O*-methyl-dehydrolophocerine, **13**

A round bottom flask containing a magnetic stir bar, Pd₂(dba)₃•CHCl₃ (0.005 mmol, 5 mol%), and bidentate ligand (0.015 mmol, 15 mol%) was placed under nitrogen and charged with 300 μL MeTHF. The mixture was stirred at 70 °C until a clear orange solution was obtained (approximately 5 min). A separate round bottom flask, containing a magnetic stir bar, was

charged with aryl iodide **12** (0.10 mmol, 100 mol%), *N*-tosylhydrazone (0.20 mmol, 200 mol%) and *t*-BuOLi (0.20 mmol, 200 mol%) under nitrogen. The catalyst solution was transferred by syringe into the flask containing aryl iodide; an additional 0.7 mL of THF was used to ensure complete transfer. The reaction mixture was placed into an oil bath at 70 °C and monitored by TLC. Once finished by TLC the reaction mixture was diluted with EtOAc and 1% (w/v) NaOH_(aq) followed by extraction with EtOAc (3×). The combined organic layer was sequentially washed with brine, dried over Na₂SO₄, filtered and concentrated *in vacuo*. Purification by flash column chromatography using hexane/EtOAc/TEA (70:25:5) affords an inseparable mixture of product and related substance impurity.

6,7-Dimethoxy-2-methyl-1-(2-methylprop-1-en-1-yl)-1,2,3,4-tetrahydroisoquinoline, (7-*O*-methyl-dehydrolophocerine) 13.



Following the general procedure, (*R,R*)-DIOP (7.5 mg, 0.015 mmol, 15 mol%), Pd₂dba₃•CHCl₃ (5.3 mg, 0.0051 mmol, 5 mol%), aryl iodide **12** (32.2 mg, 0.100 mmol, 100 mol%), *t*-BuOLi (16.2 mg, 0.202 mmol, 202 mol%) and *N*-tosylhydrazone **4** (50.7 mg, 0.201 mmol, 200 mol%) were monitored by TLC and at 8 hours an additional batch of *N*-tosylhydrazone **4** (25.7 mg, 0.102 mmol, 100 mol%) and *t*-BuOLi (8.4 mg, 0.105 mmol, 105 mol%) was added. After an additional 2 hours, work-up and purification by flash chromatography resulted in 7-*O*-methyl-dehydrolophocerine **13** as an oil (15.9 mg, 0.0487 mmol, 49%, yield based on the sample being approximately 80% pure by NMR). *R*_f = 0.15 (80:20:3 hexanes/EtOAc/TEA); ¹H NMR (600 MHz, CDCl₃) δ 6.57 (s, 1H), 6.49 (s, 1H), 5.15 (d, *J* = 9.7 Hz, 1H), 3.93 (d, *J* = 9.6 Hz, 1H), 3.84 (s, 3H), 3.79 (s, 3H), 3.07–2.99 (m, 2H), 2.68–2.64 (m, 1H), 2.54–2.50 (m, 1H), 2.38 (s, 3H),

1.85 (s, 3H) 1.83 (s, 3H); ^{13}C NMR (150 MHz, CDCl_3) δ 147.5, 147.1, 134.8, 129.7, 127.1, 126.4, 111.2, 110.6, 63.1, 55.92, 55.86, 52.1, 44.0, 29.0, 25.9, 18.4; MS (ESI) m/z calcd for $\text{C}_{16}\text{H}_{23}\text{NO}_2\text{H} (\text{M} + \text{H})^+$ 262.2, found 262.2.

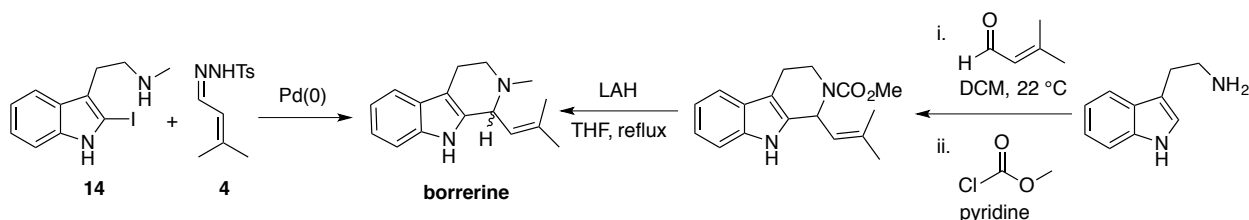
Chapter 3

Palladium-Catalyzed Carbenylative Cross-Coupling and Carbenylative Amination with Vinylcarbenes: Synthesis of *N*-Boc-Borrerine

3.1 Introduction

After gaining experience with palladium-catalyzed carbenylative cross-coupling in several model systems, we set out to apply vinylcarbene insertion directly to a target of interest. Borrerine seemed like a logical target, potentially allowing for an asymmetric alternative to the Pictet-Spengler reaction (Figure 3.1).⁶⁹ However, the need to employ a potentially sensitive 2-iodoindole introduced additional risks. Formation of the desired 2-iodo-*N*-methyltryptamine proved exceedingly problematic and only a few of the attempted routes are discussed below. *N*-Protected 2-iodotryptamines are common in synthesis but unprotected 2-iodotryptamines are rare.

Figure 3.1 Carbenylative Cross-Coupling to Form Borrerine in Comparison to Pictet-Spengler



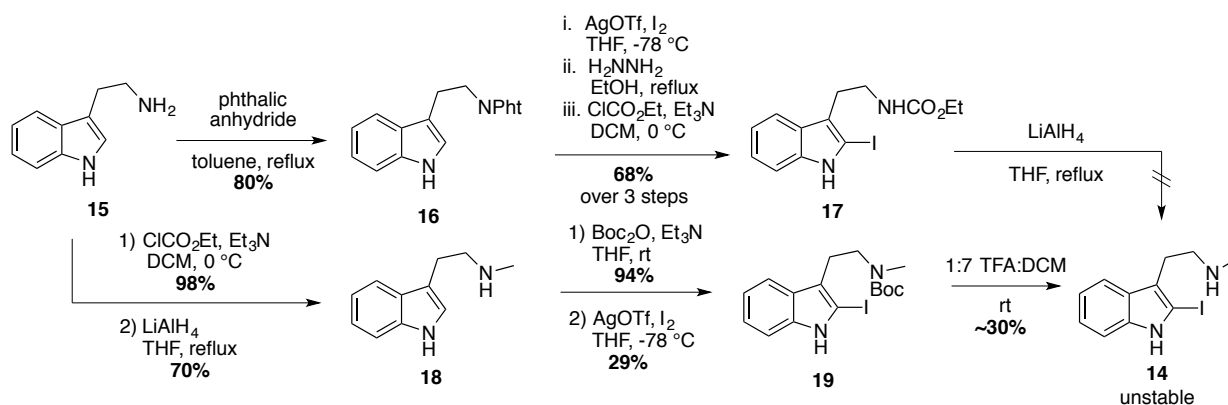
3.2 Results and Discussion

3.2.1 Initial Attempt to Synthesize 2-Iodo-*N*-methyltryptamine

One attempt to synthesize 2-iodo-*N*-methyltryptamine **14** started with the protection of tryptamine **15** as the phthalimide followed by iodination with silver triflate and molecular iodine, the resulting 2-iodotryptamine was deprotected with hydrazine and acylated with ethyl chloroformate to give **17** in 68% yield over 3 steps (Figure 3.2). During the iodination step it was found to be crucial to add sub-stoichiometric amounts of iodine and silver triflate in order to

prevent over-iodination, this is especially important as the mono- and diiodinated products were found to be inseparable by flash chromatography. Attempts to reduce carbamate **17** to the desired *N*-methylamine **14** using LiAlH₄ led to complete deiodination. Tosyl protection of the indole nitrogen of **17** before LiAlH₄ reduction also led only to deiodinated material. From this it was apparent that methylation needed to be carried out before iodination. A route to **14** that was successful started with the two-step synthesis of *N*-methyltryptamine **18** in a 70% yield. Boc protection of **18** followed by iodination with silver triflate and molecular iodine provided iodoindole **19** in moderate yield due to partial Boc deprotection by the triflic acid by-product. Deprotection of the Boc group on **19** was accompanied by partial proto-deiodination indicating that the product is acid sensitive. Once purified, the unprotected 2-iodo-*N*-methyltryptamine **14** is unstable; decomposition occurs *in vacuo* even when protected from light. The unprotected 2-iodo-*N*-methyltryptamine **14** was too sensitive for use as a substrate in our palladium-catalyzed carbenylation reaction.

Figure 3.2 Synthetic Routes to Sensitive 2-Iodo-*N*-methyltryptamine

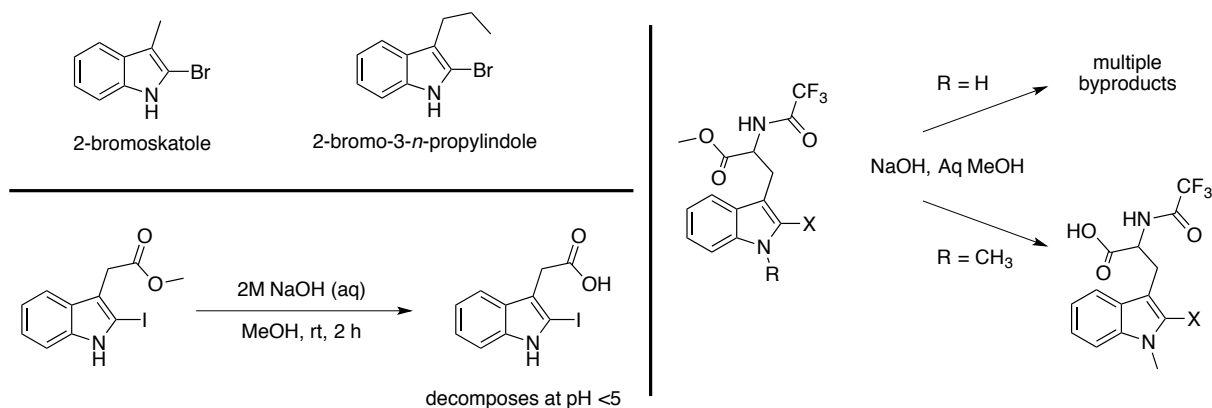


3.2.2 Haloidole Sensitivity

Numerous examples of 2-haloidoles can be found in the literature that discuss the sensitivity and the difficulties encountered during their synthesis. Simple bromoidoles are

reported to be unstable and undergo gradual decomposition on standing which is accelerated by light or acid.⁷⁰ Of note, 2-bromoskatole (Figure 3.3) could only be crystallized without decomposition after sublimation and needed to be stored in the dark, under nitrogen at -20 °C. The related 2-bromo-3-*n*-propylindole (Figure 3.3) could not be purified and attempts to distill led to decomposition. Unsworth and co-workers noted that for the workup of 2-iodoindole-3-acetic acid (Figure 3.3) careful control of pH (>5) was needed to prevent acid catalyzed decomposition.⁷¹ In addition to 2-haloindoles being acid sensitive, they are also sensitive to base decomposition. Cohen and co-workers demonstrated that the ability to deprotonate the indole hydrogen of a 2-haloindole greatly increased its susceptibility to base decomposition (Figure 3.3).⁷² By replacing the indole *N*-H with a *N*-methyl group they were able to successfully carry out a basic ester hydrolysis on 2-haloindole substrates.

Figure 3.3 Sensitivities of 2-Haloindoles



3.2.3 Route to Stable Boc-Protected 2-Iodo-*N*-methyltryptamine

Recognizing the sensitivity of 2-iodo-*N*-methyltryptamines, a route was formulated to synthesize the Boc-protected indole substrate **22** (Figure 3.4). Although the use of a Boc-indole protected substrate was less than ideal due to increase in sterics so close to the site of palladium reactivity, it was deemed a necessary risk in order to probe the application of carbenylation to

borrerine. Stewart and co-workers had previously carried out a palladium-catalyzed domino Heck-aza-Michael reaction on a Boc-protected 2-bromo-*N*-tosyltryptamine in high yields (Figure 3.5),⁷³ which is very similar to our target substrate **22** and indicates that a bulky ortho Boc group does not preclude oxidative addition or migratory insertion. Starting from *N*-methyltryptamine **18**, NsCl protection followed by iodination led to **20** in 85% yield. Subsequent protection of the indole nitrogen with Boc anhydride led to **21** in a 99% yield. *N*-Nosyl deprotection of **21** with thiophenol and cesium carbonate led to secondary amine **22** with highly variable yields between 5-40% due to formation of two major byproducts, the oxindole **23** and the protodeiodinated indole **24** (Figure 3.4). These byproducts might be due to the bicarbonate and/or hydroxide arising from the base but alternatives to cesium carbonate were not effective. In an attempt to eliminate both possible sources of byproducts, the reaction was performed by pre-forming the thiolate anion with sodium hydride prior to addition of indole **21**. This combination seemed to generate one product as indicated by thin layer chromatography, but the workup ultimately generated a mixture similar to that obtained with cesium carbonate and thiophenol. Numerous workup conditions were tested however none provided a greater yield of the iodindole **22**.

Figure 3.4 Synthetic Route to Stable Substrate for Borrerine

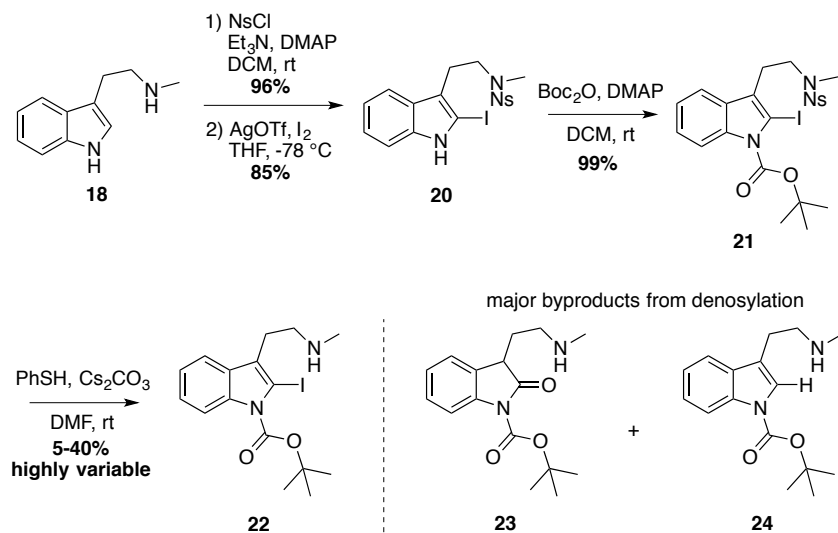
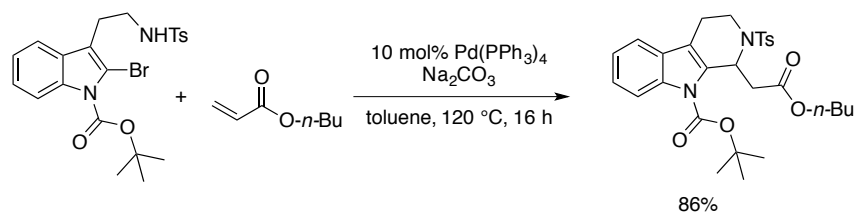


Figure 3.5 Example of Palladium Chemistry Next to a Sterically Demanding Boc Group

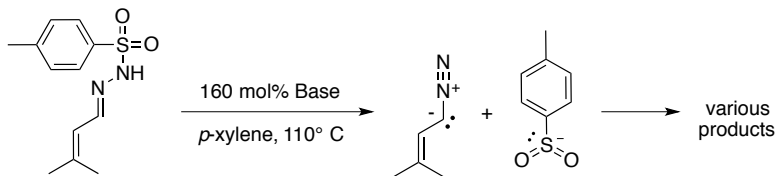


3.2.4 Synthesis of *N*-Boc-Borrerine Through Carbenylative Cross-Coupling

Although the yield for **22** was low, enough material was obtained to perform palladium-catalyzed carbenylative cyclizations (Figure 3.1). Initially the reaction was executed under conditions similar to those optimized for the 5-member ring: 50 °C, MeTHF (instead of THF), 100 mol% BTAC (instead of 10 mol%) (Table 2.2). Under these conditions no significant reaction was seen after four hours at 50 °C. The temperature was increased to 60 °C for another four hours and under these conditions the reaction was not consuming hindered aryl iodide **22** even though hydrazone **4** was being depleted. There are several reasons that the aryl iodide is failing to engage the reaction, sluggish oxidative addition and attack of the palladium by diazo compound, slow 6-membered cyclization and large steric demands due to two ortho groups, one of which is a very bulky Boc group. In an attempt to overcome these barriers the temperature was increased to reflux, 80 °C, and the reaction was complete within 30 min, consuming both of the starting materials. Unfortunately, this led to primarily unproductive pathways that led to only a small amount (<5%) of the desired product, *N*-Boc-borrerine **25** as seen by NMR. We attempted to decrease the amount of BTAC (BnNEt_3Cl) to 10 mol% and the temperature to 70 °C in an effort to slow the hydrazone decomposition rate significantly and shut down unproductive diazo side reactions. Slowing down the rate of hydrazone decomposition provided a 13% yield of *N*-Boc-borrerine **25**.

The rate of *N*-tosylhydrazone decomposition via the Bamford-Stevens reaction can be

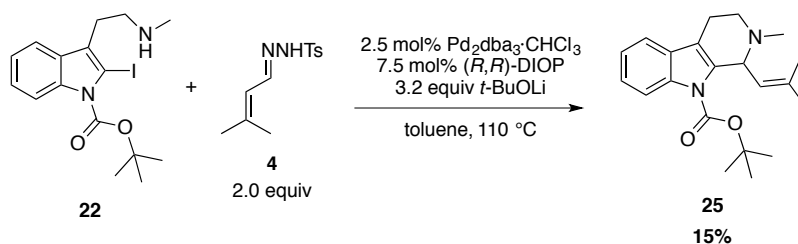
modified in a variety of ways: changing the concentration of phase transfer catalyst BTAC, altering temperature, using bases with differing solubility or strength and through solvent selection based on polarity. An independent study was carried out to determine the effect of base on *N*-tosylhydrazone decomposition (Table 3.1) in the hopes of being able to fine-tune the rate of diazo formation in our reaction. Using *p*-xylene at 110 °C for this experiment, the *t*-BuOLi, which was slightly soluble, reacted the fastest showing *N*-tosylhydrazone consumption within 15 minutes (Table 3.1, entry 2) potentially due to lithium coordination to the tosyl group stabilizing its ionization. *t*-BuOK which was also slightly soluble was moderately slower (1-2 hours, Table 3.1 entry 3) than the lithium counterpart, possibly due to weaker coordination of the tosyl group. Interestingly, the *t*-BuOK reaction generated a different distribution of byproducts, the majority of which were more polar than the byproducts seen with the other bases. Carbonate bases were all insoluble and a reverse in reaction rates compared to *t*-butoxide was seen with potassium carbonate reacting much faster compared to lithium carbonate (Table 3.1, entries 4 and 7). The reversal in activity can be attributed to solubility, due to not having a solubilizing organic functionality the lithium remains tightly bound to the insoluble carbonate whereas the potassium and cesium ions are more naked allowing for more facile deprotonation. Using a soluble non-nucleophilic amine base, DBU, kept the entire reaction in solution and was equivalent to sodium carbonate (Table 3.1, entries 6 and 8).

Table 3.1 Base Effects on Bamford-Stevens *N*-Tosylhydrazone Decomposition

Entry	Base	Solubility of Hydrazone Species	Time Until >90% Consumption
1	None	N/A	>24 h
2	<i>t</i> -BuOLi	Slightly Soluble	10-15 min
3	<i>t</i> -BuOK ^a	Slightly Soluble	1-2 h
4	K ₂ CO ₃	Insoluble	1 h
5	Cs ₂ CO ₃	Insoluble	1 h
6	Na ₂ CO ₃	Insoluble	>6 h
7	Li ₂ CO ₃	Insoluble	>>6 h
8	Hünig's Base ^b	Soluble	>6 h

Notes^a KO^t-Bu had a noticeable different set of byproducts (more polar) than the rest^b Hünig's Base kept the entire solution soluble during the reaction

Using what was learned from base effects on *N*-tosylhydrazone decomposition we set out to further optimize the reaction by adjusting the solvent, temperature, BTAC and base. Ultimately we were able to obtain a modest 15% yield of *N*-Boc-borrerine **25** by switching the solvent to toluene, increasing the temperature to 110 °C, removing BTAC and keeping *t*-BuOLi as the base. By adjusting the solvent and temperature, omitting BTAC and utilizing what we learned from base effects on *N*-tosylhydrazone decomposition we were only able to obtain a 15% yield of *N*-Boc-borrerine **25** (Figure 3.6).

Figure 3.6 Synthesis of *N*-Boc-Borrerine

Application of these conditions to the less encumbered aryl iodide **12** generated the six-

membered 7-*O*-methyl-dehydrolophocerine **13** in over twice the yield (36%, Figure 3.7) that we obtained from the 2-iodo-*N*-Boc-indole **22** (*vide supra*). Although the sterically encumbering *N*-Boc group ortho to the halide did little to inhibit Heck chemistry in a similar system (*vide supra*) can inhibit the diazo attack on the arylpalladium(II) intermediate, and raise the energy barrier for both migratory insertion and nucleophilic cyclization due to the sterically hindered environment. The low yields due to an ortho substituent has even been observed by Liang and co-workers with a much less encumbering methyl substituent resulting in a similar drop in yield from 84% to 44% (Figure 3.8).³⁵

Figure 3.7 Reaction Conditions with a Less Sterically Hindered Substrate

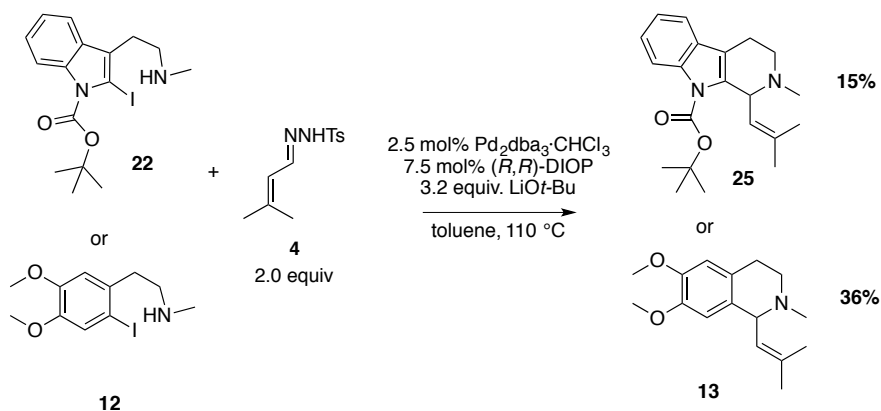
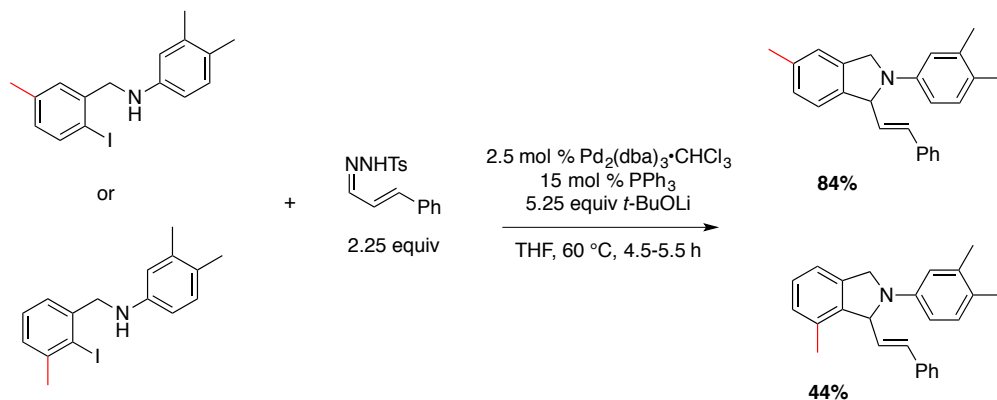


Figure 3.8 Ortho Substituents Have Been Shown to Dramatically Effect the Yield in Carbenylative Cross-Coupling Reactions



3.3 Conclusion

This work demonstrated that vinylcarbene insertion reactions can be used to assemble the heterocyclic rings of alkaloid natural products. It is clear that palladium-catalyzed carbenylative insertion is not superior to Pictet-Spengler approaches to bornerine. This work revealed the complex interplay between rates of diazo generation and the rates of reactions and side reactions in the catalytic cycle. The dramatic effects of ortho substitution on reactivity and methods for controlling of rates of diazo compound formation and decomposition will be invaluable to future method development in palladium-catalyzed carbenylative cross-coupling.

3.4 Experimental

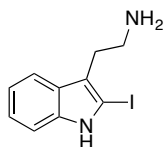
General. NMR spectral data were recorded using either a Bruker 500 or 600 MHz spectrometer. The NMR data are reported as follows: chemical shift in ppm from an internal tetramethylsilane standard on the δ scale, multiplicity (br = broad, app = apparent, s = singlet, d = doublet, t = triplet, q = quartet, and m = multiplet), coupling constants (Hz), and integration. If the tetramethylsilane signal could not be referenced the residual proton found in the NMR solvent was used (^1H NMR CDCl_3 : δ 7.26 (CHCl_3), C_6D_6 : δ 7.16 ($\text{C}_6\text{D}_5\text{H}$); ^{13}C NMR CDCl_3 : δ 77.16 (CHCl_3), C_6D_6 : δ 128.06 ($\text{C}_6\text{D}_5\text{H}$)). Analytical thin layer chromatography was performed using EM Reagents 0.25 mm silica gel 60-F plates. When triethylamine (TEA) was used as a co-eluent for thin layer chromatography, the plates were briefly pre-soaked in the eluent and allowed to dry for a few minutes before spotting with analyte. All reactions were carried out under an atmosphere of nitrogen in glassware that had been flame-dried under a stream of nitrogen or in glassware that had been flame-dried under vacuum. Unless otherwise noted, all reagents were commercially obtained and, where appropriate, purified prior to use. **16**,⁷⁴ **18**,⁷⁵ 2-(2-(2-iodo-1*H*-indol-3-yl)ethyl)isoindoline-1,3-dione (**S2**),⁷⁶ and *tert*-butyl (2-(1*H*-indol-3-

yl)ethyl)(methyl)carbamate (**S5**),⁷⁷ were synthesized according to reported literature procedures. **16**,⁷⁴ **18**,⁷⁵ **S2**⁷⁶ and **S5**⁷⁷ had spectroscopic data consistent with published values.

General procedure for the iodination of indoles

A round bottom flask containing a magnetic stir bar, protected indole (100 mol%), iodine (90 – 95 mol%) and THF (0.1 mM) was stirred vigorously at -78 °C while AgOTf (90 - 95 mol%) was added. The reaction turned from deep purple to opaque yellow. The reaction was monitored by TLC, and after completion solid NaHCO₃ (200 mol%) was added and the dry ice bath was removed. EtOAc and a 1:1 solution of Na₂S₂O₃(sat. aq):NaHCO₃(sat. aq) were added. The crude reaction mixture was filtered through a plug of Celite and washed through with EtOAc. The filtrate was extracted with EtOAc (3×), washed with brine, dried over Na₂SO₄ and then concentrated *in vacuo*. Purification by flash column chromatography in suitable eluent produces 2-iodoindole product.

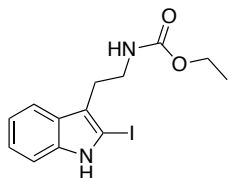
2-(2-Iodo-1*H*-indol-3-yl)ethan-1-amine (2-iodotryptamine), **S3**.



Starting from a known phthalamide protected 2-iodotryptamine **S2**, a 200 mL pear-shaped flask with condenser was charged with **S2** (1.10 g, 2.64 mmol, 100 mol%) and EtOH (40 mL). The mixture was brought to reflux while stirring and hydrazine hydrate (50%, 0.987 mL, 15.8 mmol, 600 mol%) was added in one portion. After 1 hour a white precipitate formed which was filtered and washed with CHCl₃. The filtrate was acidified with 1 mL concentrated HCl, diluted with 100 mL H₂O and extracted with CHCl₃. The aqueous layer was neutralized with solid K₂CO₃, extracted with CHCl₃ (3×), dried over MgSO₄ and concentrated *in vacuo* to obtain 2-iodotryptamine **S3** as a viscous oil (0.63 g, 2.2 mmol, 83%) in sufficient purity to use in further

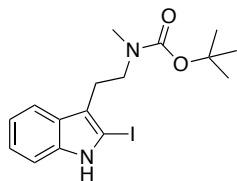
steps. The compound decomposed over several weeks to dark brown oil. ^1H NMR (600 MHz, CDCl_3) δ 9.79 (br s, 1H), 7.50 (d, $J = 7.7$ Hz, 1H), 7.22 (d, $J = 7.9$ Hz, 1H), 7.08 (t, $J = 8.1$ Hz, 1H), 7.04 (t, $J = 7.5$ Hz, 1H) 3.03 (t, $J = 6.7$ Hz, 2H), 2.87 (t, $J = 6.7$ Hz, 2H), 1.53 (br s, 2H); ^{13}C NMR (151 MHz, CDCl_3) δ 139.1, 127.6, 122.1, 119.6, 118.8, 117.9, 110.7, 79.3, 42.3, 31.0.

Ethyl (2-(2-iodo-1*H*-indol-3-yl)ethyl)carbamate, 17.



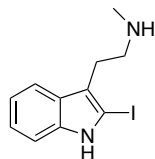
A 50 mL pear-shaped flask was charged with 2-iodotryptamine **S3** (0.55 g, 1.92 mmol, 100 mol%), TEA (0.27 mL, 1.9 mmol, 100 mol%) and DCM (10 mL). The reaction was cooled to 0 °C in an ice bath followed by dropwise addition of ethyl chloroformate (0.18 mL, 1.9 mmol, 100 mol%) while stirring. The reaction was allowed to warm to room temperature. The reaction was washed sequentially with H_2O , 1 M HCl, 5% NaHCO_3 , H_2O and brine. The organic layer was dried over Na_2SO_4 , filtered and concentrated *in vacuo* providing 0.67 g of crude material. Further purification by flash column chromatography using toluene/TEA (99:1) provided 2-iodotryptamine **17** (468.9 mg, 1.31 mmol, 68%). $R_f = 0.35$ (70:30 hexane/EtOAc) A second set of broadened peaks due to a hydrogen bonding species was observed in ^1H NMR. ^1H NMR (600 MHz, C_6D_6) δ 7.71 (br s, 1H), 7.51 (d, $J = 7.6$ Hz, 1H), 7.11 – 7.04 (m, 3H), 4.26 (br s, 1H), 4.05 (q, $J = 7.1$ Hz, 2H), 3.29 (q, $J = 6.6$ Hz, 2H), 2.80 (t, $J = 6.8$ Hz, 2H), 1.65 (s, 1H), 1.02 (t, $J = 7.1$ Hz, 3H); ^{13}C NMR (126 MHz, C_6D_6) δ 156.8, 139.3, 128.0, 122.4, 120.0, 119.0, 118.3, 111.1, 79.0, 60.7, 41.4, 27.5, 14.9.

***tert*-Butyl (2-(2-iodo-1*H*-indol-3-yl)ethyl)(methyl)carbamate, 19.**



Following the general procedure, *N*-Boc-*N*-methyltryptamine **S5** (1.46 g, 5.32 mmol, 100 mol%), iodine (1.23 g, 4.79 mmol, 90 mol%), AgOTf (1.23 g, 4.79 mmol, 90 mol%) NaHCO₃ (0.93 g, 10.6 mmol, 200 mol%) and purification by flash chromatography (90:10 hexanes/ethyl acetate) produced 2-iodotryptamine **19** as a yellow solid (0.56 g, 1.40 mmol, 29%). $R_f = 0.54$ (70:30 hexanes/EtOAc); ¹H NMR (600 MHz, CDCl₃) δ 8.35 (br s, 1H), 7.52 (br s, 1H), 7.27 (d, $J = 7.9$ Hz, 1H), 7.10 (t, $J = 7.6$ Hz, 1H), 7.05 (t, $J = 7.3$ Hz, 1H), 3.44 (t, $J = 7.1$ Hz, 2H), 2.91 (t, $J = 6.5$ Hz, 2H), 2.88 (br s, 3H), 1.41 (br s, 9H); ¹³C NMR (151 MHz, CDCl₃) δ 155.8, 139.2, 127.8, 122.4, 120.0, 119.6, 117.9, 110.6, 79.4, 78.2, 49.3, 34.9, 28.7, 25.9.

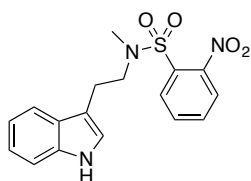
2-(2-Iodo-1*H*-indol-3-yl)-*N*-methylethan-1-amine, 14.



A 20 mL pear-shaped flask was charged with **19** (75.5 mg, 0.189 mmol, 100 mol%) and DCM (2.8 mL). While stirring, TFA (0.45 mL, 5.88 mmol, 3100 mol%) was added dropwise by syringe. After 45 minutes the reaction was neutralized with saturated NaHCO_{3(aq)} and the solution was extracted with EtOAc (3 \times). The organic layer was dried over Na₂SO₄ and concentrated *in vacuo* to provide 90.2 mg of crude material. Flash column chromatography using EtOAc/TEA (99:1) provided unstable **14** (32.7 mg, 0.109 mmol, 58%, contaminated by decomposition and grease) which turned from brown to blue-green overnight while under vacuum. Noticeable grease contamination was observed by NMR and was later attributed to the

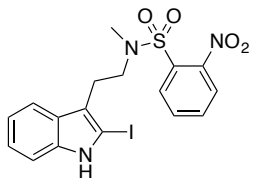
EtOAc used for purification. Decomposition of **14** occurred before repurification could be attempted after attributing the source of contamination and rectifying it. $R_f = 0.16$ (94:5:1 EtOAc/MeOH/TEA) $^1\text{H NMR}$ (600 MHz, CDCl_3) δ 9.17 (br s, 1H), 7.55 (d, $J = 7.7$, 1H), 7.26 (d, $J = 8.2$ Hz, 1H), 7.10 (t, $J = 7.4$ Hz, 1H), 7.06 (t, $J = 7.4$ Hz, 1H), 2.96 – 2.91 (m, 4H), 2.48 (s, 3H); $^{13}\text{C NMR}$ (151 MHz, CDCl_3) δ 139.2, 127.6, 122.2, 119.8, 119.3, 118.0, 110.6, 78.9, 51.8, 36.3, 27.0.

***N*-(2-(1*H*-Indol-3-yl)ethyl)-*N*-methyl-2-nitrobenzenesulfonamide, S4.**



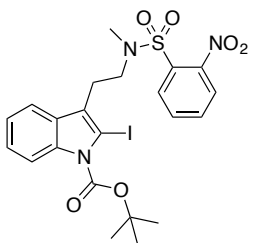
A 50 mL round-bottom flask was charged with *N*-methyltryptamine **18** (1.08 g, 6.18 mmol, 100 mol%), DMAP (76.8 mg, 0.629 mmol, 10.0 mol%), TEA (1.29 mL, 9.27 mmol, 150 mol%) and DCM (22 mL). The reaction was cooled to 0 °C in an ice bath. 2-NsCl (1.52 g, 6.86 mmol, 111 mol%) was added and the reaction vessel was allowed to warm to room temperature. After 30 minutes the reaction mixture was washed sequentially with H_2O , 1 M HCl, 5% (w/v) $\text{NaHCO}_{3(\text{aq})}$, H_2O and brine. The organic layer was dried over Na_2SO_4 and concentrated *in vacuo* to produce *N*-nosyltryptamine **S4** as a yellow oil (2.11 g, 5.87 mmol, 95%) of sufficient purity to use in further steps. $R_f = 0.40$ (50:50 hexane/EtOAc). $^1\text{H NMR}$ (500 MHz, CDCl_3) δ 8.03 (br s, 1H), 7.87 (dd, $J = 7.6, 1.2$ Hz, 1H), 7.62 – 7.518 (m, 4H), 7.32 (d, $J = 8.1$ Hz, 1H), 7.18 (t, $J = 7.6$ Hz, 1H) 7.11 (t, $J = 7.5$ Hz, 1H), 7.04 (d, $J = 2.1$ Hz, 1H), 3.55 (t, $J = 7.7$ Hz, 2H), 3.07 (t, $J = 7.6$ Hz, 2H), 2.97 (s, 3H), 1.45 (br s, 9H); $^{13}\text{C NMR}$ (151 MHz, C_6D_6) δ 148.0, 136.2, 133.3, 132.5, 131.5, 130.6, 127.1, 124.0, 122.3, 122.1, 119.5, 118.5, 111.9, 111.3, 50.6, 34.8, 24.3; HRMS (ESI) m/z calcd for $\text{C}_{17}\text{H}_{17}\text{O}_4\text{N}_3\text{SNa}$ ($\text{M} + \text{Na}$) $^+$ 382.0837, found 382.0836.

***N*-(2-(2-Iodo-1*H*-indol-3-yl)ethyl)-*N*-methyl-2-nitrobenzenesulfonamide, **20**.**



Following the general procedure, **S4** (4.16 g, 11.6 mmol, 100 mol%), iodine (2.796 g, 11.0 mmol, 95 mol%), AgOTf (2.84 g, 11.0 mmol, 95 mol%), NaHCO₃ (1.91 g, 22.7 mmol, 196 mol%) and purification by flash chromatography (80:20 hexanes/ethyl acetate) resulted in 2-iodotryptamine **20** as a yellow oil (4.76 g, 9.81 mmol 85%). $R_f = 0.53$ (50:50 hexanes/EtOAc); ¹H NMR (600 MHz, C₆D₆) δ 7.55 (d, $J = 7.9$ Hz, 1H), 7.51 (d, $J = 7.6$ Hz, 1H), 7.47 (s, 1H), 7.09–7.03 (m, 3H), 6.81 (d, $J = 7.9$ Hz, 1H), 6.75 (t, $J = 7.7$ Hz, 1H), 6.69 (t, $J = 7.6$ Hz, 1H), 3.28 (t, $J = 7.7$ Hz, 2H), 2.85 (t, $J = 7.7$ Hz, 2H), 2.69 (s, 3H); ¹³C NMR (151 MHz, C₆D₆) δ 148.4, 139.3, 133.1, 132.8, 131.2, 130.5, 127.7, 123.9, 122.6, 120.3, 118.2, 118.1, 111.1, 78.9, 50.2, 34.9, 26.4; HRMS (ESI) m/z calcd for C₁₇H₁₆O₄SIN₃Na (M + Na)⁺ 507.9804, found 507.9802.

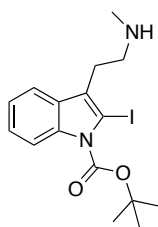
***tert*-Butyl 2-iodo-3-(2-((*N*-methyl-2-nitrophenyl)sulfonamido)ethyl)-1*H*-indole-1-carboxylate, **21**.**



A 25 mL pear-shaped flask was charged with **20** (436 mg, 0.898 mmol, 100 mol%), DMAP (19.8 mg, 0.162 mmol, 18.0 mol%), Boc₂O (215.6 mg, 0.988 mmol, 110 mol%) and DCM (5 mL). After mixing for 1 hour the reaction mixture was concentrated *in vacuo*. Flash column chromatography using hexane/EtOAc (70:30) provided Boc-indole **21** as a yellow oil (520 mg,

0.888 mmol, 99%,). $R_f = 0.26$ (70:30 hexane/EtOAc); $^1\text{H NMR}$ (600 MHz, C_6D_6) δ 8.20 (d, $J = 8.3$ Hz, 1H), 7.61 (d, $J = 7.6$ Hz, 1H), 7.46 (d, $J = 7.3$ Hz, 1H), 7.13 – 7.08 (m, 2H), 6.92 (d, $J = 7.8$ Hz, 1H) 6.89 (t, $J = 7.7$ Hz, 1H), 6.83 (t, $J = 7.7$ Hz, 1H), 3.27 (t, $J = 7.8$ Hz, 2H), 2.87 (t, $J = 7.8$ Hz, 2H), 2.76 (s, 3H), 1.45 (br s, 9H); $^{13}\text{C NMR}$ (151 MHz, C_6D_6) δ 149.2, 148.4, 138.6, 133.3, 132.8, 131.3, 130.5, 129.8, 126.1, 124.8, 124.0, 123.3, 118.5, 116.0, 84.9, 79.7, 49.3, 35.1, 28.1, 27.4; HRMS (ESI) m/z calcd for $\text{C}_{22}\text{H}_{24}\text{O}_6\text{N}_3\text{SINa}$ ($\text{M} + \text{Na}$) $^+$ 608.0328, found 608.0323.

***tert*-Butyl 2-iodo-3-(2-(methylamino)ethyl)-1*H*-indole-1-carboxylate, **22**.**



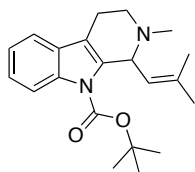
A 500 mL round-bottom flask was charged with **21** (4.56 g, 7.79 mmol, 100 mol%), Cs_2CO_3 (7.63 g, 23.4 mmol, 300 mol%) and DMF (130 mL). The reaction mixture became opaque and slowly turned light pink in color. PhSH (0.957 mL, 9.35 mmol, 120 mol%) was added dropwise to the reaction, which changed the color of the reaction from light pink to orange. The reaction was monitored by TLC and after 3 hours additional PhSH (0.500 mL, 4.89 mmol, 63 mol%) was added dropwise and allowed to react for an additional 30 minutes. Upon completion, the reaction was diluted with Et_2O (480 mL) followed by addition of 10% (w/v) $\text{K}_2\text{CO}_{3(\text{aq})}$ (240 mL). The aqueous layer was extracted with Et_2O (2 \times 200 mL) and the combined organic layers were washed with H_2O (2 \times 300 mL), brine (300 mL), dried over anhydrous K_2CO_3 and concentrated *in vacuo* to provide 4.12 g of crude material. Flash column chromatography using EtOAc/TEA (95:5) provided *N*-methyltryptamine **22** as an orange solid (493 mg, 1.23 mmol, 16%). $R_f = 0.31$ (95:5 EtOAc/TEA) $^1\text{H NMR}$ (500 MHz, C_6D_6) δ 8.37 (d, $J = 8.4$ Hz, 1H), 7.43 (d, $J = 7.8$ Hz, 1H), 7.18 – 7.14 (m, 1H), 7.09 (td, $J = 7.5, 1.1$ Hz, 1H), 2.87 (t, $J = 7.3$ Hz, 2H), 2.7022-H (t, $J =$

7.3 Hz, 2H), 2.21 (s, 3H), 1.41 (s, 9H), 0.73 (s, 1H); ^{13}C NMR (126 MHz, C_6D_6) δ 149.5, 139.0, 130.4, 128.5, 124.7, 122.9, 118.8, 116.1, 84.4, 79.5, 51.6, 36.6, 28.9, 28.1; HRMS (ESI) m/z calcd for $\text{C}_{16}\text{H}_{21}\text{O}_2\text{N}_2\text{INa}$ ($\text{M} + \text{Na}$) $^+$ 423.0545, found 423.0530.

General procedure for the carbenylative coupling to form Boc-borrerine, **25**

A round bottom flask containing a magnetic stir bar, $\text{Pd}_2(\text{dba})_3 \cdot \text{CHCl}_3$ (0.0025 mmol, 2.5 mol%), and bidentate ligand (0.0075 mmol, 7.5 mol%) was placed under nitrogen and charged with 500 μL toluene. The purple suspension was stirred at 110 $^\circ\text{C}$ until a clear orange solution was obtained (approximately 5 min). A separate round bottom flask, containing a magnetic stir bar, was charged with 2-iodoindole (0.10 mmol, 100 mol%), *N*-tosylhydrazone (0.20 mmol, 200 mol%) and *t*-BuOLi (0.32 mmol, 320 mol%) under nitrogen. The palladium complex solution was then transferred by syringe to the hydrazone containing round bottom flask, washing three times with a total 1.0 mL of toluene. The reaction mixture was then placed into an oil bath at 110 $^\circ\text{C}$ and monitored by TLC. The crude reaction mixture was diluted with EtOAc and 1% (w/v) aq. NaOH followed by extraction with EtOAc three times. The organic layer was washed with brine, dried over Na_2SO_4 , filtered and concentrated *in vacuo*. Purification by flash column chromatography using hexane/EtOAc/MeOH (20:80:0 to 0:98:2) affords product.

Boc-borrerine - *tert*-butyl 2-methyl-1-(2-methylprop-1-en-1-yl)-1,2,3,4-tetrahydro-9*H*-pyrido[3,4-*b*]indole-9-carboxylate, **25**.



Following the general procedure utilizing the ligand (*R,R*)-DIOP, **22** (40.0 mg, 0.100 mmol, 100 mol%), and *N*-tosylhydrazone **4** (52.9 mg, 0.210 mmol, 210 mol%) were reacted and monitored by TLC. The reaction was complete after 2.5 hours. Purification by flash chromatography

produced Boc-borrerine **25** (5.0 mg, 0.0147 mmol, 15%). $R_f = 0.29$ (98:2 EtOAc/MeOH); ^1H NMR (500 MHz, CDCl_3) δ 7.92 (d, $J = 8.1$ Hz, 1H), 7.43 (d, $J = 7.3$ Hz, 1H), 7.24 – 7.19 (m, 2H), 5.10 (d, $J = 9.0$ Hz, 1H), 4.89 (d, $J = 8.9$ Hz, 1H), 3.14 – 3.08 (m, 1H), 2.87 – 2.80 (m, 2H), 2.71 – 2.67 (m, 1H), 2.50 (s, 3H), 1.83 (s, 3H), 1.72 (s, 3H), 1.63 (s, 9H); ^{13}C NMR (126 MHz, CDCl_3) δ 150.0, 137.1, 136.9, 136.0, 129.2, 123.6, 122.9, 122.2, 118.0, 114.9, 114.4, 83.2, 57.8, 47.0, 41.9, 28.1, 26.0, 19.8, 18.9; MS (ESI) m/z calcd for $\text{C}_{21}\text{H}_{28}\text{N}_2\text{O}_2\text{H}$ ($\text{M} + \text{H}$) $^+$ 341.2, found 341.5.

¹ (a) Heck, R. F.; Nolley, J. P. "Palladium-catalyzed vinylic hydrogen substitution reactions with (b) Negishi, E.; King, A. O.; Okukado, N. "Selective carbon-carbon bond formation via transition metal catalysis. 3. A highly selective synthesis of unsymmetrical biaryls and diarylmethanes by the nickel- or palladium-catalyzed reaction of aryl- and benzylzinc derivatives with aryl halides" *J. Org. Chem.* **1977**, *42*, 1821–1823.

(c) Miyaura, N.; Yamada, K.; Suzuki, A. "A new stereospecific cross-coupling by the palladium-catalyzed reaction of 1-alkenylboranes with 1-alkenyl or 1-alkynyl halides" *Tetrahedron Lett.* **1979**, *20*, 3437–3440.

(d) Seechurn, C. C. C. J.; Kitching, M. O.; Colacot, T. J.; Snieckus, V. "Palladium-Catalyzed Cross-Coupling: A Historical Contextual Perspective to the 2010 Nobel Prize" *Angew. Chem. Int. Ed.* **2012**, *51*, 5062–5085.

² The Nobel Prize in Chemistry 2010.

http://www.nobelprize.org/nobel_prizes/chemistry/laureates/2010/ (accessed Jan 22, 2017).

³ (a) Peng, C.; Wang, Y.; Wang, J. "Palladium-Catalyzed Cross-Coupling of α -Diazocarbonyl Compounds with Arylboronic Acids" *J. Am. Chem. Soc.* **2008**, *130*, 1566–1567.

(b) Tsoi, Y-T; Zhou, Z.; Chan, A. S. C.; Yu, W-Y. "Palladium-Catalyzed Oxidative Cross-Coupling Reaction of Arylboronic Acids with Diazoesters for Stereoselective Synthesis of (*E*)- α,β -Diarylacrylates" *Org. Lett.* **2010**, *12*, 4506–4509.

⁴ (a) Barluenga, J.; Escribano, M.; Moriel, P.; Aznar, F.; Valdés, C. "Synthesis of Enol Ethers and Enamines by Pd-Catalyzed Tosylhydrazide-Promoted Cross-Coupling Reactions" *Chem. Eur. J.* **2009**, *15*, 13291–13294.

(b) Barluenga, J.; Tomás-Gamasa, M.; Aznar, F.; Valdés, C. "Synthesis of 2-Arylacrylates from Pyruvate by Tosylhydrazide-Promoted Pd-Catalyzed Coupling with Aryl Halides" *Chem. Eur. J.* **2010**, *16*, 12801–12803.

(c) Barluenga, J.; Escribano, M.; Aznar, F.; Valdés, C. "Arylation of α -Chiral Ketones by Palladium-Catalyzed Cross-Coupling Reactions of Tosylhydrazones with Aryl Halides" *Angew. Chem. Int. Ed.* **2010**, *49*, 6856–6859.

(d) Ojha, D. P.; Prabhu, K. R. "Heteroaryl Halides in the Absence of External Ligands: Synthesis of Substituted Olefins" *J. Org. Chem.* **2012**, *77*, 11027–11033.

(e) Roche, M.; Hamze, A.; Brion, J.-D.; Alami, M. "Catalytic Three-Component One-Pot Reaction of Hydrazones, Dihaloarenes, and Amines" *Org. Lett.* **2013**, *15*, 148–151.

-
- (f) Roche, M.; Hamze, A.; Provot, O.; Brion, J.-D.; Alami, M. "Synthesis of Ortho/Ortho'-Substituted 1,1-Diarylethylenes through Cross-Coupling Reactions of Sterically Encumbered Hydrazones and Aryl Halides" *J. Org. Chem.* **2013**, *78*, 445–454.
- (g) Jimenéz-Aquino, A.; Vega, J. A.; Trabanco, A. A.; Valdés, C. "A General Synthesis of α -Trifluoromethylstyrenes through Palladium-Catalyzed Cross-Couplings with 1,1,1-Trifluoroacetone Tosylhydrazone" *Adv. Synth. Catal.* **2014**, *356*, 1079–1084.
- (h) Barluenga, J.; Florentino, L.; Aznar, F.; Valdés, C. "Synthesis of Polysubstituted Olefins by Pd-Catalyzed Cross-Coupling Reaction of Tosylhydrazones and Aryl Nonaflates" *Org. Lett.* **2011**, *13*, 510–513.
- (i) Florentino, L.; Aznar, F.; Valdés, C. "Synthesis of Polysubstituted Isoquinolines through Cross-Coupling Reactions with α -Alkoxytosylhydrazones" *Org. Lett.* **2012**, *14*, 2323–2325.
- (j) Florentino, L.; Aznar, F.; Valdés, C. "Synthesis of (*Z*)-*N*-Alkenylazoles and Pyrroloisoquinolines from α -*N*-Azoleketones through Pd-Catalyzed Tosylhydrazone Cross-Couplings" *Chem. Eur. J.* **2013**, *19*, 10506–10510.
- (k) Patel, P. K.; Dalvadi, J. P.; Chikhalia, K. H. "Pd-Catalyzed Cross-Coupling Reactions of less Activated Alkenyl Electrophiles (for Tosylates and Mesylates) with Tosylhydrazones: Synthesis of Various 1,3-Dienes" *RSC Adv.* **2014**, *4*, 55354–55361.
- (l) Barluenga, J.; Escribano, M.; Moriel, P.; Aznar, F.; Valdés, C. "Synthesis of Enol Ethers and Enamines by Pd-Catalyzed Tosylhydrazide-Promoted Cross-Coupling Reactions" *Chem. Eur. J.* **2009**, *15*, 13291–13294.
- (m) Roche, M.; Frison, G.; Brion, J.-D.; Provot, O.; Hamze, A.; Alami, M. "Csp²-N Bond Formation via Ligand-Free Pd-Catalyzed Oxidative Coupling Reaction of *N*-Tosylhydrazones and Indole Derivatives" *J. Org. Chem.* **2013**, *78*, 8485–8495.
- (n) Barluenga, J.; Moriel, P.; Valdés, C.; Aznar, F. "*N*-Tosylhydrazones as Reagents for Cross-Coupling Reactions: A Route to Polysubstituted Olefins" *Angew. Chem., Int. Ed.* **2007**, *46*, 5587–5590.
- (o) Barluenga, J.; Tomas-Gamasa, M.; Moriel, P.; Aznar, F.; Valdés, C. "Pd-Catalyzed Cross-Coupling Reactions with Carbonyls: Application in a Very Efficient Synthesis of 4-Aryltetrahydropyridines" *Chem. Eur. J.* **2008**, *14*, 4792–4795.
- (p) Peng, C.; Wang, Y.; Wang, J. "Palladium-Catalyzed Cross-Coupling of α -Diazocarbonyl Compounds with Arylboronic Acids" *J. Am. Chem. Soc.* **2008**, *130*, 1566–1567.
- (q) Xia, Y.; Xia, Y.; Lin, Z.; Zhang, Y.; Wang, J. "Palladium-Catalyzed Cross-Coupling Reaction of Diazo Compounds and Vinyl Boronic Acids: An Approach to 1,3-Diene Compounds" *J. Org. Chem.* **2014**, *79*, 7711–7717.
- ⁵ Roche, M.; Bignon, J.; Brion, J.-D.; Hamze, A.; Alami, M. "Tandem One-Pot Palladium-Catalyzed Coupling of Hydrazones, Haloindoles, and Amines: Synthesis of Amino-*N*-vinylindoles and Their Effect on Human Colon Carcinoma Cells" *J. Org. Chem.* **2014**, *79*, 7583–7592.
- ⁶ Devine S. K. J.; Van Vranken, D. L. "Palladium-Catalyzed Carbene Insertion and Trapping with Carbon Nucleophiles" *Org. Lett.* **2008**, *10*, 1909–1911.
- ⁷ Devine, S. K. J.; Van Vranken, D. L. "Palladium-Catalyzed Carbene Insertion into Vinyl Halides and Trapping with Amines" *Org. Lett.* **2007**, *9*, 2047–2049.
- ⁸ Peng, C.; Yan, G.; Wang, Y.; Jiang, Y.; Zhang, Y.; Wang, J. "Palladium-Catalyzed Coupling Reaction of α -Diazocarbonyl Compounds with Aromatic Boronic Acids or Halides" *Synthesis*, **2010**, 4154–4168.

-
- ⁹ (a) Trost, B. M.; Van Vranken, D. L. "Asymmetric Transition Metal-Catalyzed Allylic Alkylations" *Chem. Rev.*, **1996**, *96*, 395–422.
- (b) Trost, B. M.; Crawley, M. L. "Asymmetric Transition-Metal-Catalyzed Allylic Alkylations: Applications in Total Synthesis" *Chem. Rev.*, **2003**, *103*, 2921–2944.
- ¹⁰ Chen, S.; Wang, J. "Palladium-catalyzed reaction of allyl halides with α -diazocarbonyl compounds" *Chem. Commun.* **2008**, 4198–4200.
- ¹¹ Greenman, K. L.; Carter, D. S.; Van Vranken, D. L. "Palladium-Catalyzed Insertion Reactions of Trimethylsilyldiazomethane" *Tetrahedron* **2001**, *57*, 5219–5225.
- ¹² Greenman, K. L.; Van Vranken, D. L. "Palladium-catalyzed carbene insertion into benzyl bromides" *Tetrahedron*, **2005**, *61*, 6438–6441.
- ¹³ Yu, W.-Y.; Tsoi, Y.-T.; Zhou, Z.; Chan, A. S. C. "Palladium-Catalyzed Cross Coupling Reaction of Benzyl Bromides with Diazoesters for Stereoselective Synthesis of (*E*)- α,β -Diarylacrylates" *Org. Lett.*, **2009**, *11*, 469–472.
- ¹⁴ Tréguier, B.; Hamze, A.; Provot, O.; Brion, J.-D.; Alami, M. "Expeditious synthesis of 1,1-diarylethylenes related to isocombretastatin A-4 (isoCA-4) via palladium-catalyzed arylation of *N*-tosylhydrazones with aryl triflates" *Tetrahedron Lett.* **2009**, 6549–6552.
- ¹⁵ Chen, Z.-S.; Duan, X.-H.; Wu, L.-Y.; Ali, S.; Ji, K.-G.; Zhou, P.-X.; Liu, X.-Y.; Liang, Y.-M. "Palladium-Catalyzed Coupling of Propargylic Carbonates with *N*-Tosylhydrazones: Highly Selective Synthesis of Substituted Propargylic *N*-Sulfonylhydrazones and Vinylallenes" *Chem. Eur. J.* **2011**, *17*, 6918–6921.
- ¹⁶ Ye, T.; McKervey, M. A. "Organic Synthesis with α -Diazo Carbonyl Compounds" *Chem. Rev.* **1994**, *94*, 1091–1160.
- ¹⁷ Gutiérrez-Bonet, Á.; Juliá-Hernández, F.; de Luis, B.; Martin, R. "Pd-Catalyzed C(sp³)-H Functionalization/Carbenoid Insertion: All-Carbon Quaternary Centers via Multiple C–C Bond Formation" *J. Am. Chem. Soc.* **2016**, 6384–6387.
- ¹⁸ (a) Bertz, S. H.; Dabbagh, G. "Improved Preparations of Some Arenesulfonylhydrazones" *J. Org. Chem.* **1983**, *48*, 116–119.
- (b) Wu, P.-L.; Peng, S.-Y.; Magrath, J. "Tosylhydrazines by the Reduction of Tosylhydrazones with Triethylsilane in Trifluoroacetic Acid" *Synthesis* **1996**, 249–252.
- ¹⁹ Bamford, W. R.; Stevens, T. S. "The Decomposition of Toluene-*p*-sulphonylhydrazones by Alkali" *J. Chem. Soc.* **1952**, 4735–4740.
- ²⁰ Ihara, E.; Haida, N.; Lio, M.; Inoue, K. "Palladium-Mediated Polymerization of Alkyl Diazoacetates To Afford Poly(alkoxycarbonylmethylene)s. First Synthesis of Polymethylenes Bearing Polar Substituents" *Macromolecules*, **2003**, 36–41.
- ²¹ Fulton, J. R.; Aggarwal, V. K.; de Vicente, J. "The Use of Tosylhydrazone Salts as a Safe Alternative for Handling Diazo Compounds and Their Applications in Organic Synthesis" *Eur. J. Org. Chem.* **2005**, 1479–1492.
- ²² Amrich, M. J.; Bell, J. A. "Photoisomerization of Diazirine" *J. Am. Chem. Soc.* **1964**, 292–293.
- ²³ Nevado, C.; Charruault, L.; Michelet, V.; Nieto-Oberhuber, C.; Muñoz, M. P.; Méndez, M.; Rager, M.-N.; Genêt, J.-P.; Echavarren, A. M. "On the Mechanism of Carbohydroxypalladation of Enynes. Additional Insights on the Cyclization of Enynes with Electrophilic Metal Complexes" *Eur. J. Org. Chem.* **2003**, 706–713.

- ²⁴ Sierra, M. A.; Mancheño, M. J.; Sáez, E.; del Amo, J. C. "Chromium(0)–Carbene Complexes as Carbene Sources: Self-Dimerization and Inter- and Intramolecular C–H Insertion Reactions Catalyzed by Pd(OAc)₂" *J. Am. Chem. Soc.* **1998**, *120*, 6812–6813.
- ²⁵ Hine, J. "Carbon Dichloride as an Intermediate in the Basic Hydrolysis of Chloroform. A Mechanism for Substitution Reactions at a Saturated Carbon Atom" *J. Am. Chem. Soc.* **1950**, 2438–2445.
- ²⁶ Chen, Z.-S.; Huang, L.-Z.; Jeon, H. J.; Xuan, Z.; Lee, S.-G. "Cooperative Pd(0)/Rh(II) Dual Catalysis: Interceptive Capturing of π -Allyl Pd(II) Complexes with α -Imino Rh(II) Carbenoids" *ACS Catal.* **2016**, 4914–4919.
- ²⁷ Kudirka, R.; Van Vranken, D. L. "Cyclization Reactions Involving Palladium-Catalyzed Carbene Insertion into Aryl Halides" *J. Org. Chem.* **2008**, 3585–3588.
- ²⁸ Arunprasath, D.; Muthupandi, P.; Sekar, G. "Palladium-Catalyzed Intermolecular Carbene Insertion Prior to Intramolecular Heck Cyclization: Synthesis of 2-Arylidene-3-aryl-1-indanones" *Org. Lett.* **2015**, *17*, 5448–5451.
- ²⁹ Zhang, Z.; Liu, Y.; Gong, M.; Zhao, X.; Zhang, Y.; Wang, J. "Palladium-Catalyzed Carbonylation/Acyl Migratory Insertion Sequence" *Angew. Chem. Int. Ed.* **2010**, *49*, 1139–1142.
- ³⁰ Xia, Y.; Hu, F.; Liu, Z.; Qu, P.; Ge, R.; Ma, C.; Zhang, Y.; Wang, J. "Palladium-Catalyzed Diarylmethyl C(sp³)-C(sp²) Bond Formation: A New Coupling Approach toward Triarylmethanes" *Org. Lett.* **2013**, *15*, 1784–1787.
- ³¹ Zhou, L.; Ye, F.; Zhang, Y.; Wang, J. "Pd-Catalyzed Three-Component Coupling of *N*-Tosylhydrazone, Terminal Alkyne, and Aryl Halide" *J. Am. Chem. Soc.* **2010**, *132*, 13590–13591.
- ³² Zhou, P.-X.; Ye, Y.-Y.; Zhao, L.-B.; Hou, J.-Y.; Kang, X.; Chen, D.-Q.; Tang, Q.; Zhang, J.-Y.; Huang, Q.-X.; Zheng, L.; Ma, J.-W.; Xu, P.-F.; Liand, Y.-M. "Using *N*-Tosylhydrazone as a Double Nucleophile in the Palladium-Catalyzed Cross-Coupling Reaction To Synthesize Allylic Sulfones" *Chem. Eur. J.* **2014**, *20*, 16093–16096.
- ³³ Premachandra, I. D. U. A.; Nguyen, T. A.; Shen, C.; Gutmen, E. S.; Van Vranken, D. L. "Carbenylative Amination and Alkylation of Vinyl Iodides via Palladium Alkylidene Intermediates" *Org. Lett.* **2015**, 5464–5467.
- ³⁴ Zhou, P.-X.; Zhou, Z.-Z.; Chen, Z.-S.; Ye, Y.-Y.; Zhao, L.-B.; Yang, Y.-F.; Xia, X.-F.; Luo, J.-Y.; Liang, Y.-M. "Palladium-catalyzed insertion of α -diazocarbonyl compounds for the synthesis of cyclic amino esters" *Chem. Commun.* **2013**, *49*, 561–563.
- ³⁵ Zhou, P.-X.; Luo, J.-Y.; Zhao, L.-B.; Ye, Y.-Y.; Liang, Y.-M. "Palladium-catalyzed insertion of *N*-tosylhydrazones for the synthesis of isoindolines" *Chem. Commun.* **2013**, *49*, 3254–3256.
- ³⁶ Brennfürer, A.; Neumann, H.; Beller, M. "Palladium-Catalyzed Carbonylation Reactions of Aryl Halides and Related Compounds" *Angew. Chem. Int. Ed.* **2009**, *48*, 4114–4133.
- ³⁷ Mori, M.; Chiba, K.; Ban, Y. "Reactions and syntheses with organometallic compounds. 7. Synthesis of benzolactams by palladium-catalyzed amidation" *J. Org. Chem.* **1978**, *43*, 1684–1687.
- ³⁸ Keinan, E.; Sahai, M. "Regioselectivity in Organo-transition-metal Chemistry. A Remarkable Steric Effect in π -Allyl Palladium Chemistry" *J. Chem. Soc., Chem. Commun.* **1984**, 648–650.
- ³⁹ (a) Kobayashi, S.; Ishitani, H.; Ueno, M. "Catalytic Asymmetric Synthesis of Both Syn- and Anti- β -Amino Alcohols" *J. Am. Chem. Soc.* **1998**, *120*, 431–432.

(b) Ibrahem, I.; Casas, J.; Córdova, A. “Direct Catalytic Enantioselective α -Aminomethylation of Ketones” *Angew. Chem. Int. Ed.* **2004**, *43*, 6528–6531.

⁴⁰ Gutman, E. S.; Arredondo, V.; Van Vranken, D. L. “Cyclization of η^3 -Benzylpalladium Intermediates Derived from Carbene Insertion” *Org. Lett.* **2014**, *16*, 5498–5501.

⁴¹ Huang, L.; Arndt, M.; Gooben, K.; Heydt, H.; Gooben, L. “Late Transition Metal-Catalyzed Hydroamination and Hydroamidation” *Chem. Rev.* **2015**, *115*, 2596–2697.

⁴² Kawatsura, M.; Hartwig, J. “Palladium-Catalyzed Intermolecular Hydroamination of Vinylarenes Using Arylamines” *J. Am. Chem. Soc.* **2000**, *122*, 9546–9547.

⁴³ Ney, J. E.; Wolfe, J. P. “Palladium-Catalyzed Synthesis of *N*-Aryl Pyrrolidines from γ -(*N*-Arylamino) Alkenes: Evidence for Chemoselective Alkene Insertion into Pd-N Bonds” *Angew. Chem. Int. Ed.* **2004**, *43*, 3605–3608.

⁴⁴ Wolfe, J. P. “Stereoselective Synthesis of Saturated Heterocycles via Palladium-Catalyzed Alkene Carboetherification and Carboamination Reaction” *Synlett* **2008**, 2913–2937.

⁴⁵ White, D. R.; Hutt, J. T.; Wolfe, J. P. “Asymmetric Pd-Catalyzed Alkene Carboamination Reactions for the Synthesis of 2-Aminoindane Derivatives” *J. Am. Chem. Soc.* **2015**, *137*, 11246–11249.

⁴⁶ Kudirka, R.; Devine, S. K. J.; Adams, C. S.; Van Vranken, D. L. “Palladium-Catalyzed Insertion of α -Diazoesters into Vinyl Halides To Generate α,β -Unsaturated γ -Amino Esters” *Angew. Chem. Int. Ed.* **2009**, *48*, 3677–3680.

⁴⁷ Khanna, A.; Maung, C.; Johnson, K. R.; Luong, T. T.; Van Vranken, D. L. “Carbenylative Amination with *N*-Tosylhydrazones” *Org. Lett.* **2012**, *14*, 3233–3235.

⁴⁸ Kitamura, M.; Yuasa, R.; Van Vranken, D. L. “Synthesis of the cyclic prenylguanidine nitensidine E using a palladium-catalyzed carbenylative amination” *Tetrahedron Lett.* **2015**, *56*, 3027–3031.

⁴⁹ (a) 2,4,6-Triisopropylbenzenesulfonylhydrazide. *Encyclopedia of Reagents for Organic Synthesis* [Online]; Wiley & Sons, Posted September 15, 2008.

<http://onlinelibrary.wiley.com/doi/10.1002/047084289X.rt259.pub2/pdf> (accessed January 10, 2017).

(b) *p*-Toluenesulfonylhydrazide. *Encyclopedia of Reagents for Organic Synthesis* [Online]; Wiley & Sons, Posted September 17, 2007.

<http://onlinelibrary.wiley.com/doi/10.1002/047084289X.rt137.pub2/pdf> (accessed January 10, 2017).

⁵⁰ (a) Zhang, Y.; Wang, J. “Recent Developments in Pd-Catalyzed Reactions of Diazo Compounds” *Eur. J. Org. Chem.* **2011**, 1015–1026.

(b) Xiao, Q.; Zhang, Y.; Wang, J. “Diazo Compounds and *N*-Tosylhydrazones: Novel Cross-Coupling Partners in Transition-Metal-Catalyzed Reactions” *Acc. Chem. Res.* **2013**, *46*, 236–247.

⁵¹ Xiao, Q.; Ma, J.; Yang, Y.; Zhang, Y.; Wang, J. “Pd-Catalyzed C=C Double-Bond Formation by Coupling of *N*-Tosylhydrazones with Benzyl Halides” *Org. Lett.* **2009**, *11*, 4732–4735.

⁵² Faller, J. W.; Wilt, J. C. “Palladium/BINAP(S)-Catalyzed Asymmetric Allylic Amination” *Org. Lett.* **2005**, *7*, 633–636.

⁵³ Hayashi, T.; Yamamoto, A.; Ito, Y.; Nishioka, E.; Miura, H.; Yanagi, K. “Asymmetric Synthesis Catalyzed by Chiral Ferrocenylphosphine-Transition-Metal Complexes. 8. Palladium-Catalyzed Asymmetric Allylic Amination” *J. Am. Chem. Soc.* **1989**, *111*, 6301–6311.

⁵⁴ Šebesta, R.; Škvorcová, A.; Horváth, B. “Asymmetric allylic substitutions on symmetrical and

non-symmetrical substrates using [5]ferrocenophane ligands” *Tetrahedron: Asymmetry*, **2010**, *21*, 1910–1915.

⁵⁵ Grellier, M.; Pfeffer, M. “Heterocyclization, deprotection and isomerization in an intramolecular palladium-catalyzed tertiary amine-allyl coupling reaction” *Chem. Commun.* **1996**, 2257–2258.

⁵⁶ Miyabe, H.; Yoshida, K.; Kobayashi, Y.; Matsumura, A.; Takemoto, Y. “Synthesis of Azacycles Based on Iridium-Catalyzed Sequential Allylic Amination” *Synlett*. **2003**, 1031–1033.

⁵⁷ Rajamaki, S.; Kilburn, J. D. “Lewis acid mediated endo-cyclisation of trimethylsilylmethylenecyclopropyl imines—a stereoselective route to indolizidines” *Chem. Commun.* **2005**, 1637–1639.

⁵⁸ Tang, M.; Zhang, F.-M. “Efficient One-Pot Synthesis of Substituted Pyrazoles” *Tetrahedron*, **2013**, *69*, 1427–1433.

⁵⁹ Péron, F.; Fossey, C.; Santos, J. S.-de O.; Cailly, T.; Fabis, F. “Room-Temperature *ortho*-Alkoxylation and -Halogenation of *N*-Tosylbenzamides by Using Palladium(II)-Catalyzed C-H Activation” *Chem. Eur. J.* **2014**, *20*, 7507–7513.

⁶⁰ Ye, Y.-Y.; Zhou, P.-X.; Luo, J.-Y.; Zhong, M.-J.; Liang, Y.-M. “Palladium-catalyzed insertion of α,β -unsaturated *N*-tosylhydrazones and trapping with carbon nucleophiles” *Chem. Commun.* **2013**, *49*, 10190–10192.

⁶¹ Faller, J. W.; Wilt, J. C.; Parr, J. “Kinetic Resolution and Unusual Regioselectivity in Palladium-Catalyzed Allylic Alkylations with a Chiral P,S Ligand” *Org. Lett.* **2004**, *6*, 1301–1304.

⁶² Aggarwal, V. K.; Alonso, E.; Bae, I.; Hynd, G.; Lydon, K. M.; Palmer, M. J.; Patel, M.; Porcelloni, M.; Richardson, J.; Stenson, R. A.; Studley, J. R.; Vasse, J.; Winn, C. L. “A New Protocol for the In Situ Generation of Aromatic, Heteroaromatic, and Unsaturated Diazo Compounds and Its Application in Catalytic and Asymmetric Epoxidation of Carbonyl Compounds. Extensive Studies To Map Out Scope and Limitations, and Rationalization of Diastereo- and Enantioselectivities” *J. Am. Chem. Soc.* **2003**, *125*, 10926–10940.

⁶³ Jeffs, P. W.; Hansen, J. F.; Brine, G. A. “Photochemical Synthesis of 6,7-dihydro-5*H*-dibenz[*c,e*]azepine and 5,6,7,8-tetrahydrodibenz[*c,e*]azocine Derivatives” *J. Org. Chem.* **1975**, *40*, 2883–2890.

⁶⁴ Jiang, X.; Yang, Q.; Yu, Y.; Fu, C.; Ma, S. “Highly Regio- and Stereoselective Synthesis of Nine- to Twelve-Membered Cyclic Compounds by a Pd⁰-Catalyzed Cyclization Reaction between Allenes with a Nucleophilic Functionality and Organic Halides” *Chem. Eur. J.* **2009**, *15*, 7283–7286.

⁶⁵ Sawant, R. T.; Waghmode, S. B. “Synthesis of *N*-Boc-C1 Vinyl Tetrahydroisoquinoline via Zn-Mediated Intramolecular Cyclization of *N*-Boc Protected Iodo Acetonide” *Synth. Commun.* **2011**, *41*, 2385–2391.

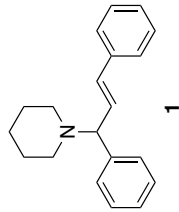
⁶⁶ Chapman, C. J.; Frost, C. G.; Gill-Carey, M. P.; Kociok-Köhn, G.; Mahon, M. F.; Weller, A. S.; Willis, M. C. “Diphosphine mono-sulfides: readily available chiral monophosphines” *Tetrahedron: Asymmetry*, **2003**, *14*, 705–710.

⁶⁷ Majumdar, K. C.; Mondal, S. “Synthesis of Polycyclic Sultams by Palladium-Catalyzed Intramolecular Cyclization” *Synthesis*, **2009**, *18*, 3127–3135.

⁶⁸ Villani, F. J. Jr.; Costanzo, M. J.; Inners, R. R.; Mutter, M. S.; McClure, D. E. “Determination of Enantiomeric Purity of Tertiary Amines by ¹H NMR of α -Methoxy- α -(trifluoromethyl)phenylacetic Acid Complexes” *J. Org. Chem.* **1986**, *51*, 3715–3718.

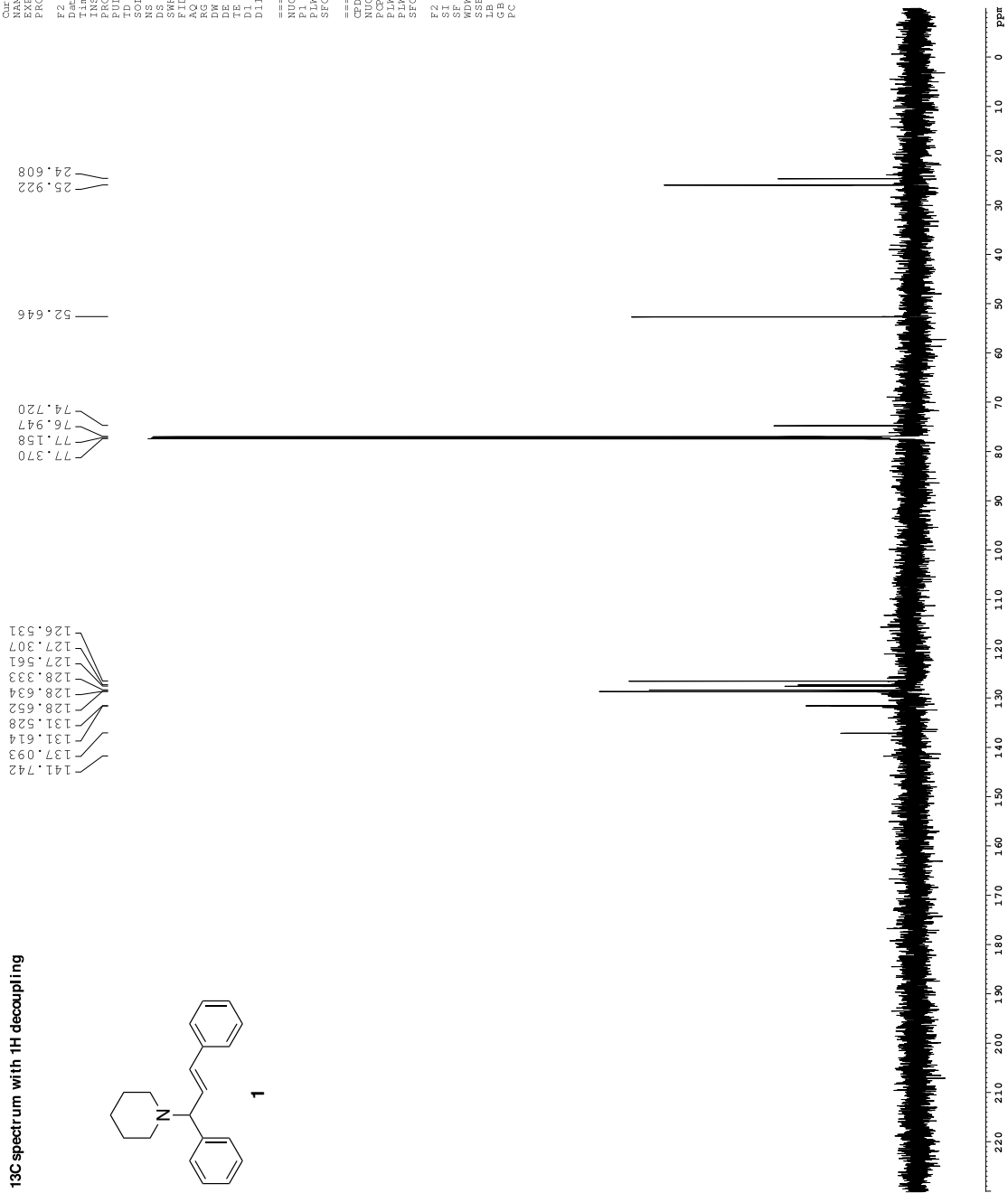
-
- ⁶⁹ Vallakati, R.; May, J. A. “Biomimetic Synthesis of the Antimalarial Flindersial Alkaloids” *J. Am. Chem. Soc.* **2012**, *134*, 6396–6939.
- ⁷⁰ Hinman, R. L.; Bauman, C. P. “Reactions of N-Bromosuccinimide and Indoles. A Simple Synthesis of 3-Bromooxindoles¹” *J. Org. Chem.* **1964**, *29*, 1206–1215
- ⁷¹ Liddon, J. T. R.; Clarke, A. K.; Taylor, R. J. K.; Unsworth, W. P. “Preparation and Reactions of Indoleninyl Halides: Scaffolds for the Synthesis of Spirocyclic Indole Derivatives” *Org. Lett.* **2016**, *18*, 6328–6331.
- ⁷² Phillips, R. S.; Cohen, L. A. “Intramolecular General Acid and General Base Catalyses in the Hydrolysis of 2-Halotryptophans and Their Analogues” *J. Am. Chem. Soc.* **1986**, *108*, 2023–2030.
- ⁷³ Priebbenow, D. L.; Henderson, L. C.; Pfeffer, F. M.; Stewart, S. G. “Domino Heck-Aza-Michael Reactions: Efficient Access to 1-Substituted Tetrahydro- β -carbolines” *J. Org. Chem.* **2010**, *75*, 1787–1790.
- ⁷⁴ Feng, P.; Fan, Y.; Xue, F.; Liu, W.; Li, S.; Shi, Y. “An Approach to the Hexacyclic Skeleton of Trigonoliimines” *Org. Lett.* **2011**, *13*, 5827–5829.
- ⁷⁵ Ignatenko, V. A.; Zhang, P.; Viswanathan, R. “Step-economic synthesis of (\pm)-debromoflustramine A using indole C3 activation strategy” *Tetrahedron Lett.* **2011**, *52*, 1269–1272.
- ⁷⁶ Han, S.; Movassaghi, M. “Concise Total Synthesis and Stereochemical Revision of all (–)-Trigonoliimines” *J. Am. Chem. Soc.* **2011**, *133*, 10768–10771.
- ⁷⁷ Snell, R. H.; Woodward, R. L.; Willis, M. C. “Catalytic Enantioselective Total Synthesis of Hodgkinsine B” *Angew. Chem. Int. Ed.* **2011**, *50*, 9116–9119.

¹³C spectrum with ¹H decoupling

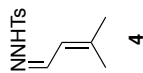


```

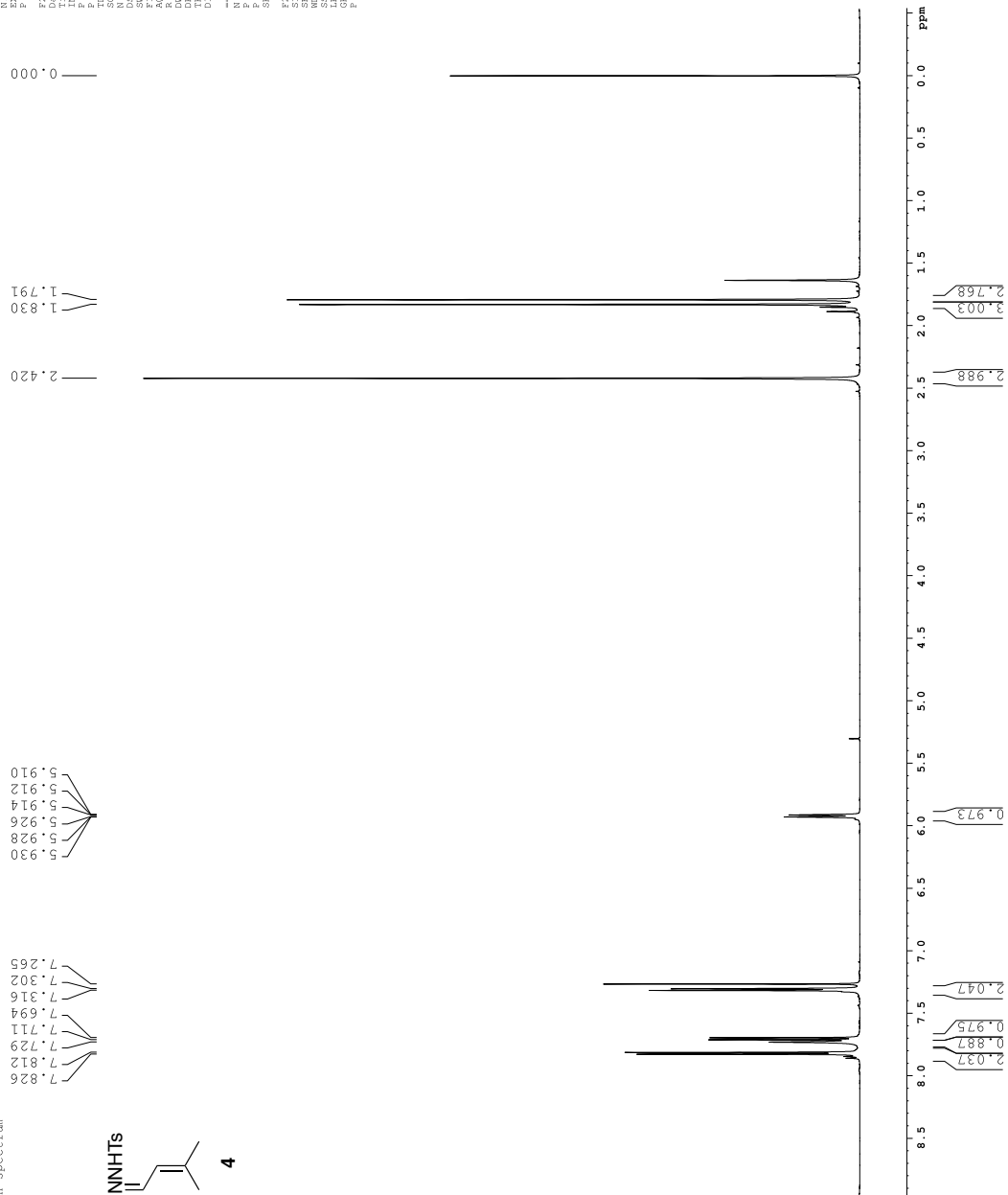
Current Data Parameters
NAME      CEA-I-152P-rodac
EXPNO    3
PROCNO   1
F2 - Acquisition Parameters
Date_    20110818
Time     11.21
INSTRUM  spect
PROBHD   5 mm TBI 1H/13
PULPROG  zgpg30
TD        65536
CONVENT  1
NS        176
DS        4
SRR       36231.882
LORRES    3.94598
AQ         0.904988
RG         2050
DW         13.800
DE         1.000
TE         298.0
D1         0.40000001
D11        0.03000000
===== CHANNEL f1 =====
NUC1       13C
P1         15.00
PLW1      107.15190125
SFO1      125.76134989
===== CHANNEL f2 =====
CDEPRG [2] waltz16
PCPD2     70.00
PLW2      0 W
SFO2      600.1350010
F2 - Processing parameters
SI         65536
SF         150.9027928
MDW        0
SSB        0
LB         2.00
GB         0
PC         1.00
  
```



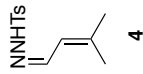
1H spectrum



Current Data Parameters
NAME: 1175
EXPNO: 2
PROCNO: 1
F2 - Acquisition Parameters
Time: 20.11436
INSTRUM: av600
PULPROG: zgpg30
SOLVENT: CDCl3
NS: 8
DSH: 5707.763 Hz
FIDRES: 0.058139 Hz
RG: 8.531256
OR: 87.000 usec
TE: 293.1 K
DI: 0.10000000 sec
----- CHANNEL f1 -----
P1: 8.00 usec
PL1: 23.03441956 W
SFO1: 60.1325629 MHz
F2 - Processing Parameters
SF: 600.1300324 MHz
SSB: 0
LB: 0
PC: 1.00

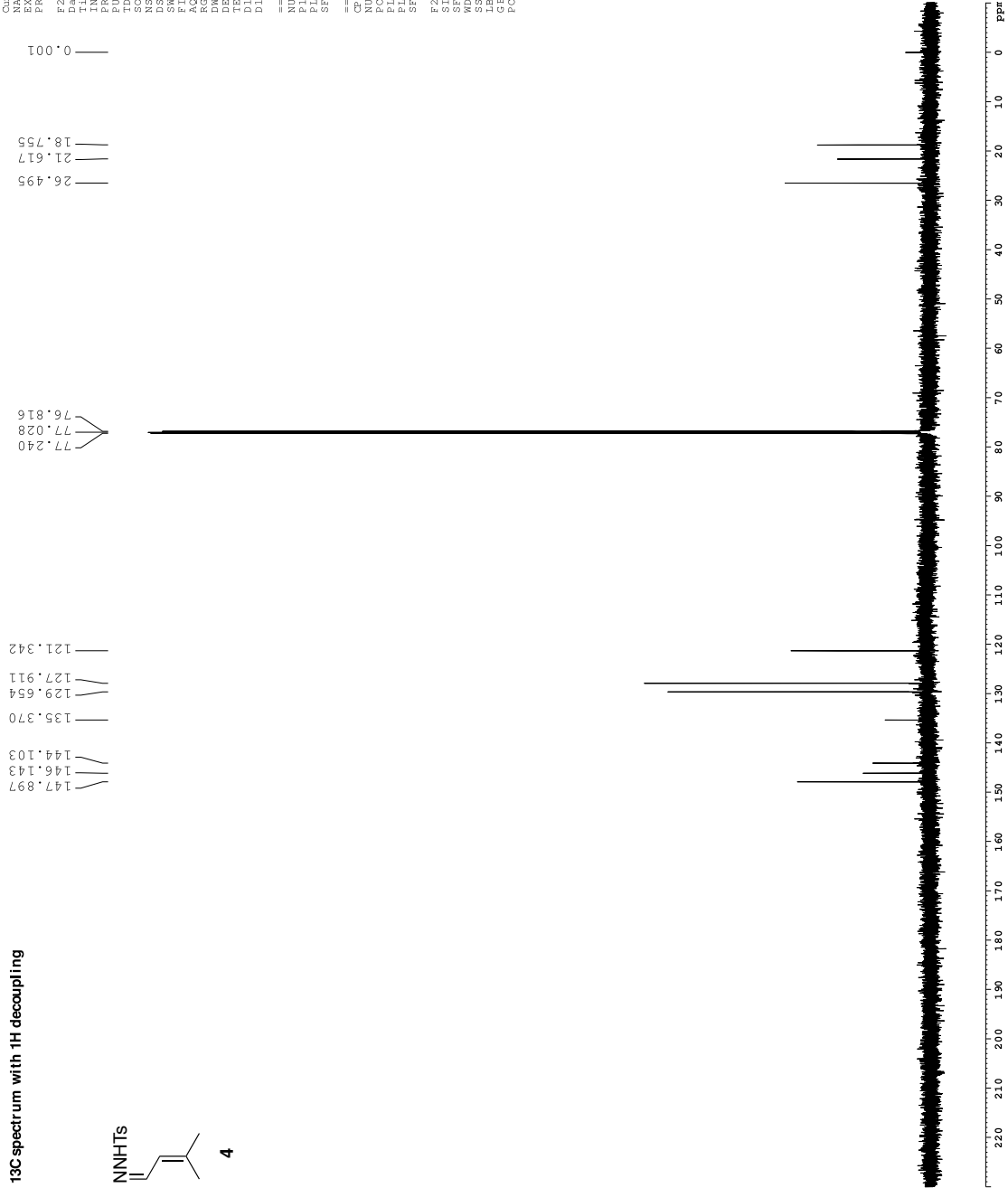


¹³C spectrum with ¹H decoupling



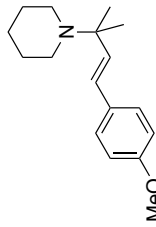
```

Current Data Parameters
NAME      CRA-I-179
EXPNO    3
PROCNO   1
F2 - Acquisition Parameters
Date_    20110906
Time     11.01
INSTRUM  spect
PROBHD   5 mm TBI 1H/13
PULPROG  zgpg30
TD        65536
SOLVENT  CDCl3
NS        573
DS        4
SWH       36231.882
FIDRES    0.99582
AQ         0.904988
RG         2050
DM         13.800
DE         2.00
TE         294.0
D1         0.40000001
D11        0.03000000
===== CHANNEL f1 =====
NUC1       13C
P1         15.00
PLW1       107.15190125
SFO1       125.761354689
===== CHANNEL f2 =====
CDEPRG [2] waltz16
PCPD2      70.00
PLW2       0 W
SFO2       0.30199519
===== Processing parameters =====
SI         65536
SF         125.761354689
WDW        0
SSB        0
LB         0
GB         0
PC         1.00
    
```

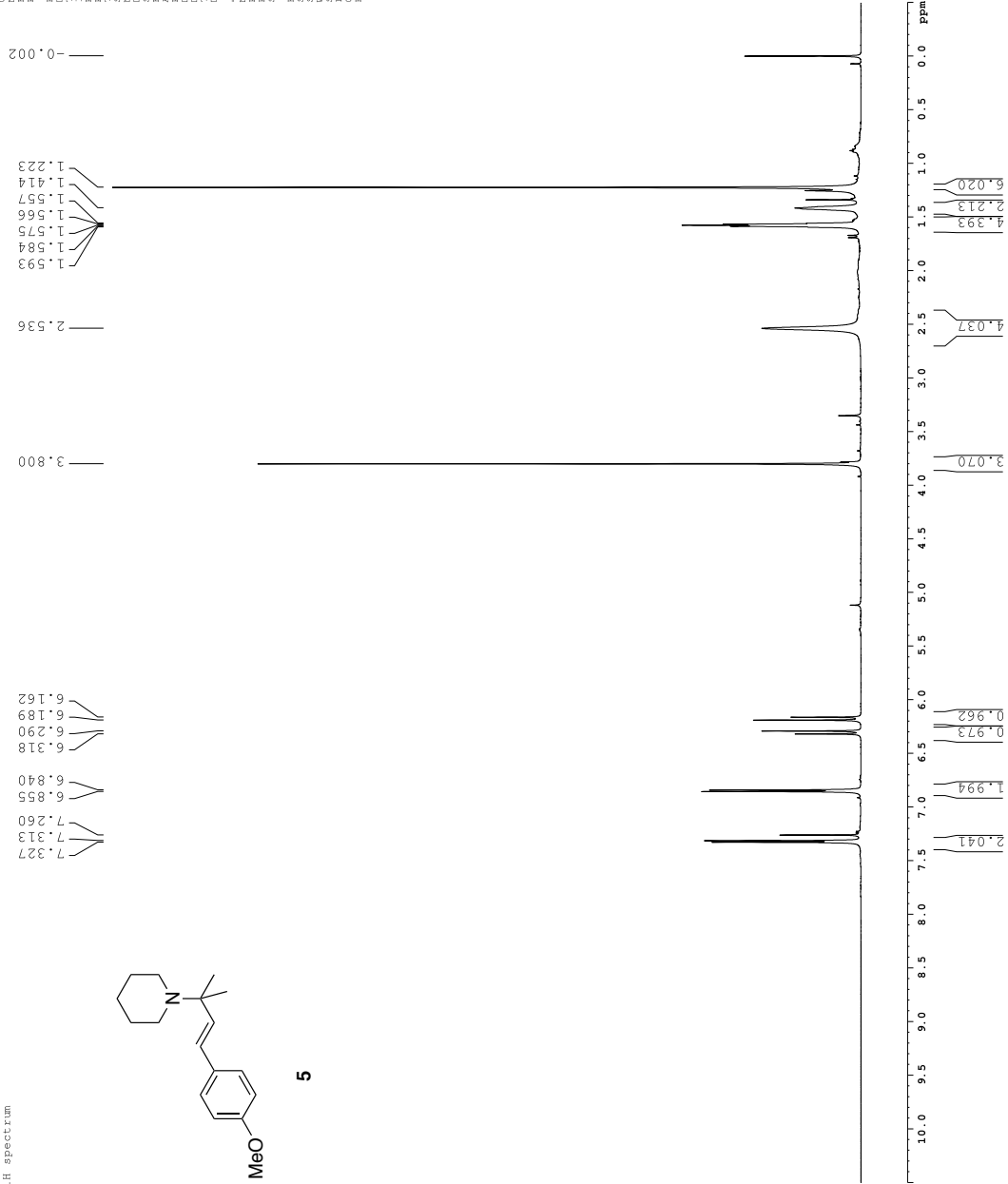


1H spectrum

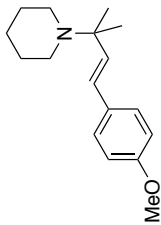
Current Data Parameters
NAME: DATA1318018
EXPNO: 1
PROCNO: 1
F2 - Acquisition Parameters
Time: 12.42
INSTRUM: av600
PULPROG: zgpg30
SOLVENT: CDCl3
NS: 8
DSH: 9615.85 Hz
FIDRES: 0.098042 Hz
RG: 5.000 Hz
AQ: 80.6 sec
DM: 52.000 usec
TE: 292.5 K
DE: 0.10000000 sec
===== CHANNEL f1 =====
NUC1: 13C
P1: 8.00 usec
PL1: 23.0441956 W
SFO1: 60.1320000 MHz
F2 - Processing parameters
SF: 600.1300354 MHz
WDW: EM
SSB: 0
LB: 0.30 Hz
GB: 0
PC: 1.00



5



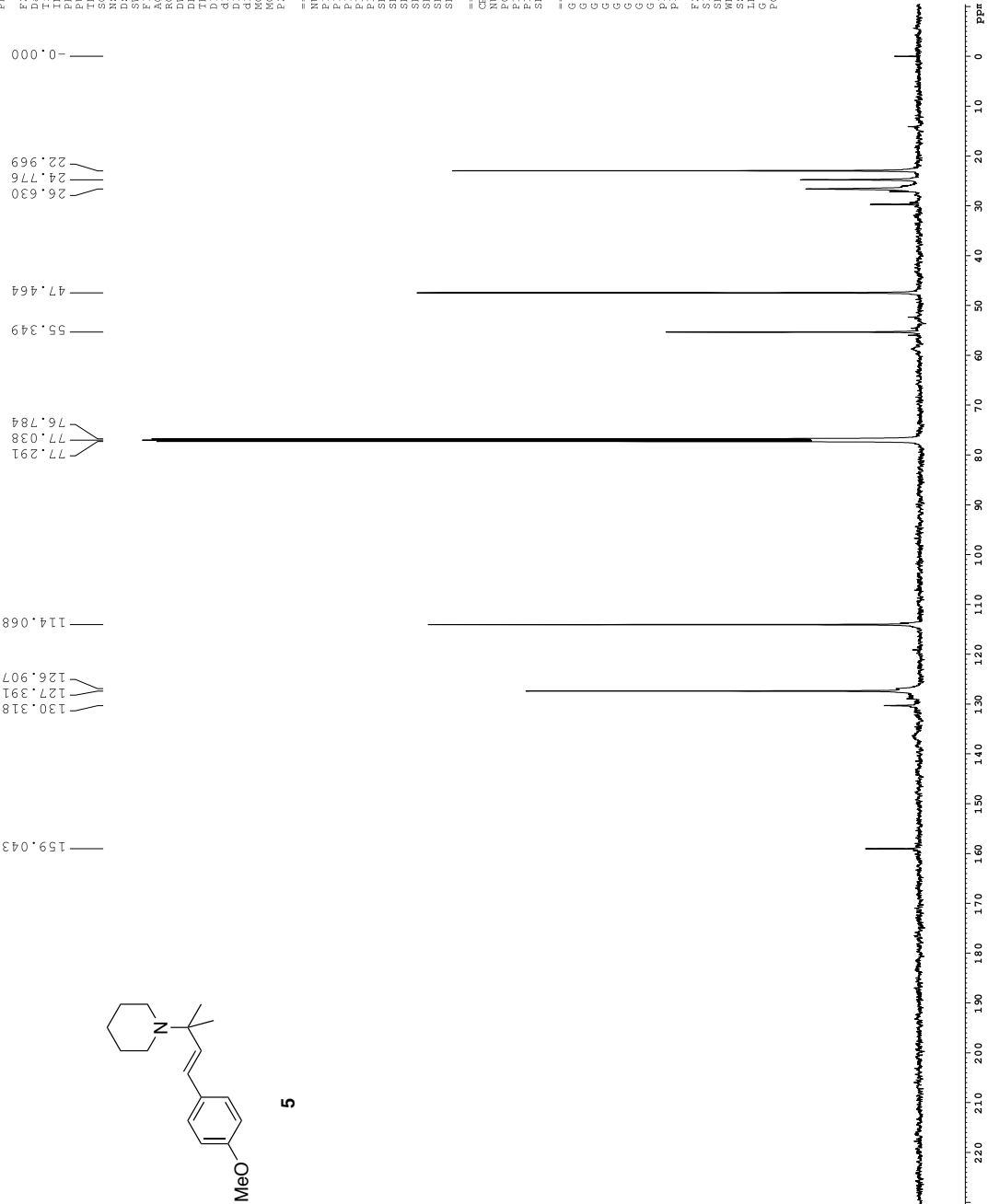
Z-restored spin-echo 13C spectrum with 1H decoupling



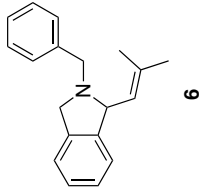
5

```

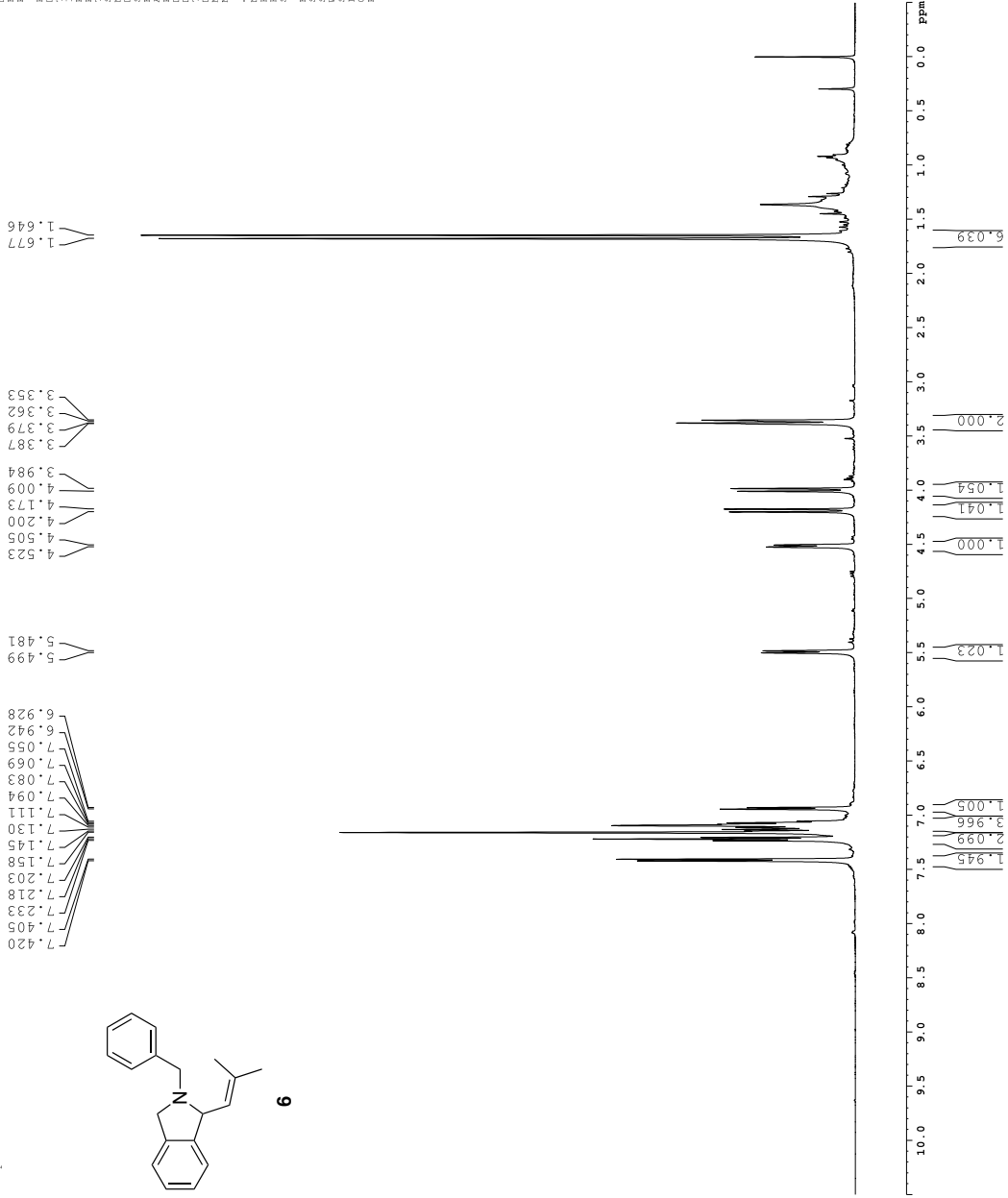
Current Data Parameters
NAME CEA-I-189prodcr
EXPNO 4
PROCNO 1
F2 - Acquisition Parameters
Date_ 20111120
Time 8.44
TimeOff 0
PROBHD 5 mm CPYCI 1H-
PULPROG SpineEcho309p.
TD 65536
SFOFF 0
NS 277
DS 16
RG 3032.031
SRH 0
AQ 0.02584
RG 1.0813440
RG 7298.2
DM 16.500
TE 313.0
D1 1.50000000
d11 0.03000000
d12 0.00290000
d17 0.00290000
MCREST 0 sec. 0.0019000
MORCK 0.01500000
P2 31.00
===== CHANNEL F1 =====
NUC1 13C
P1 1
P2 1
P3 5.50
P4 2000.00
P5 120.00
P6 120.00
P7 125.794500
P8 3.20
P9 3.20
SFNAM[1] CPFG0.5,20.1
SFNAM[2] CPFG60comp.4
SFOFF[1] 0 Hz
SFOFF[2] 0 Hz
===== CHANNEL F2 =====
CPDPRG[2] waltz16
NUC2 1H
P1 1
P2 100.00
P3 24.00
P4 24.00
P5 500.2225011
SFO2 500.2225011
===== GRADIENT CHANNEL
GPNAM[1] SINE.100
GPNAM[2] SINE.100
GEX1 0 %
GEX2 0 %
GFX3 0 %
GFY1 0 %
GFY2 0 %
GEZ1 30.00
GEZ2 50.00
GFI1 1000.00
GFI2 1000.00
P16 1000.00
F2 - Processing Parameters
SF 125.760189
WDW EM
SSB 0
GB 0
PC 2.00
  
```



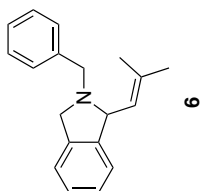
1H spectrum



Current Data Parameters
NAME: 04-11-4ppm2_1sum2
EXPNO: 2
PROCNO: 1
F2 - Acquisition Parameters
Time: 20.913 s
INSTRUM: spect
PULPROG: zgpg30
SOLVENT: DMSO
NS: 16
DSH: 8012.820 Hz
FIDRES: 0.098043 Hz
RG: 5.039627 s
AQ: 62.400 usec
RG: 298.0 K
TE: 1.00000000 sec
MCNRF1: 0.01500000 sec
----- CHANNEL f1 -----
NUC1: 1H
P1: 7.160 usec
PL1: 1.60 dB
SFO1: 500.2235015 MHz
F2 - Processing parameters
SI: 32768
SF: 500.220021 MHz
WDW: EM
SSB: 0
GB: 0
PC: 4.00



Z-restored spin-echo 13C spectrum with 1H decoupling



```

Current Data Parameters
NAME  CEA-II-41prodco
EXPNO  3
PROCNO  1

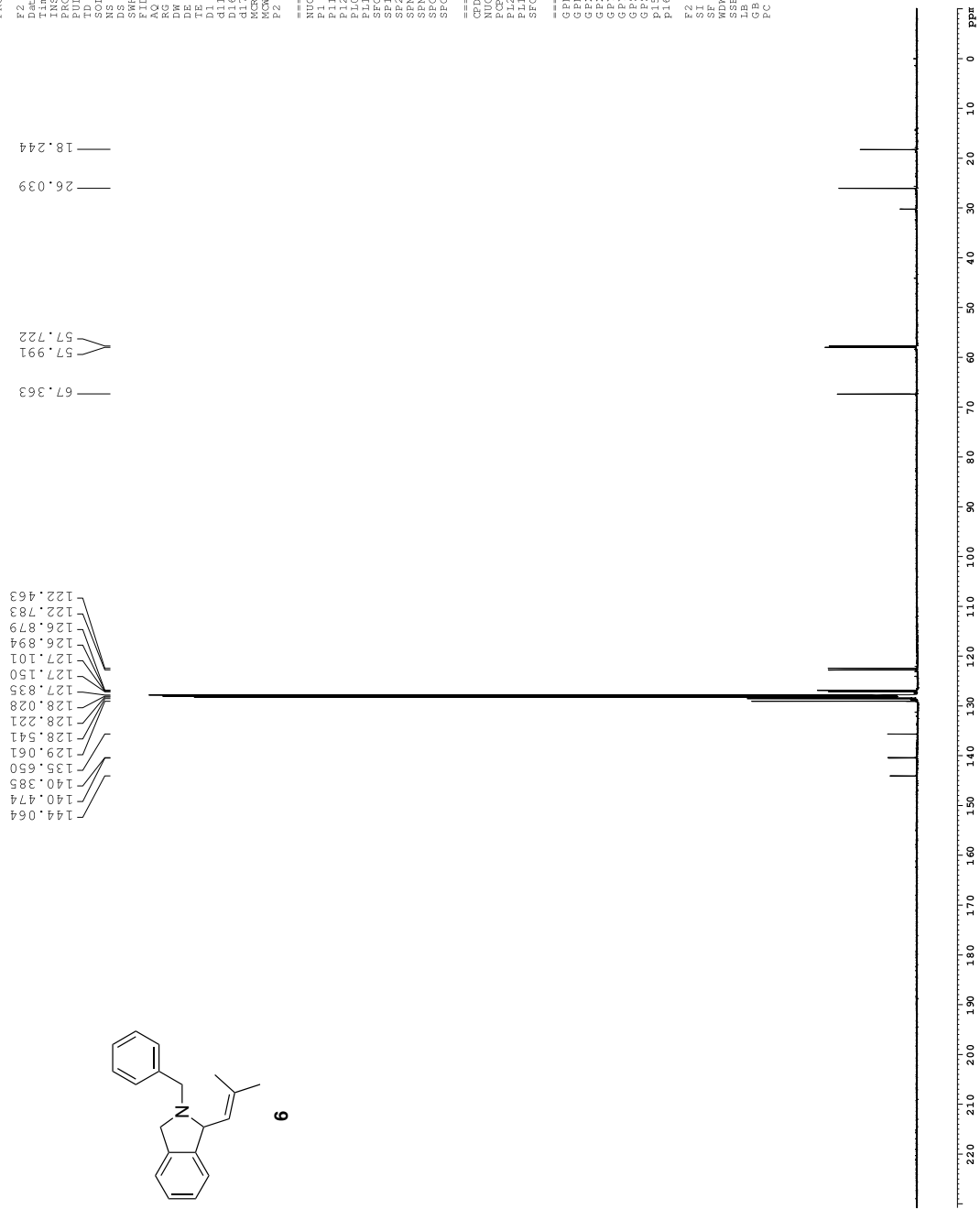
F2 - Acquisition Parameters
Date_  20111118
Time  9.37
Time0  9.37
PROBHD  5 mm CPYCI 1H-
PULPROG  Spinecho930gp.
TD  65536
SOLVENT  CDCl3
NS  720
DS  16
SWH  30302.031
AQ  0.06288
RG  1.0813440
RG  51160.6
DM  16.500
DE  288.0
TE  298.0
D1  0.25000000
d11  0.03000000
d12  0.03000000
d17  0.00290000
d18  0.00290000
MCOREST  0 sec. 0.0019000
MORAK  0.01500000
P2  31.00

===== CHANNEL f1 =====
NUC1  13C
P1  15.50
P2  15.50
P10  2000.00
P12  2000.00
P13  120.00
P14  120.00
P15  125.794500
P16  125.794500
P17  3.20
P18  3.20
SFO1  125.7600000
SFO2  500.1360000
SFO3  500.1360000
SFO4  500.1360000
SFO5  500.1360000
SFO6  500.1360000
SFO7  500.1360000
SFO8  500.1360000
SFO9  500.1360000
SFO10  500.1360000
SFO11  500.1360000
SFO12  500.1360000
SFO13  500.1360000
SFO14  500.1360000
SFO15  500.1360000
SFO16  500.1360000
SFO17  500.1360000
SFO18  500.1360000
SFO19  500.1360000
SFO20  500.1360000
SFO21  500.1360000
SFO22  500.1360000
SFO23  500.1360000
SFO24  500.1360000
SFO25  500.1360000
SFO26  500.1360000
SFO27  500.1360000
SFO28  500.1360000
SFO29  500.1360000
SFO30  500.1360000
SFO31  500.1360000
SFO32  500.1360000
SFO33  500.1360000
SFO34  500.1360000
SFO35  500.1360000
SFO36  500.1360000
SFO37  500.1360000
SFO38  500.1360000
SFO39  500.1360000
SFO40  500.1360000
SFO41  500.1360000
SFO42  500.1360000
SFO43  500.1360000
SFO44  500.1360000
SFO45  500.1360000
SFO46  500.1360000
SFO47  500.1360000
SFO48  500.1360000
SFO49  500.1360000
SFO50  500.1360000
SFO51  500.1360000
SFO52  500.1360000
SFO53  500.1360000
SFO54  500.1360000
SFO55  500.1360000
SFO56  500.1360000
SFO57  500.1360000
SFO58  500.1360000
SFO59  500.1360000
SFO60  500.1360000
SFO61  500.1360000
SFO62  500.1360000
SFO63  500.1360000
SFO64  500.1360000
SFO65  500.1360000
SFO66  500.1360000
SFO67  500.1360000
SFO68  500.1360000
SFO69  500.1360000
SFO70  500.1360000
SFO71  500.1360000
SFO72  500.1360000
SFO73  500.1360000
SFO74  500.1360000
SFO75  500.1360000
SFO76  500.1360000
SFO77  500.1360000
SFO78  500.1360000
SFO79  500.1360000
SFO80  500.1360000
SFO81  500.1360000
SFO82  500.1360000
SFO83  500.1360000
SFO84  500.1360000
SFO85  500.1360000
SFO86  500.1360000
SFO87  500.1360000
SFO88  500.1360000
SFO89  500.1360000
SFO90  500.1360000
SFO91  500.1360000
SFO92  500.1360000
SFO93  500.1360000
SFO94  500.1360000
SFO95  500.1360000
SFO96  500.1360000
SFO97  500.1360000
SFO98  500.1360000
SFO99  500.1360000
SFO100  500.1360000

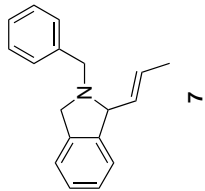
===== CHANNEL f2 =====
CPDPRG12  waltz16
NUC2  1H
PCPD2  100.00
P1  2.00
P2  2.00
P10  2.00
P12  2.00
P13  2.00
P14  2.00
P15  2.00
P16  2.00
P17  2.00
P18  2.00
P19  2.00
P20  2.00
P21  2.00
P22  2.00
P23  2.00
P24  2.00
P25  2.00
P26  2.00
P27  2.00
P28  2.00
P29  2.00
P30  2.00
P31  2.00
P32  2.00
P33  2.00
P34  2.00
P35  2.00
P36  2.00
P37  2.00
P38  2.00
P39  2.00
P40  2.00
P41  2.00
P42  2.00
P43  2.00
P44  2.00
P45  2.00
P46  2.00
P47  2.00
P48  2.00
P49  2.00
P50  2.00
P51  2.00
P52  2.00
P53  2.00
P54  2.00
P55  2.00
P56  2.00
P57  2.00
P58  2.00
P59  2.00
P60  2.00
P61  2.00
P62  2.00
P63  2.00
P64  2.00
P65  2.00
P66  2.00
P67  2.00
P68  2.00
P69  2.00
P70  2.00
P71  2.00
P72  2.00
P73  2.00
P74  2.00
P75  2.00
P76  2.00
P77  2.00
P78  2.00
P79  2.00
P80  2.00
P81  2.00
P82  2.00
P83  2.00
P84  2.00
P85  2.00
P86  2.00
P87  2.00
P88  2.00
P89  2.00
P90  2.00
P91  2.00
P92  2.00
P93  2.00
P94  2.00
P95  2.00
P96  2.00
P97  2.00
P98  2.00
P99  2.00
P100  2.00

===== GRADIENT CHANNEL =====
GNAME1  0 %
GNAME2  0 %
GX1  0 %
GX2  0 %
GY1  0 %
GY2  0 %
GZ1  30.00
GZ2  50.00
GZ3  50.00
GZ4  50.00
GZ5  50.00
GZ6  50.00
GZ7  50.00
GZ8  50.00
GZ9  50.00
GZ10  50.00
GZ11  50.00
GZ12  50.00
GZ13  50.00
GZ14  50.00
GZ15  50.00
GZ16  1000.00

F2 - Processing Parameters
SI  32768
SF  125.7603784
WDW  EM
SSB  0
GB  0
PC  2.00
    
```

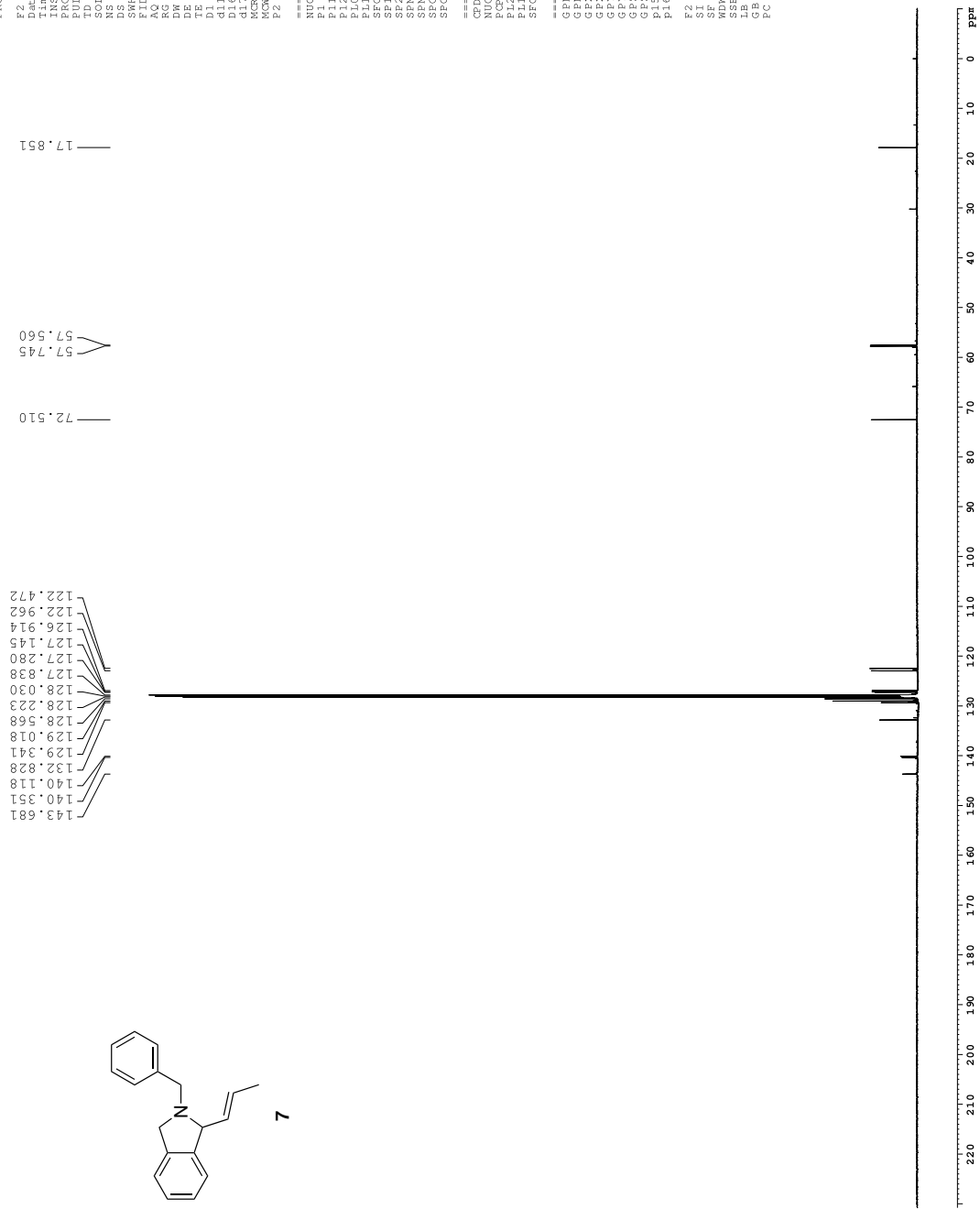


Z-restored spin-echo 13C spectrum with 1H decoupling

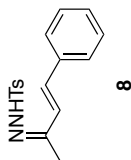


```

Current Data Parameters
NAME      CFA-II-42prod
EXPNO     3
PROCNO    1
F2 - Acquisition Parameters
Date_     20111117
Time      16.23
TimeOff   1.00
PROBHD    5 mm CPFGH-1H-
PULPROG   SpinEcho30gp.
TD        65536
SFOFF     0 Hz
RG        800
DS        16
SRH       3030.031
AQ        0.00000000
RG        1.0813440
RG        6502
DM        16.500
TE        298.0
D1        1.00000000
d11       0.03000000
d12       0.00000000
d13       0.00000000
d14       0.00000000
d15       0.00000000
d16       0.00000000
d17       0.00000000
d18       0.00000000
d19       0.00000000
d20       0.00000000
MCREST    0 sec. 00019600
MORF      0.01500000
P2        31.00
===== CHANNEL F1 =====
NUC1      13C
P1        5.50
P2        5.50
P3        2000.00
P4        2000.00
P5        120.00
P6        120.00
P7        125.7941500
P8        3.20
P9        3.20
P10       3.20
P11       3.20
P12       3.20
P13       3.20
P14       3.20
P15       3.20
P16       3.20
SFOFF[1] 0 Hz 60comp.4
SFOFF[2] 0 Hz
SFOFF[3] 0 Hz
SFOFF[4] 0 Hz
===== CHANNEL F2 =====
CPDPRG12  waltz16
NUC2      13C
P1        100.00
P2        100.00
P3        24.00
P4        24.00
P5        500.2225011
P6        500.2225011
P7        500.2225011
P8        500.2225011
P9        500.2225011
P10       500.2225011
P11       500.2225011
P12       500.2225011
P13       500.2225011
P14       500.2225011
P15       500.2225011
P16       500.2225011
===== GRADIENT CHANNEL =====
GPM1[1]   0 %
GPM1[2]   0 %
GPM1[3]   0 %
GPM1[4]   0 %
GPM1[5]   0 %
GPM1[6]   0 %
GPM1[7]   0 %
GPM1[8]   0 %
GPM1[9]   0 %
GPM1[10]  0 %
GPM1[11]  0 %
GPM1[12]  0 %
GPM1[13]  0 %
GPM1[14]  0 %
GPM1[15]  0 %
GPM1[16]  0 %
GPM1[17]  0 %
GPM1[18]  0 %
GPM1[19]  0 %
GPM1[20]  0 %
GPM1[21]  0 %
GPM1[22]  0 %
GPM1[23]  0 %
GPM1[24]  0 %
GPM1[25]  0 %
GPM1[26]  0 %
GPM1[27]  0 %
GPM1[28]  0 %
GPM1[29]  0 %
GPM1[30]  0 %
GPM1[31]  0 %
GPM1[32]  0 %
GPM1[33]  0 %
GPM1[34]  0 %
GPM1[35]  0 %
GPM1[36]  0 %
GPM1[37]  0 %
GPM1[38]  0 %
GPM1[39]  0 %
GPM1[40]  0 %
GPM1[41]  0 %
GPM1[42]  0 %
GPM1[43]  0 %
GPM1[44]  0 %
GPM1[45]  0 %
GPM1[46]  0 %
GPM1[47]  0 %
GPM1[48]  0 %
GPM1[49]  0 %
GPM1[50]  0 %
GPM1[51]  0 %
GPM1[52]  0 %
GPM1[53]  0 %
GPM1[54]  0 %
GPM1[55]  0 %
GPM1[56]  0 %
GPM1[57]  0 %
GPM1[58]  0 %
GPM1[59]  0 %
GPM1[60]  0 %
GPM1[61]  0 %
GPM1[62]  0 %
GPM1[63]  0 %
GPM1[64]  0 %
GPM1[65]  0 %
GPM1[66]  0 %
GPM1[67]  0 %
GPM1[68]  0 %
GPM1[69]  0 %
GPM1[70]  0 %
GPM1[71]  0 %
GPM1[72]  0 %
GPM1[73]  0 %
GPM1[74]  0 %
GPM1[75]  0 %
GPM1[76]  0 %
GPM1[77]  0 %
GPM1[78]  0 %
GPM1[79]  0 %
GPM1[80]  0 %
GPM1[81]  0 %
GPM1[82]  0 %
GPM1[83]  0 %
GPM1[84]  0 %
GPM1[85]  0 %
GPM1[86]  0 %
GPM1[87]  0 %
GPM1[88]  0 %
GPM1[89]  0 %
GPM1[90]  0 %
GPM1[91]  0 %
GPM1[92]  0 %
GPM1[93]  0 %
GPM1[94]  0 %
GPM1[95]  0 %
GPM1[96]  0 %
GPM1[97]  0 %
GPM1[98]  0 %
GPM1[99]  0 %
GPM1[100] 0 %
===== Processing Parameters =====
SI        32768
SF        125.7603781
WDW       EM
SSB       0
GB        0
PC        2.00
  
```



Z-restored spin-echo 13C spectrum with 1H decoupling



```

Current Data Parameters
NAME      CEA-III-10crude
EXPNO     2
PROCNO    1

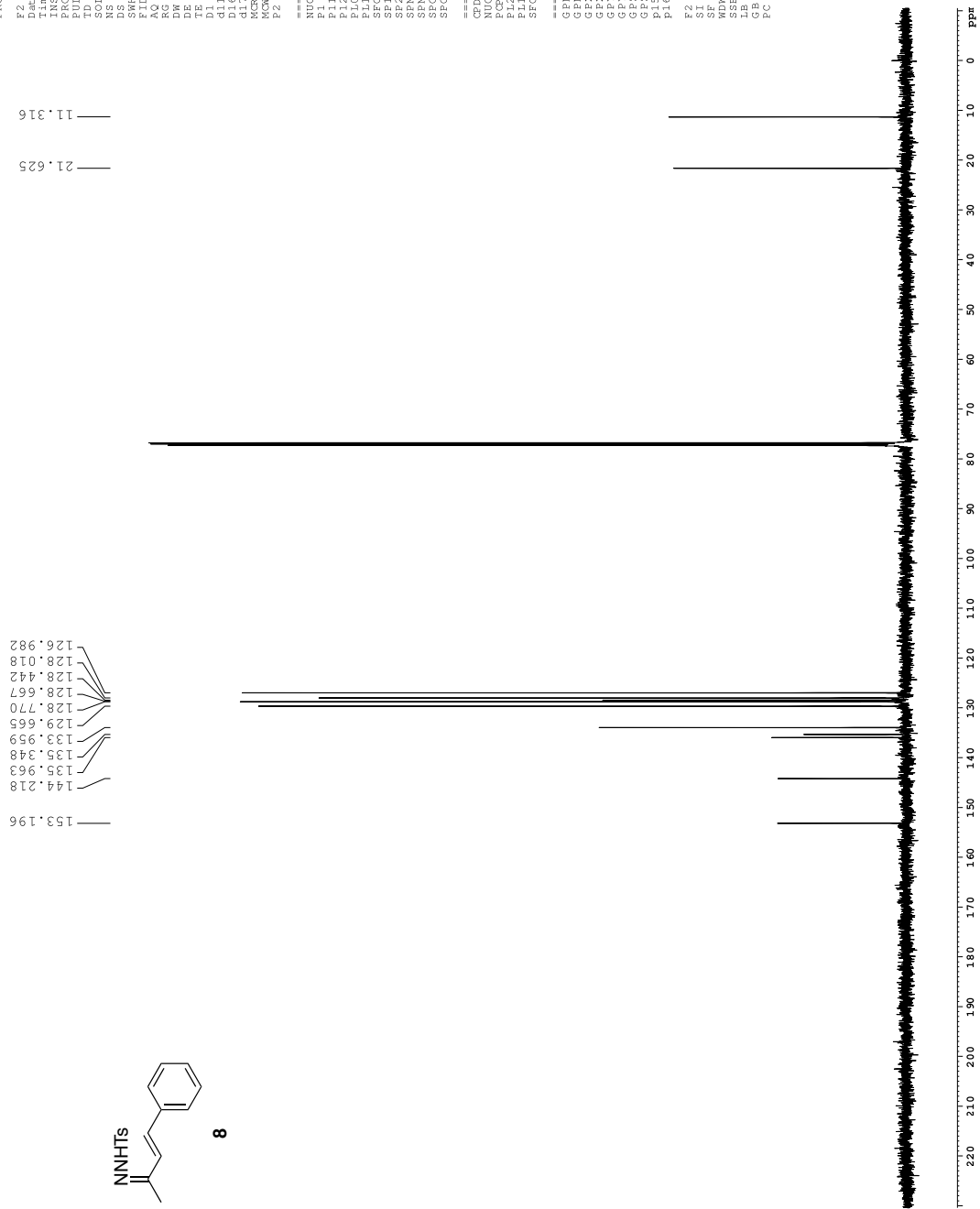
F2 - Acquisition Parameters
Date_     20130402
Time      15.40
INSTRUM   spect
PROBHD    5 mm CPXI 1H-
PULPROG   Spinecho30gp
TD         65536
SFOFF     0 Hz
NS         400
DS         16
SR        3030.031
AQ         0.02588
RG         1.0813440
RG         11585.2
DW         16.500
TE         298.0
D1         0.25000000
d11        0.03000000
d12        0.03000000
d13        0.00290000
d14        0.00290000
d15        0.00290000
d16        0.00290000
d17        0.00290000
d18        0.00290000
d19        0.00290000
d20        0.00290000
MCRET     0 sec. 0.0019000
MORPR     0.01500000
P2         31.00

===== CHANNEL F1 =====
NUC1       13C
P1         5.50
P2         2000.00
P10        120.00
P11        125.7941500
P12        125.7941500
P13        125.7941500
P14        125.7941500
P15        125.7941500
P16        125.7941500
SFOFF      0 Hz
SFOFF2     0 Hz
SFOFF3     0 Hz
SFOFF4     0 Hz
SFOFF5     0 Hz
SFOFF6     0 Hz
SFOFF7     0 Hz
SFOFF8     0 Hz
SFOFF9     0 Hz
SFOFF10    0 Hz
SFOFF11    0 Hz
SFOFF12    0 Hz
SFOFF13    0 Hz
SFOFF14    0 Hz
SFOFF15    0 Hz
SFOFF16    0 Hz
SFOFF17    0 Hz
SFOFF18    0 Hz
SFOFF19    0 Hz
SFOFF20    0 Hz
SFOFF21    0 Hz
SFOFF22    0 Hz
SFOFF23    0 Hz
SFOFF24    0 Hz
SFOFF25    0 Hz
SFOFF26    0 Hz
SFOFF27    0 Hz
SFOFF28    0 Hz
SFOFF29    0 Hz
SFOFF30    0 Hz
SFOFF31    0 Hz
SFOFF32    0 Hz
SFOFF33    0 Hz
SFOFF34    0 Hz
SFOFF35    0 Hz
SFOFF36    0 Hz
SFOFF37    0 Hz
SFOFF38    0 Hz
SFOFF39    0 Hz
SFOFF40    0 Hz
SFOFF41    0 Hz
SFOFF42    0 Hz
SFOFF43    0 Hz
SFOFF44    0 Hz
SFOFF45    0 Hz
SFOFF46    0 Hz
SFOFF47    0 Hz
SFOFF48    0 Hz
SFOFF49    0 Hz
SFOFF50    0 Hz
SFOFF51    0 Hz
SFOFF52    0 Hz
SFOFF53    0 Hz
SFOFF54    0 Hz
SFOFF55    0 Hz
SFOFF56    0 Hz
SFOFF57    0 Hz
SFOFF58    0 Hz
SFOFF59    0 Hz
SFOFF60    0 Hz
SFOFF61    0 Hz
SFOFF62    0 Hz
SFOFF63    0 Hz
SFOFF64    0 Hz
SFOFF65    0 Hz
SFOFF66    0 Hz
SFOFF67    0 Hz
SFOFF68    0 Hz
SFOFF69    0 Hz
SFOFF70    0 Hz
SFOFF71    0 Hz
SFOFF72    0 Hz
SFOFF73    0 Hz
SFOFF74    0 Hz
SFOFF75    0 Hz
SFOFF76    0 Hz
SFOFF77    0 Hz
SFOFF78    0 Hz
SFOFF79    0 Hz
SFOFF80    0 Hz
SFOFF81    0 Hz
SFOFF82    0 Hz
SFOFF83    0 Hz
SFOFF84    0 Hz
SFOFF85    0 Hz
SFOFF86    0 Hz
SFOFF87    0 Hz
SFOFF88    0 Hz
SFOFF89    0 Hz
SFOFF90    0 Hz
SFOFF91    0 Hz
SFOFF92    0 Hz
SFOFF93    0 Hz
SFOFF94    0 Hz
SFOFF95    0 Hz
SFOFF96    0 Hz
SFOFF97    0 Hz
SFOFF98    0 Hz
SFOFF99    0 Hz
SFOFF100   0 Hz

===== CHANNEL F2 =====
CPDPRG12  waltz16
NUC2       1H
PCPD2     100.00
P1         2.00
P2         2.00
P10        120.00
P11        125.7941500
P12        125.7941500
P13        125.7941500
P14        125.7941500
P15        125.7941500
P16        125.7941500
SFOFF      0 Hz
SFOFF2     0 Hz
SFOFF3     0 Hz
SFOFF4     0 Hz
SFOFF5     0 Hz
SFOFF6     0 Hz
SFOFF7     0 Hz
SFOFF8     0 Hz
SFOFF9     0 Hz
SFOFF10    0 Hz
SFOFF11    0 Hz
SFOFF12    0 Hz
SFOFF13    0 Hz
SFOFF14    0 Hz
SFOFF15    0 Hz
SFOFF16    0 Hz
SFOFF17    0 Hz
SFOFF18    0 Hz
SFOFF19    0 Hz
SFOFF20    0 Hz
SFOFF21    0 Hz
SFOFF22    0 Hz
SFOFF23    0 Hz
SFOFF24    0 Hz
SFOFF25    0 Hz
SFOFF26    0 Hz
SFOFF27    0 Hz
SFOFF28    0 Hz
SFOFF29    0 Hz
SFOFF30    0 Hz
SFOFF31    0 Hz
SFOFF32    0 Hz
SFOFF33    0 Hz
SFOFF34    0 Hz
SFOFF35    0 Hz
SFOFF36    0 Hz
SFOFF37    0 Hz
SFOFF38    0 Hz
SFOFF39    0 Hz
SFOFF40    0 Hz
SFOFF41    0 Hz
SFOFF42    0 Hz
SFOFF43    0 Hz
SFOFF44    0 Hz
SFOFF45    0 Hz
SFOFF46    0 Hz
SFOFF47    0 Hz
SFOFF48    0 Hz
SFOFF49    0 Hz
SFOFF50    0 Hz
SFOFF51    0 Hz
SFOFF52    0 Hz
SFOFF53    0 Hz
SFOFF54    0 Hz
SFOFF55    0 Hz
SFOFF56    0 Hz
SFOFF57    0 Hz
SFOFF58    0 Hz
SFOFF59    0 Hz
SFOFF60    0 Hz
SFOFF61    0 Hz
SFOFF62    0 Hz
SFOFF63    0 Hz
SFOFF64    0 Hz
SFOFF65    0 Hz
SFOFF66    0 Hz
SFOFF67    0 Hz
SFOFF68    0 Hz
SFOFF69    0 Hz
SFOFF70    0 Hz
SFOFF71    0 Hz
SFOFF72    0 Hz
SFOFF73    0 Hz
SFOFF74    0 Hz
SFOFF75    0 Hz
SFOFF76    0 Hz
SFOFF77    0 Hz
SFOFF78    0 Hz
SFOFF79    0 Hz
SFOFF80    0 Hz
SFOFF81    0 Hz
SFOFF82    0 Hz
SFOFF83    0 Hz
SFOFF84    0 Hz
SFOFF85    0 Hz
SFOFF86    0 Hz
SFOFF87    0 Hz
SFOFF88    0 Hz
SFOFF89    0 Hz
SFOFF90    0 Hz
SFOFF91    0 Hz
SFOFF92    0 Hz
SFOFF93    0 Hz
SFOFF94    0 Hz
SFOFF95    0 Hz
SFOFF96    0 Hz
SFOFF97    0 Hz
SFOFF98    0 Hz
SFOFF99    0 Hz
SFOFF100   0 Hz

===== GRADIENT CHANNEL =====
GPM1[1]   SINE
GPM1[2]   SINE
GPM1[3]   SINE
GPM1[4]   SINE
GPM1[5]   SINE
GPM1[6]   SINE
GPM1[7]   SINE
GPM1[8]   SINE
GPM1[9]   SINE
GPM1[10]  SINE
GPM1[11]  SINE
GPM1[12]  SINE
GPM1[13]  SINE
GPM1[14]  SINE
GPM1[15]  SINE
GPM1[16]  SINE
GPM1[17]  SINE
GPM1[18]  SINE
GPM1[19]  SINE
GPM1[20]  SINE
GPM1[21]  SINE
GPM1[22]  SINE
GPM1[23]  SINE
GPM1[24]  SINE
GPM1[25]  SINE
GPM1[26]  SINE
GPM1[27]  SINE
GPM1[28]  SINE
GPM1[29]  SINE
GPM1[30]  SINE
GPM1[31]  SINE
GPM1[32]  SINE
GPM1[33]  SINE
GPM1[34]  SINE
GPM1[35]  SINE
GPM1[36]  SINE
GPM1[37]  SINE
GPM1[38]  SINE
GPM1[39]  SINE
GPM1[40]  SINE
GPM1[41]  SINE
GPM1[42]  SINE
GPM1[43]  SINE
GPM1[44]  SINE
GPM1[45]  SINE
GPM1[46]  SINE
GPM1[47]  SINE
GPM1[48]  SINE
GPM1[49]  SINE
GPM1[50]  SINE
GPM1[51]  SINE
GPM1[52]  SINE
GPM1[53]  SINE
GPM1[54]  SINE
GPM1[55]  SINE
GPM1[56]  SINE
GPM1[57]  SINE
GPM1[58]  SINE
GPM1[59]  SINE
GPM1[60]  SINE
GPM1[61]  SINE
GPM1[62]  SINE
GPM1[63]  SINE
GPM1[64]  SINE
GPM1[65]  SINE
GPM1[66]  SINE
GPM1[67]  SINE
GPM1[68]  SINE
GPM1[69]  SINE
GPM1[70]  SINE
GPM1[71]  SINE
GPM1[72]  SINE
GPM1[73]  SINE
GPM1[74]  SINE
GPM1[75]  SINE
GPM1[76]  SINE
GPM1[77]  SINE
GPM1[78]  SINE
GPM1[79]  SINE
GPM1[80]  SINE
GPM1[81]  SINE
GPM1[82]  SINE
GPM1[83]  SINE
GPM1[84]  SINE
GPM1[85]  SINE
GPM1[86]  SINE
GPM1[87]  SINE
GPM1[88]  SINE
GPM1[89]  SINE
GPM1[90]  SINE
GPM1[91]  SINE
GPM1[92]  SINE
GPM1[93]  SINE
GPM1[94]  SINE
GPM1[95]  SINE
GPM1[96]  SINE
GPM1[97]  SINE
GPM1[98]  SINE
GPM1[99]  SINE
GPM1[100] SINE

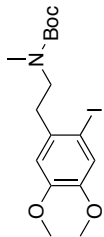
===== Processing Parameters =====
SI         32768
SF         125.760273
WDW        EM
SSB        0
GB         0
PC         2.00
  
```



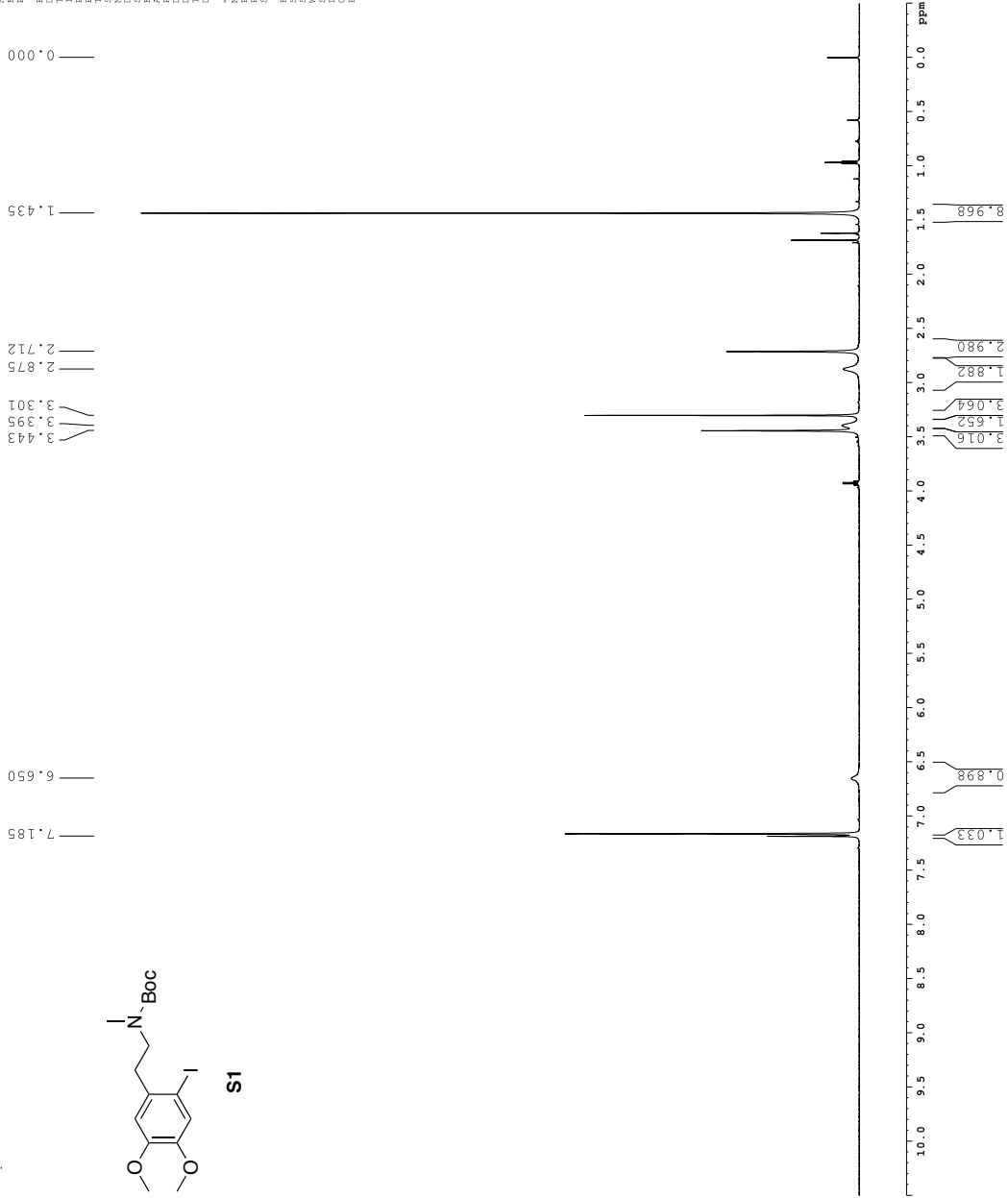
1H spectrum

```

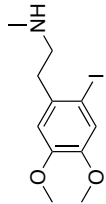
Current Data Parameters
NAME: CHN112-145-192-343K
EXPNO: 1
PROCNO: 1
F2 - Acquisition Parameters
Time: 20.117
Time: 4.11
INSTRUM: spect
PULPROG: zgpg30
SOLVENT: CDCl3
NS: 8
DS: 4
SFO: 9615.365 Hz
FIDRES: 0.099042 Hz
AQ: 0.039618 sec
RG: 812
DK: 52.000 usec
TE: 342.7 K
D1: 0.1000000 sec
***** CHANNEL f1 *****
NUC1: 13C
P1: 8.00 usec
PL1: 23.0141856 MHz
SFO1: 600.1342000 MHz
F2 - Processing parameters
SI: 32768
SF: 600.1259533 MHz
WDW: EM
SSB: 0
LB: 0.30 Hz
GB: 0
PC: 1.00
  
```



S1



1H spectrum

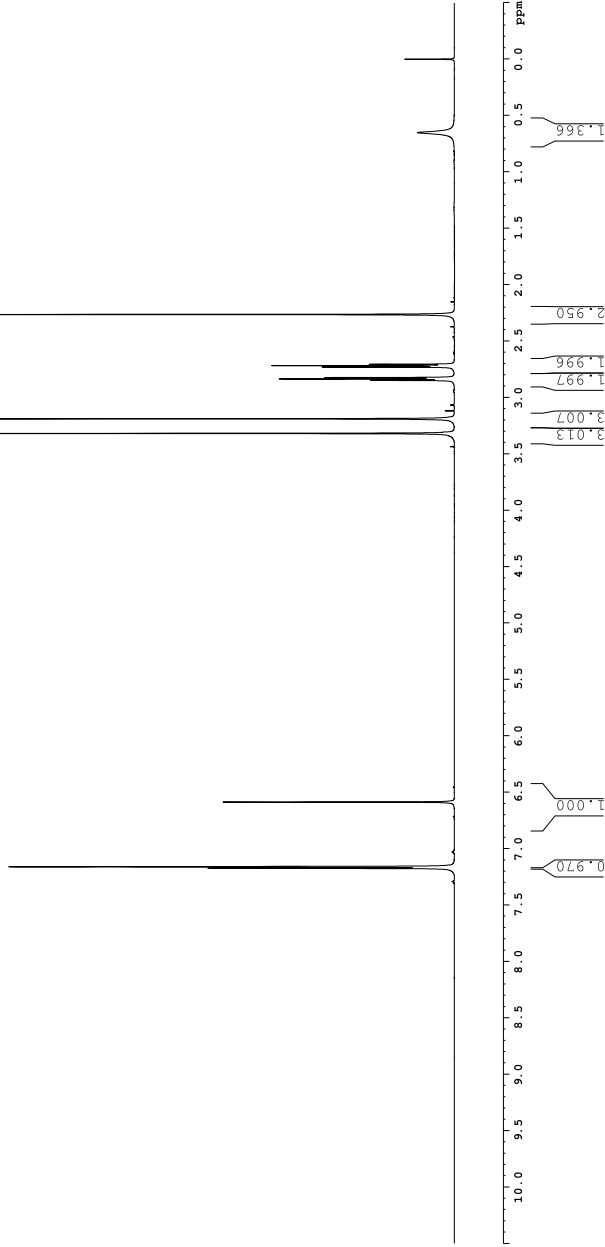


12

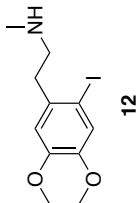
Current Data Parameters
NAME: 12-12-19-01-1 copy
EXPNO: 1
PROCNO: 1
F2 - Acquisition Parameters
Time: 17.05
INSTRUM: av600
PULPROG: zgpg30
SOLVENT: DMSO
NS: 16
DSH: 9615.785 Hz
FIDRES: 0.098042 Hz
RG: 5.000000 sec
AQ: 80.16 sec
DM: 52.000 usec
TE: 298.0 K
TD: 0.10000000 sec
----- CHANNEL f1 -----
NUC1: 1H
P1: 8.00 usec
PL1: 23.01 dB
SFO1: 600.134209 MHz
F2 - Processing parameters
SI: 65536
SF: 600.129959 MHz
RG: 655
GB: 0
PC: 1.00

2.264
2.275
2.717
2.729
2.823
2.835
2.847
3.188
3.188
3.077
1.997
1.996
2.950
0.651

7.173
6.586



Z-restored spin-echo 13C spectrum with 1H decoupling



```

Current Data Parameters
NAME      CEA-II-282co12
EXPNO     2
PROCNO    1

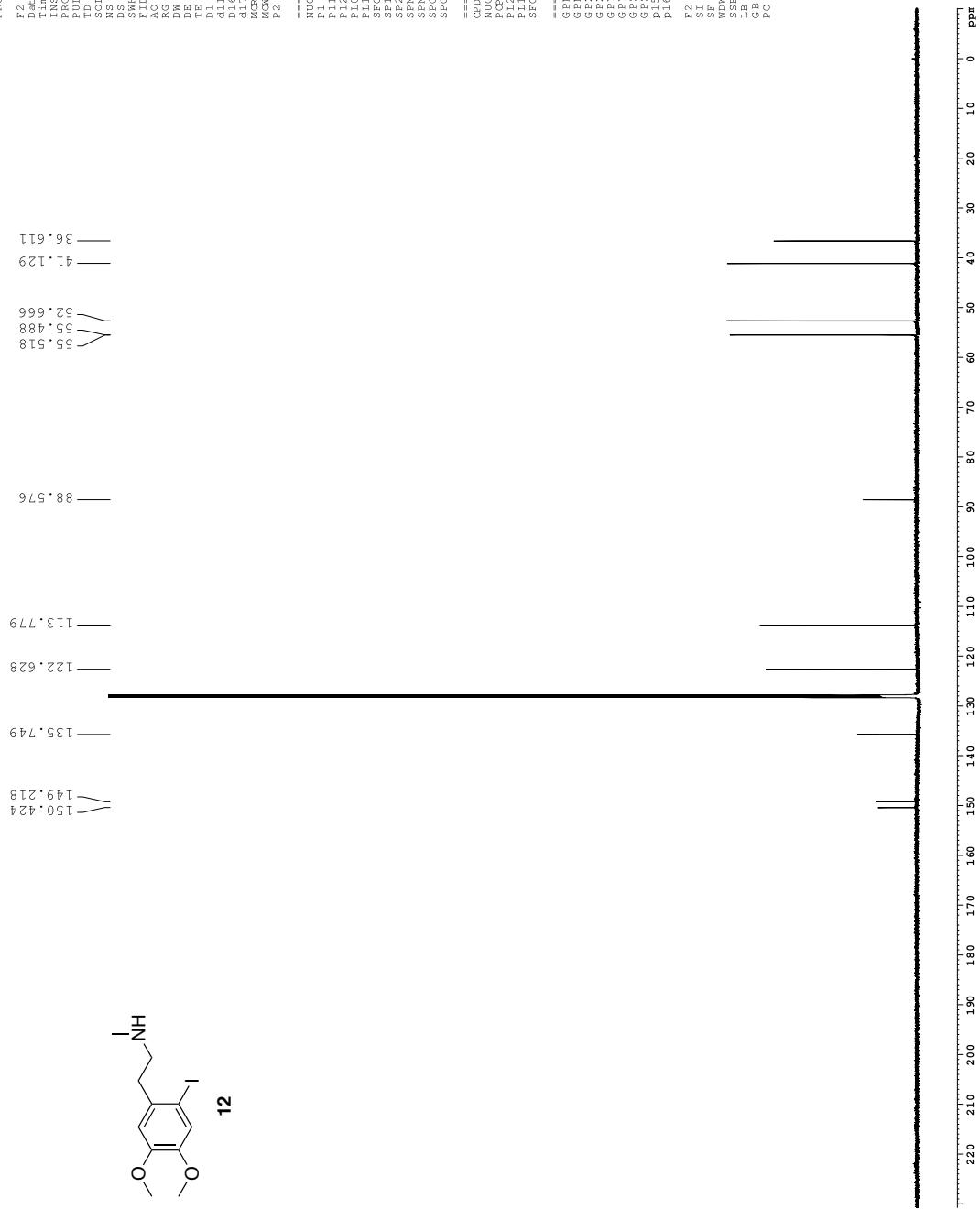
F2 - Acquisition Parameters
Date_     20130214
Time      17.12
PROBHD    5 mm CPYCI 1H-
PULPROG   SpineEcho309p.
TD         65536
SFOFF     31.00
AQ        0.25000000
RG         16.500
TE         298.0
D1         0.25000000
d11        0.03000000
d12        0.00000000
d13        0.00000000
d14        0.00000000
d15        0.00000000
d16        0.00000000
d17        0.00000000
d18        0.00000000
d19        0.00000000
d20        0.00000000
MCREST    0 sec. 00019000
MORBRK    0.01500000
P2         31.00

===== CHANNEL F1 =====
NUC1       13C
P1         1.00000000
PCPD2      100.00
P12        2000.00
P10        120.00
P11        125.7945000
SP1        3.20
SP2        3.20
SFOFF[1]   0 Hz
SFOFF[2]   0 Hz
SFOFF[3]   0 Hz
SFOFF[4]   0 Hz

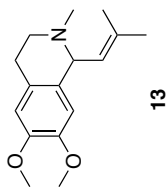
===== CHANNEL F2 =====
CPDPRG12   waltz16
NUC2       1H
PCPD2      100.00
P12        2000.00
P10        120.00
P11        125.7945000
SP1        3.20
SP2        3.20
SFOFF[1]   0 Hz
SFOFF[2]   0 Hz
SFOFF[3]   0 Hz
SFOFF[4]   0 Hz

===== GRADIENT CHANNEL =====
GNUM[1]    0
GNUM[2]    0
GFX1       0 %
GFX2       0 %
GFY1       0 %
GFY2       0 %
GEZ1       30.00
GEZ2       50.00
GFL1       1000.00
GFL2       1000.00
GFL3       1000.00
GFL4       1000.00

F2 - Processing Parameters
SI          32768
SF          125.7603793
WDW         EM
SSB         0
GB          0
PC          2.00
  
```

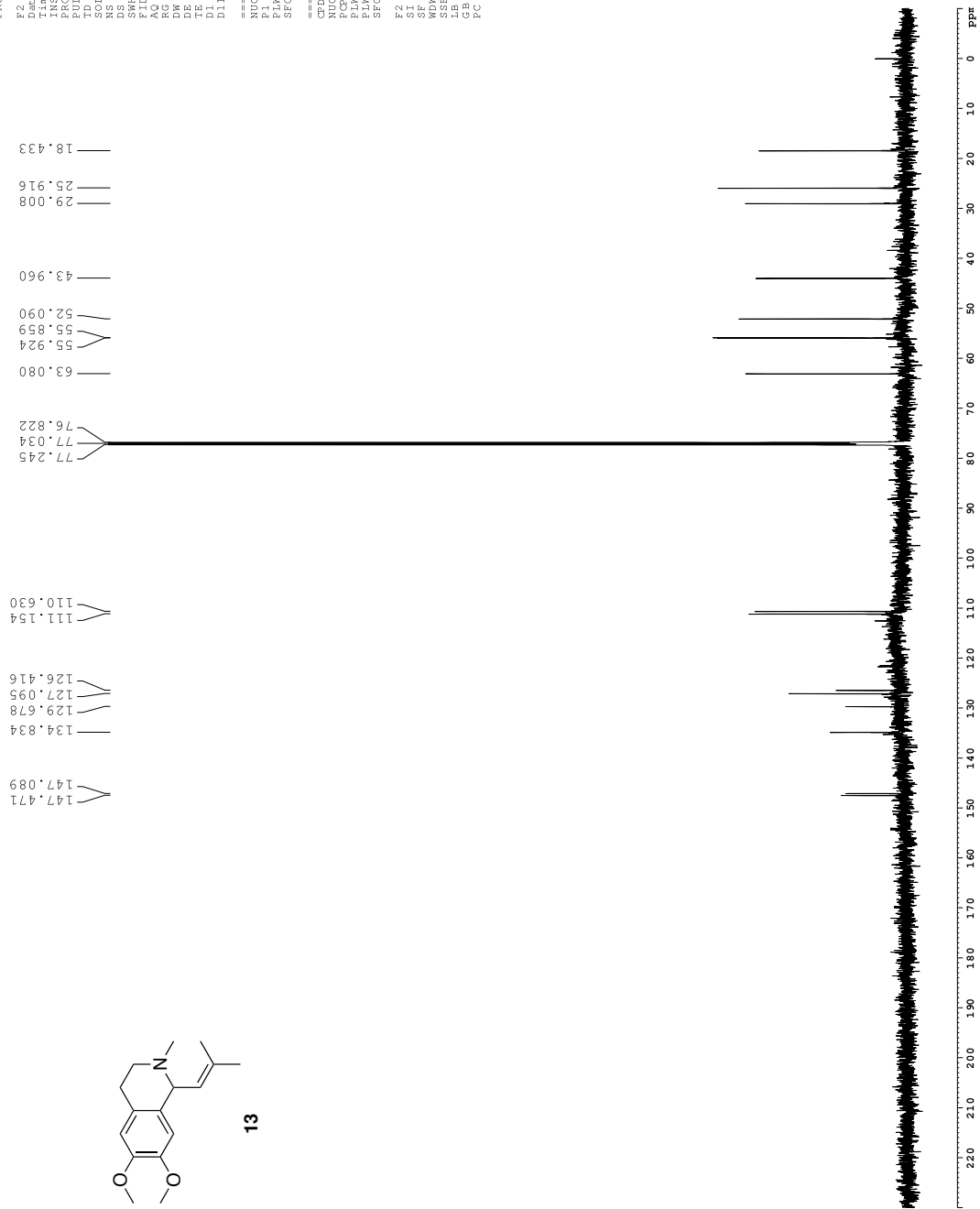


¹³C spectrum with ¹H decoupling

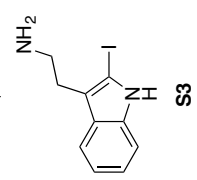
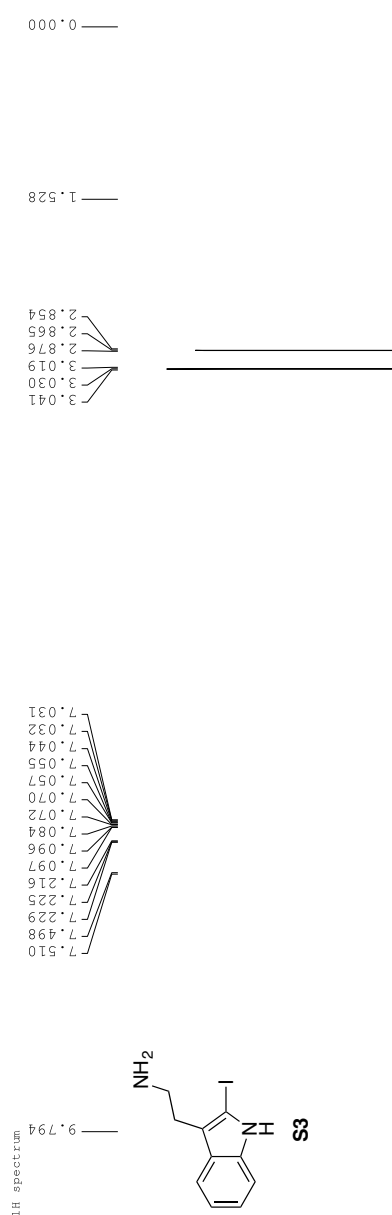


```

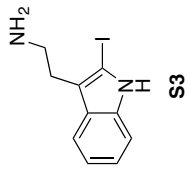
Current Data Parameters
NAME   CEA-II-284-44-9
EXPNO  1
PROCNO 1
F2 - Acquisition Parameters
Date_  20130207
Time   10.39
INSTRUM  spect
PROBHD  5 mm TBI 1H/13
PULPROG zgpg30
TD      65536
SOLVENT CDCl3
NS      800
DS      4
SWH     36231.882
AQ      0.9043982
RG      0.9043988
RG      1030
DM      13.800
DE      1.000
TE      298.0
D1      0.40000001
D11     0.03000000
===== CHANNEL f1 =====
NUC1    13C
P1      15.00
PLW1    107.15190125
SFO1    125.76134668
===== CHANNEL f2 =====
CDEPRG [2] waltz16
PCPD2   0 W
PLW2    70.00
PLW2    0.30199519
SFO2    600.1350010
F2 - Processing parameters:
SI      65536
SF      150.90281126
WDW     0
SSB     0
LB      3.00
GB      0
PC      1.00
  
```



Current Data Parameters
 NAME: 2-AMINOTOLUENE
 EXPNO: 2
 PROCNO: 1
 F2 - Acquisition Parameters
 Date_Time: 2013.12.12
 INSTRUM: av600
 PULPROG: zgpg30
 SOLVENT: CDCL3T
 NS: 16
 DS: 4
 SWH: 7812.500 Hz
 FIDRES: 0.079659 Hz
 RG: 40.3
 RC: 40.3 sec
 DR: 64.000 usec
 DE: 298.0 K
 TE: 1.00000000 sec
 DI: 1.00000000 sec
 ===== CHANNEL f1 =====
 P1: 8.00 usec
 PL1: 23.01441956 W
 SFO1: 60.130054 MHz
 F2 - Processing Parameters
 SF: 600.130055 MHz
 SSF: 0
 LB: 0.30 Hz
 PC: 1.00

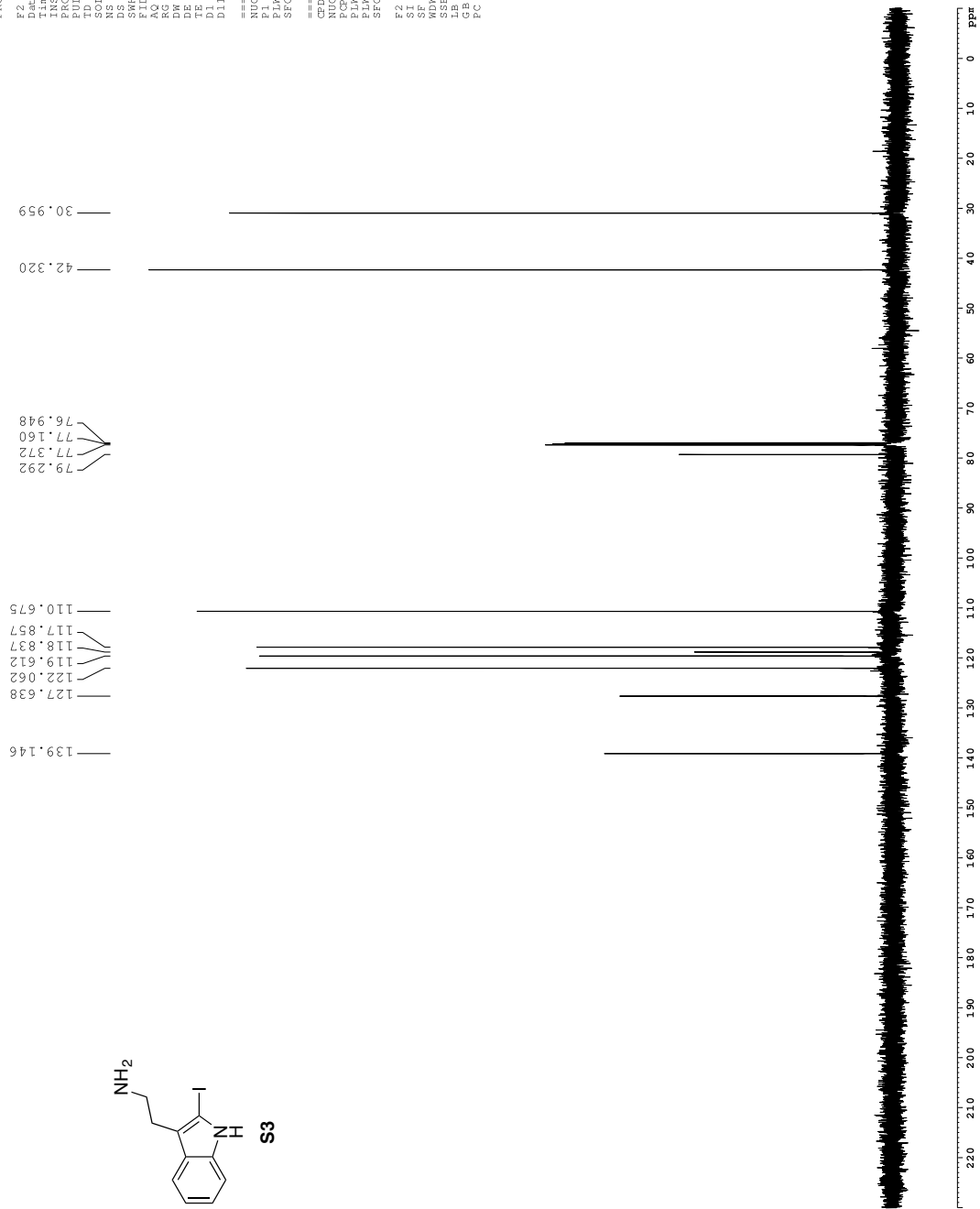


¹³C spectrum with ¹H decoupling

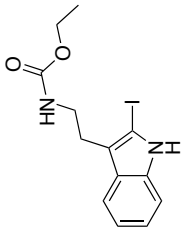


```

Current Data Parameters
NAME   CEA-II-117crude
EXPNO  3
PROCNO 1
F2 - Acquisition Parameters
Date_  20120308
Time   3.21
INSTR  spect
PROBHD 5 mm TBI 1H/13
PULPROG zgpg30
TD      65536
SFO2    125.760320
NS      240
DS      4
SRH     36231.882
AQ       0.045888
RG       0.904368
DM       13.800
TE       298.15
D1       0.40000001
D11      0.03000000
===== CHANNEL f1 =====
NUC1     13C
P1       15.00
PLW1    107.15190125
SFO1    125.760320
===== CHANNEL f2 =====
CDEPRG [2] waltz16
PCPD2   70.00
PLW2    0 W
SFO2    600.1350019
F2 - Processing parameters:
SI       65536
SF       150.9028028
WDW      0
SSB      0
LB       1.00
GB       0
PC       1.00
    
```

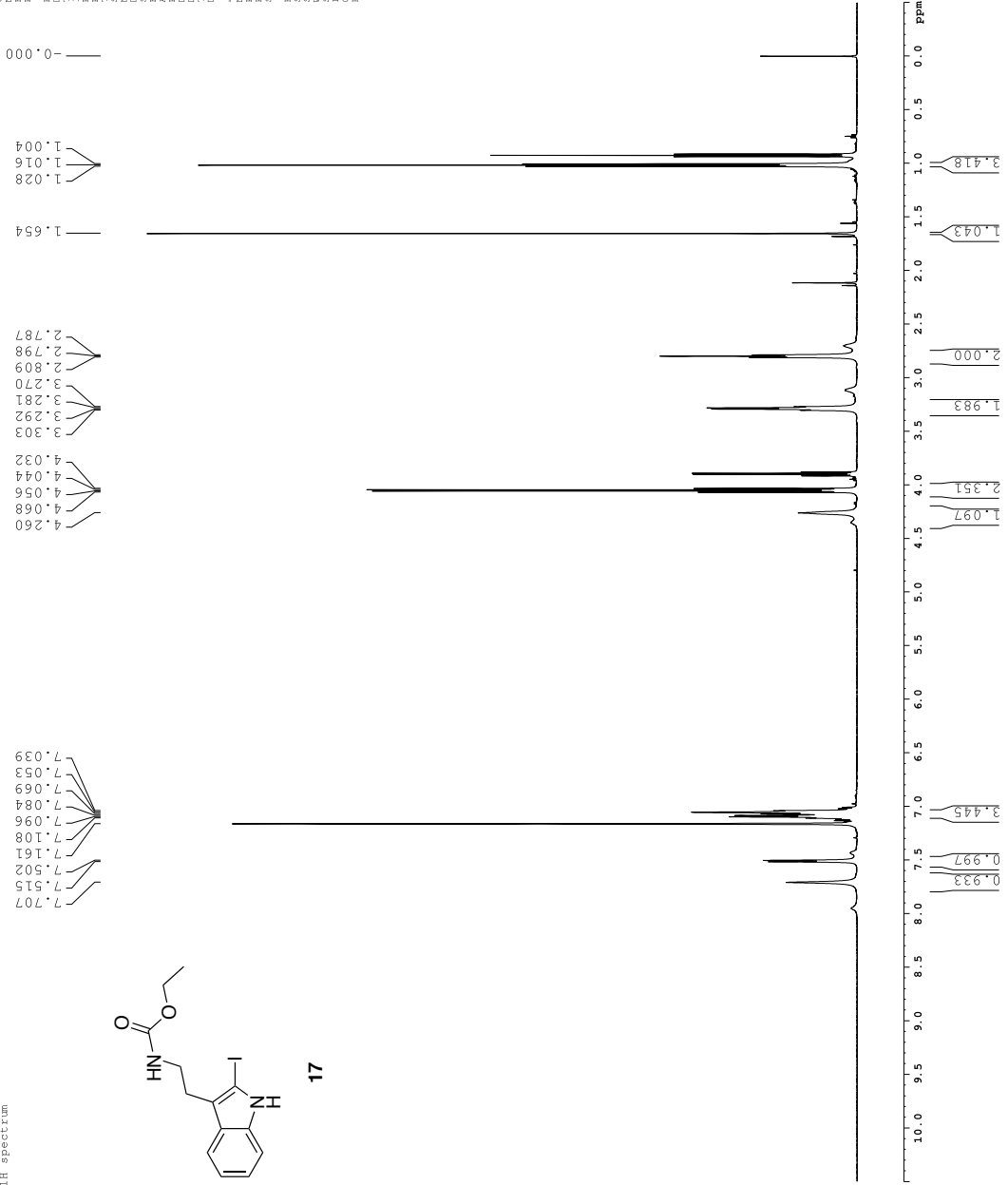


1H spectrum

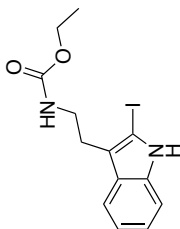


17

Current Data Parameters
NAME: 041111011_2-25-3
EXPNO: 1
PROCNO: 1
PROCGR: 1
F2 - Acquisition Parameters
Time: 5.35
INSTRUM: av600
PULPROG: 5 mm TBL 2420
SOLVENT: CDCl3
NS: 16
DSH: 9615.785 Hz
FIDRES: 0.098042 Hz
RG: 5.039645
OR: 52.000 usec
TE: 298.0 K
D1: 0.10000000 sec
----- CHANNEL f1 -----
P1: 8.00 usec
PL1: 23.0441956 W
SFO1: 60.136207 MHz
F2 - Processing Parameters
SF: 600.129956 MHz
WDW: EM
SSB: 0
LB: 0.30 Hz
GB: 0
PC: 1.00



Z-restored spin-echo 13C spectrum with 1H decoupling



17

```

Current Data Parameters
NAME      CEA-II-110col1m
EXPNO     4
PROCNO    1

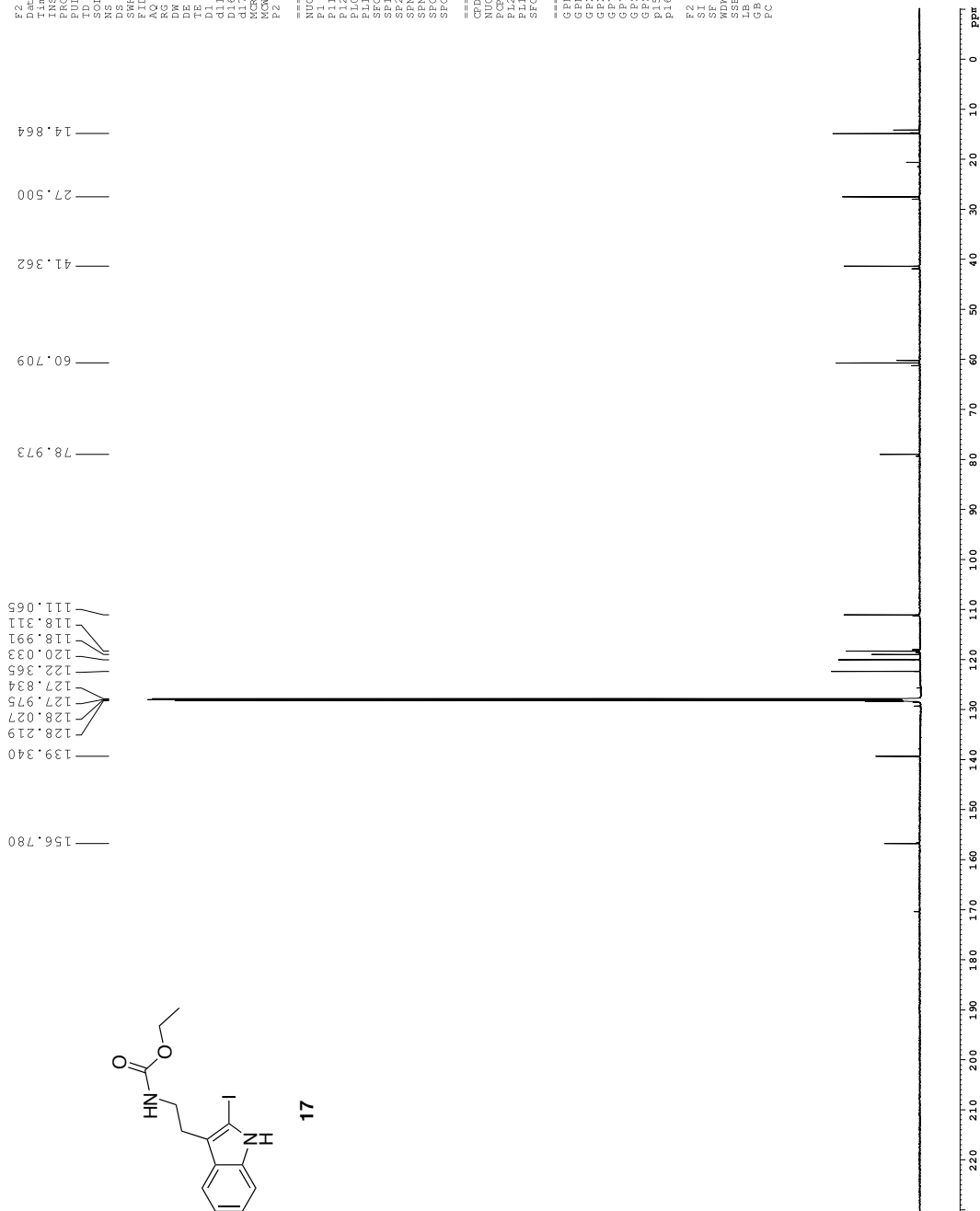
F2 - Acquisition Parameters
Date_     20120304
Time      6.23
INSTRUM   cryo
PROBHD    5 mm CPXI 1H-
PULPROG   Spinecho30gp
TD         65536
SFOF1     400
NS         400
DS         16
SRH        30302.031
AQ         0.02588
RG         1.0813440
DM         16.500
DE         278.0
TE         0.25000000
D1         0.03000000
d11        0.03000000
d12        0.00290000
d17        0.00290000
MCREST    0 sec. 0.0019000
MORBRK    0.01500000
P2         31.00

===== CHANNEL F1 =====
NUC1       13C
P1         5.50
P2         2000.00
P10        120.00
P11        125.794500
P12        3.20
P13        3.20
SFOF2      500.2225011
SFOF1[1]   CpF60.0.5.20.1
SFOF1[2]   CpF60comp.4
SFOFF1     0 Hz
SFOFF2     0 Hz

===== CHANNEL F2 =====
CPDPRG12   waltz16
NUC2        1H
PCPD2      100.00
P12        24.00
P13        24.00
SFO2       500.2225011

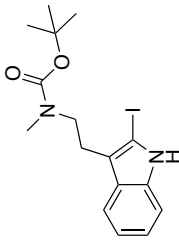
===== GRADIENT CHANNEL
GPM1[1]    SINE
GPM1[2]    SINE.100
GFX1       0 %
GFX2       0 %
GFY1       0 %
GFY2       0 %
GEZ1       30.00
GFZ2       50.00
PI6        1000.00

F2 - Processing Parameters
SI          32768
SF          125.7603874
WDW         0
SSB         0
GB          0
PC          2.00
    
```

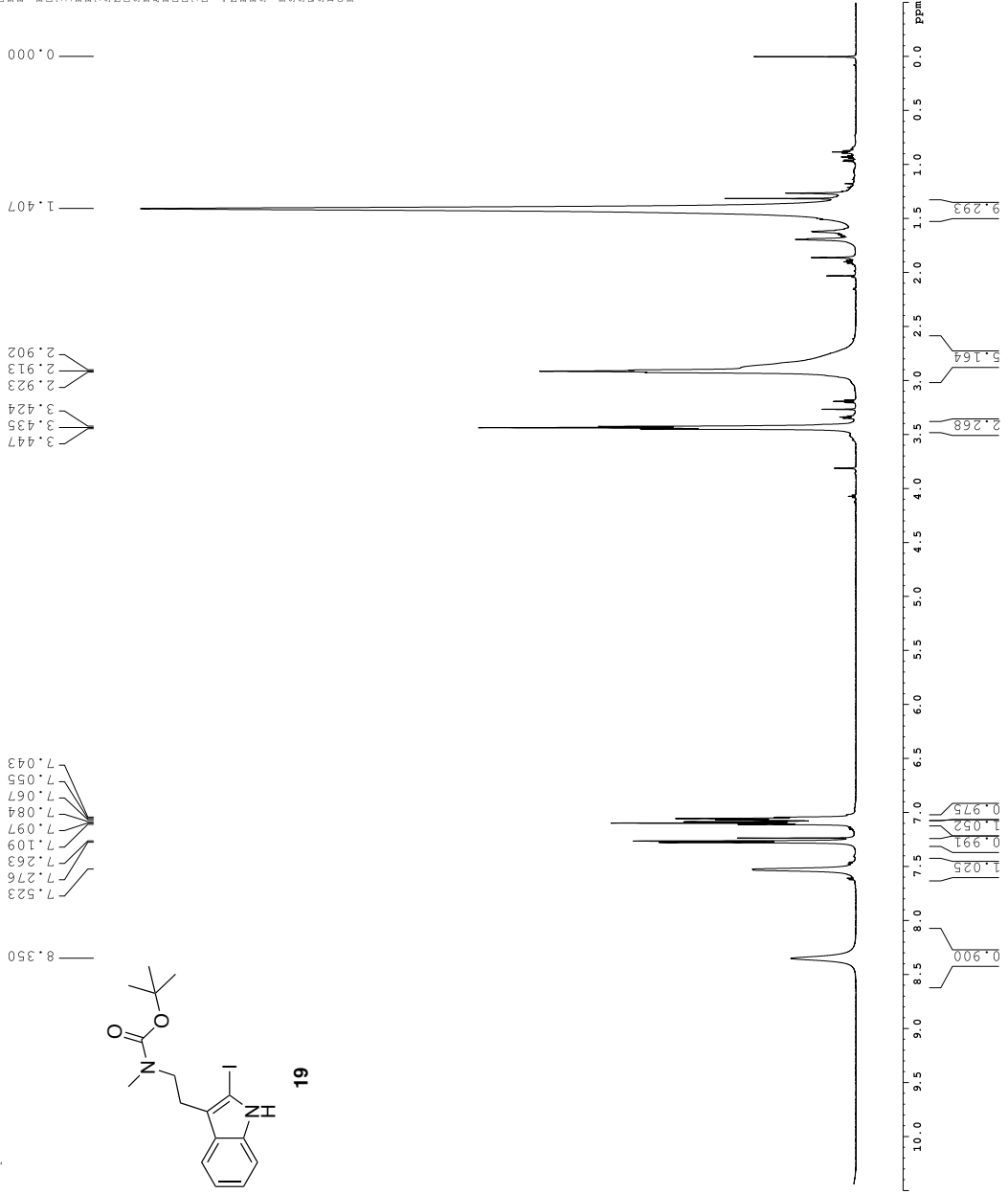


1H spectrum

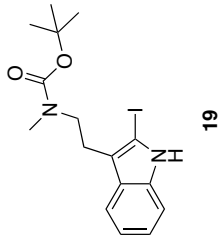
Current Data Parameters
NAME: DATA110102
EXPNO: 1
PROCNO: 1
F2 - Acquisition Parameters
Time: 14.22
INSTRUM: av600
PULPROG: zgpg30
SOLVENT: CDCl3
NS: 16
DSH: 6613.757 Hz
FIDRES: 0.167456 Hz
RG: 7.449228
AQ: 5.28 sec
OR: 75.000 usec
TE: 323.2 K
DE: 0.10000000 sec
===== CHANNEL f1 =====
NUC1: 13C
P1: 8.00 usec
PL1: 23.0144356 W
SFO1: 60.130041 MHz
F2 - Processing Parameters
SF: 600.1300482 MHz
WDW: EM
SSB: 0
LB: 0.30 Hz
GB: 0
PC: 1.00



19

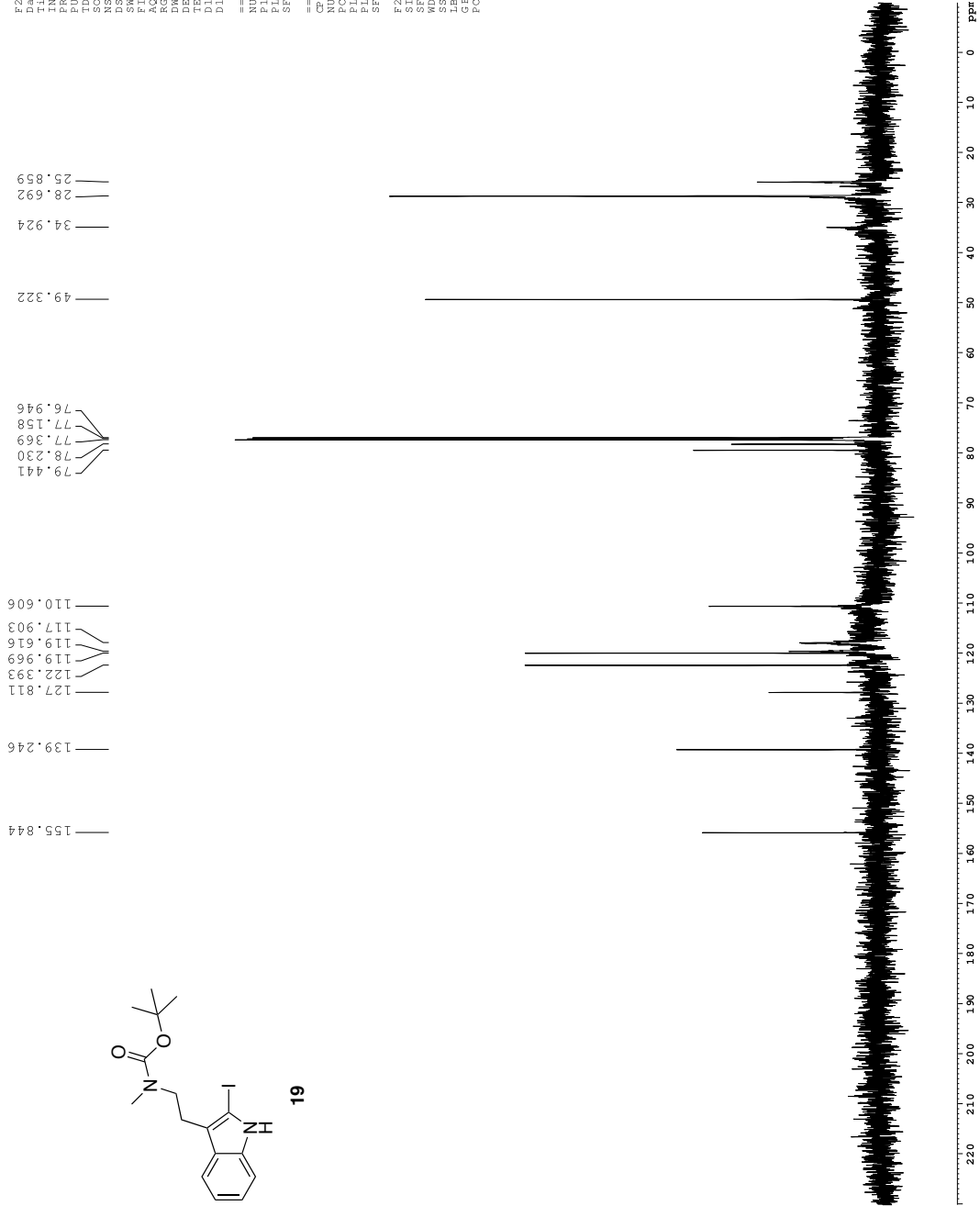


¹³C spectrum with ¹H decoupling



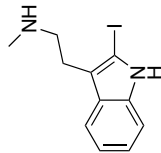
```

Current Data Parameters
NAME  CEA-II-161co12
EXPNO  3
PROCNO  1
F2 - Acquisition Parameters
Date_  20120512
Time   14.27
INSTRUM  spect
PROBHD  5 mm TBI 1H/13
PULPROG  zgpg30
TD      65536
SFO1    125.760340
NS      240
DS      4
SWH     36231.882
FIDRES  0.9045988
AQ      0.9045988
RG      912
DM      13.800
DE      323.0
TE      300.2
D1      0.40000001
D11     0.03000000
===== CHANNEL f1 =====
NUC1    13C
P1      15.00
PLW1   107.15190125
SFO1   125.760340
===== CHANNEL f2 =====
CDEPRG [2  waltz16
PCPD2   70.00
PLW2    0 W
SFO2    600.1350010
F2 - Processing parameters
SI      65536
SF      150.9027824
WDW     0
SSB     0
LB      0
GB      0
PC      1.00
  
```



1H spectrum

9.173

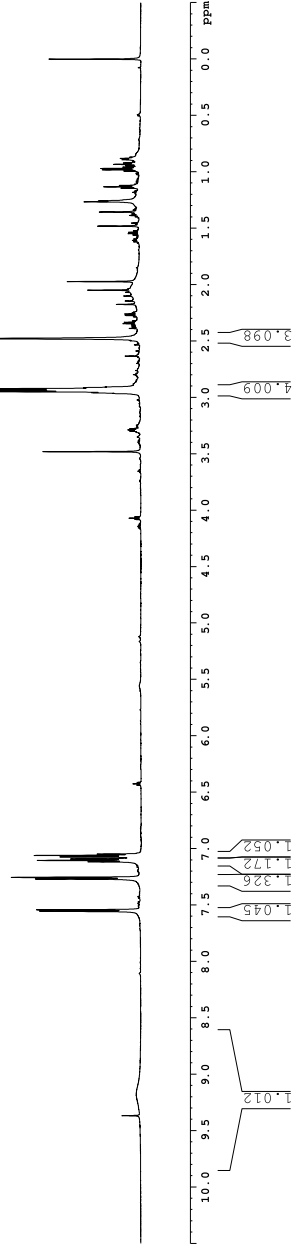


14

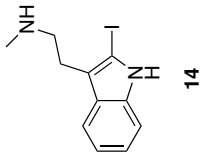
2.964
2.957
2.948
2.939
2.930
2.922
2.913
2.906
2.478

7.554
7.541
7.268
7.254
7.115
7.103
7.091
7.072
7.059
7.047

Current Data Parameters
NAME: 04-11-14-01-16
EXPNO: 1
PROCNO: 1
F2 - Acquisition Parameters
Date_Time: 2011.11.14
INSTRUM: spect
PULPROG: zgpg30
SOLVENT: CDCl3
NS: 16
DSH: 9615.785 Hz
FIDRES: 0.098042 Hz
RG: 5.039687 sec
DM: 52.000 usec
TE: 298.0 K
D1: 0.10000000 sec
----- CHANNEL f1 -----
P1: 8.00 usec
PL1: 23.0441956 W
SFO1: 60.1300000 MHz
F2 - Processing parameters
SF: 60.1300000 MHz
SSB: 0 Hz
LB: 0 Hz
PC: 1.00

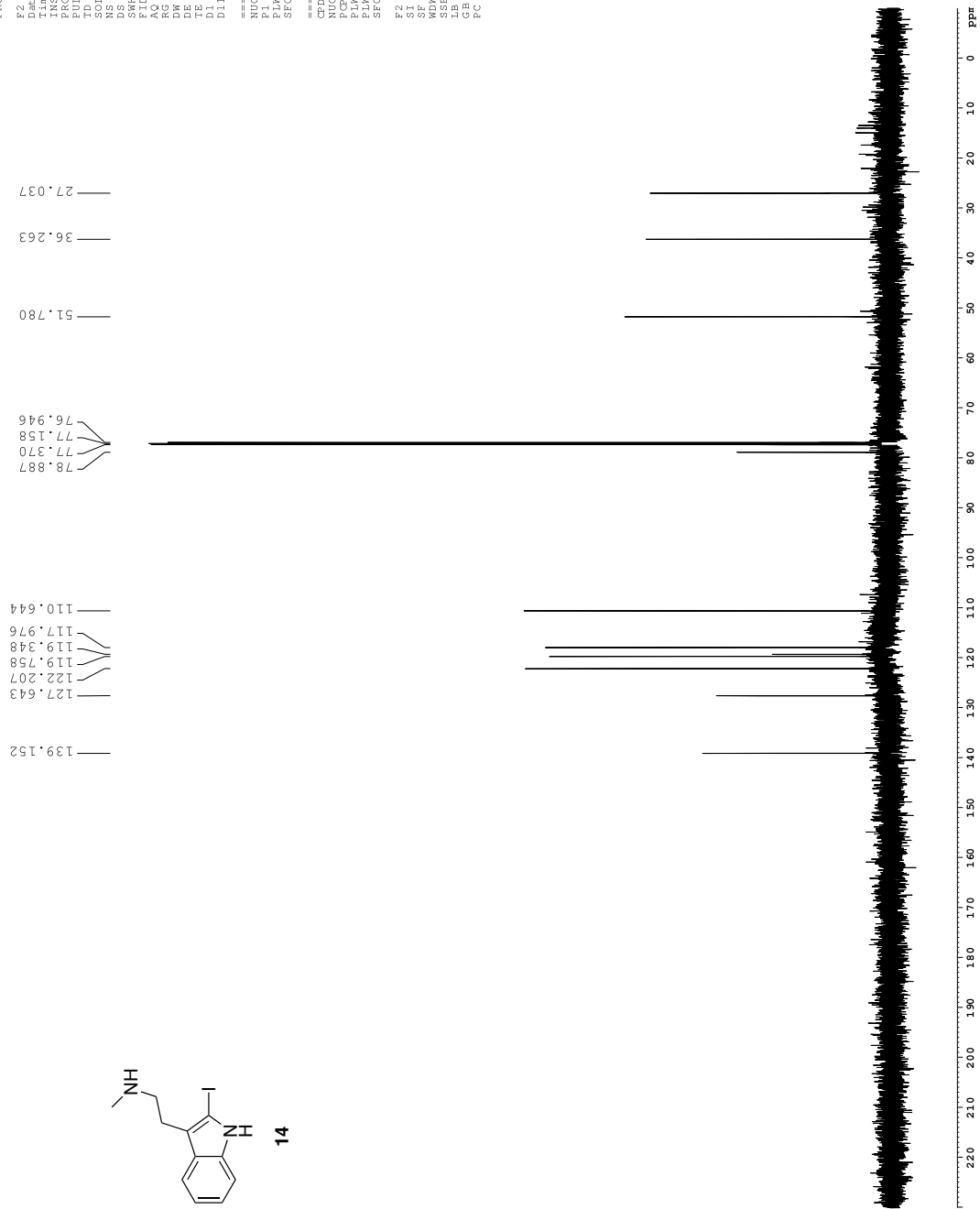


¹³C spectrum with ¹H decoupling



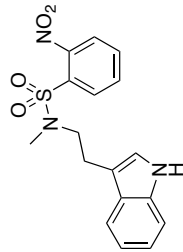
```

Current Data Parameters
NAME   CEA-II-166-30-7
EXPNO  2
PROCNO 1
F2 - Acquisition Parameters
Date_  20120518
Time   21.41
INSTR  zgpg30
PROBHD 5 mm TBI 1H/13
PULPROG zgpg30
TD      65536
SFO2    125.760300
NS      400
DS      4
SWH     36231.882
AQ      0.9943988
RG      645
DM      13.800
TE      298.1
D1      0.40000001
D11     0.03000000
===== CHANNEL f1 =====
NUC1    13C
P1      15.00
PLW1    107.15190125
SFO1    125.76030000
===== CHANNEL f2 =====
CDEPRG [2] waltz16
PCPD2   70.00
PLW2    0 W
SFO2    600.1350010
F2 - Processing parameters:
SI      65536
SF      150.90280000
WDW     0
SSB     0
LB      1.00
GB      0
PC      1.00
  
```



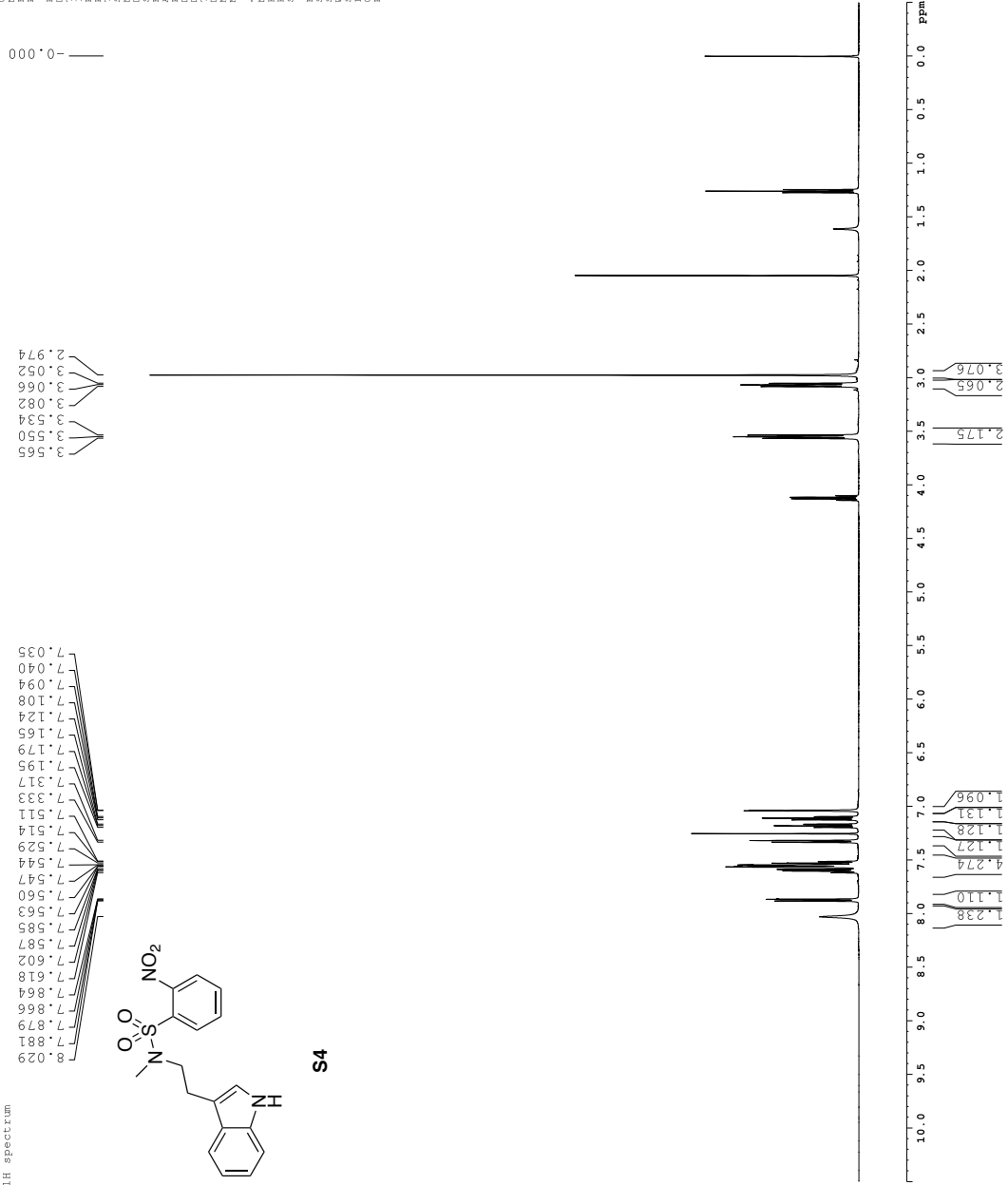
1H spectrum

8.029
7.881
7.879
7.866
7.864
7.868
7.802
7.877
7.587
7.585
7.563
7.560
7.547
7.544
7.529
7.514
7.511
7.333
7.317
7.195
7.179
7.165
7.124
7.108
7.094
7.040
7.035

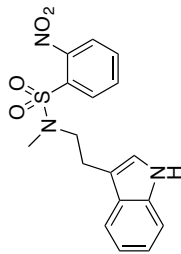


5.565
5.550
5.534
5.082
5.066
5.052
2.974

Current Data Parameters
NAME: S4-11-11-11
EXPNO: 1
PROCNO: 1
F2 - Acquisition Parameters
Time: 20.535
INSTRUM: spect
PULPROG: zgpg30
SOLVENT: CDCl3
NS: 8
DSH: 8012.820 Hz
FIDRES: 0.098073 Hz
RG: 5.039663 Hz
AQ: 62.400 usec
DM: 0.2980 Hz
TE: 0.10000000 sec
MCNRF2: 0.01500000 sec
----- CHANNEL f1 -----
NUC1: 1H
P1: 7.160 usec
PL1: 1.60 dB
SFO1: 500.2235015 MHz
F2 - Processing parameters
SF: 500.2203344 MHz
WDW: EM
SSB: 0
GB: 0
PC: 4.00

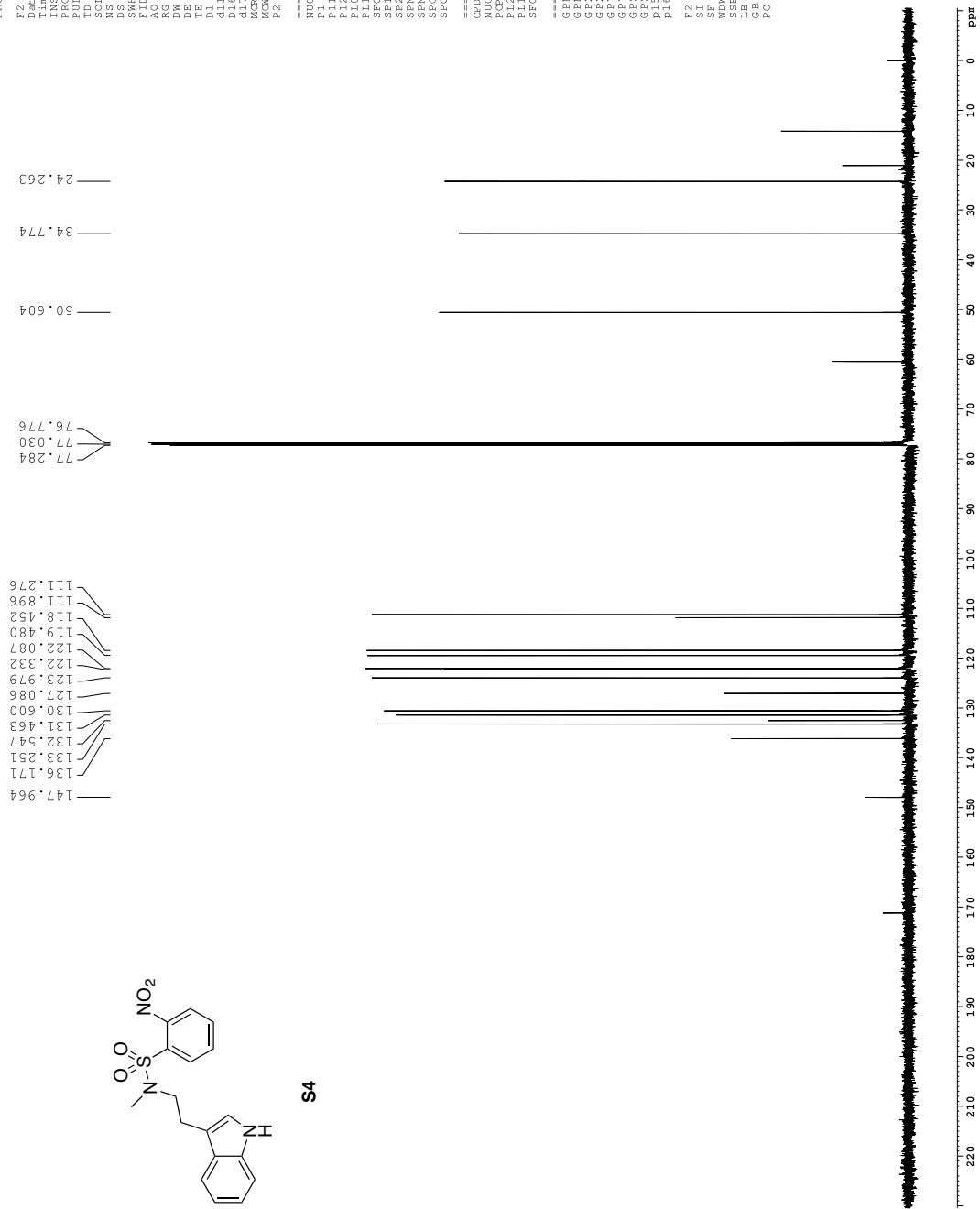


Z-restored spin-echo 13C spectrum with 1H decoupling

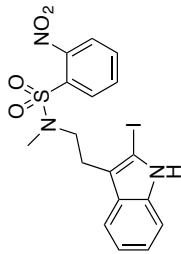


```

Current Data Parameters
NAME      CEA-II-181crude
EXPNO     2
PROCNO    1
F2 - Acquisition Parameters
Date_     20120621
Time      5.40
PROBHD    5 mm CPYCI 1H-
PULPROG   SpineEcho309p.
TD         65536
CONVENT   3.60
DS         16
SFOF1     3002.031
SFOF2     125.761
AQ         1.0813440
RG         13004
DM         16.500
TE         298.0
D1         0.25000000
d11        0.03000000
d12        0.00200000
d13        0.00200000
d14        0.00200000
d15        0.00200000
d16        0.00200000
d17        0.00200000
d18        0.00200000
d19        0.00200000
d20        0.00200000
MCREST    0 sec. 0.0019000
MORBRK    0.01500000
P2         31.00
===== CHANNEL F1 =====
NUC1       13C
P1         1.13C
F1         50.50
P2         2000.00
P10        120.00
P11        125.761500
P12        125.761500
P13        125.761500
P14        125.761500
P15        125.761500
P16        125.761500
SFOF1      3002.031
SFOF2      125.761500
SFOF3      125.761500
SFOF4      125.761500
SFOF5      125.761500
SFOF6      125.761500
SFOF7      125.761500
SFOF8      125.761500
SFOF9      125.761500
SFOF10     125.761500
SFOF11     125.761500
SFOF12     125.761500
SFOF13     125.761500
SFOF14     125.761500
SFOF15     125.761500
SFOF16     125.761500
SFOF17     125.761500
SFOF18     125.761500
SFOF19     125.761500
SFOF20     125.761500
===== CHANNEL F2 =====
CPDPRG12  waltz16
NUC2       1H
P2         100.00
P1         2.00
P10        2.00
P11        2.00
P12        2.00
P13        2.00
P14        2.00
P15        2.00
P16        2.00
SFOF1      500.2225011
SFOF2      500.2225011
===== GRADIENT CHANNEL
GPM1[1]   SINE
GPM1[2]   SINE
GPM2[1]   SINE
GPM2[2]   SINE
GFX1      0 %
GFX2      0 %
GFY1      0 %
GFY2      0 %
GEZ1      0 %
GEZ2      0 %
GFX3      0 %
GFY3      0 %
GEZ3      0 %
GFX4      0 %
GFY4      0 %
GEZ4      0 %
GFX5      0 %
GFY5      0 %
GEZ5      0 %
GFX6      0 %
GFY6      0 %
GEZ6      0 %
F2 - Processing Parameters
SI         32768
SF         125.760285
WDW        EM
SSB        0
GB         0
PC         2.00
  
```

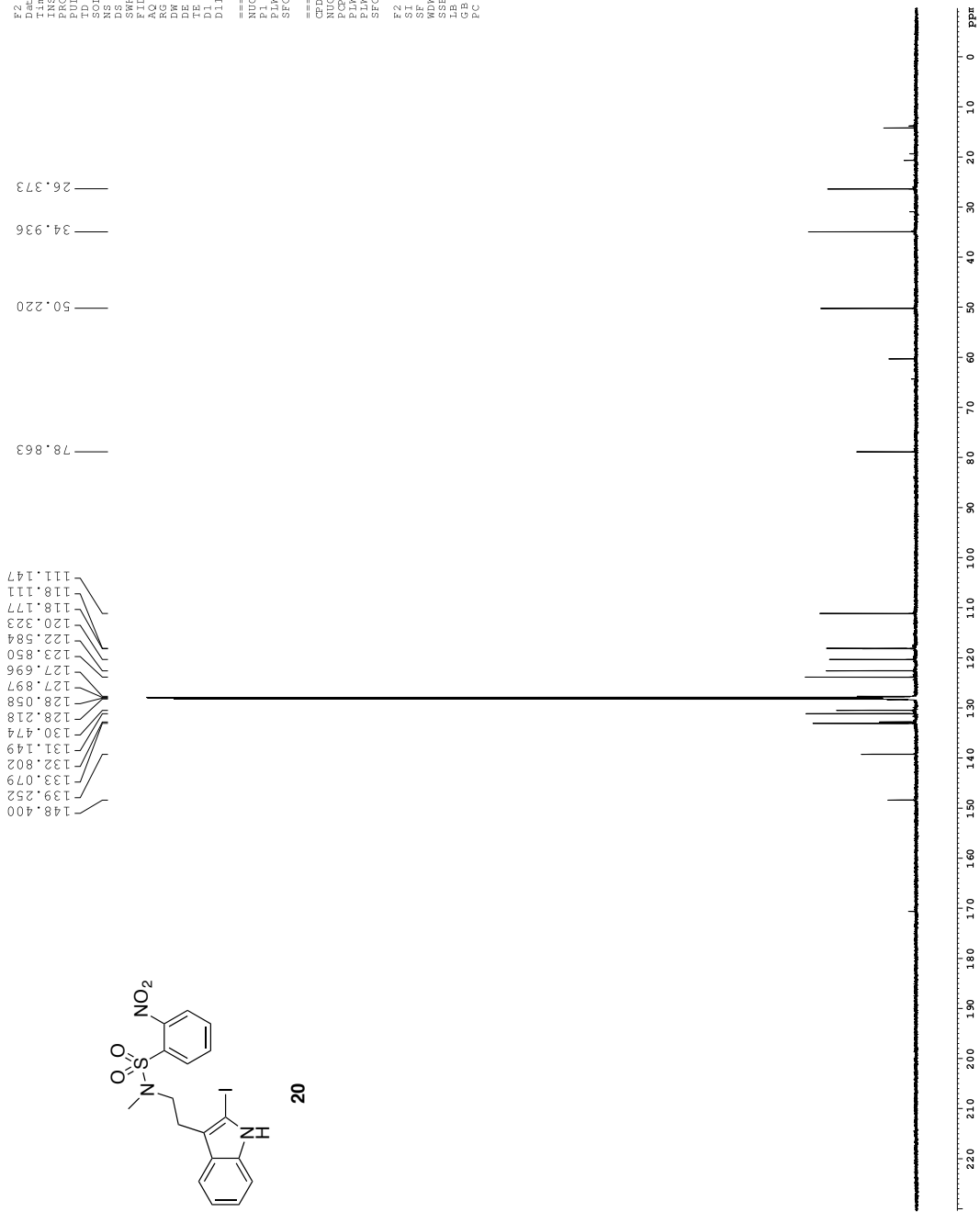


¹³C spectrum with ¹H decoupling



```

Current Data Parameters
NAME      CEA-II-200co12p
EXPNO     2
PROCNO    1
F2 - Acquisition Parameters
Date_     20120810
Time      10.21
INSTRUM   spect
PROBHD    5 mm TBI 1H/13
PULPROG   zgpg30
TD         65536
SOLVENT   CDCl3
NS         512
DS         4
SWH        36231.882
AQ         0.9943988
RG         101
DM         13.800
DE         288.0
TE         0.40000001
D1         0.03000000
D11        0.03000000
===== CHANNEL f1 =====
NUC1       13C
P1         15.00
PLW1       107.15190125
SFO1       125.761354669
===== CHANNEL f2 =====
CDEPRG [2] waltz16
PCPD2      70.00
PLW2       0 W
SFO2       600.1350010
F2 - Processing parameters:
SI         65536
SF         150.9027581
WDW        0
SSB        0
LB         1.00
GB         0
PC         1.00
    
```



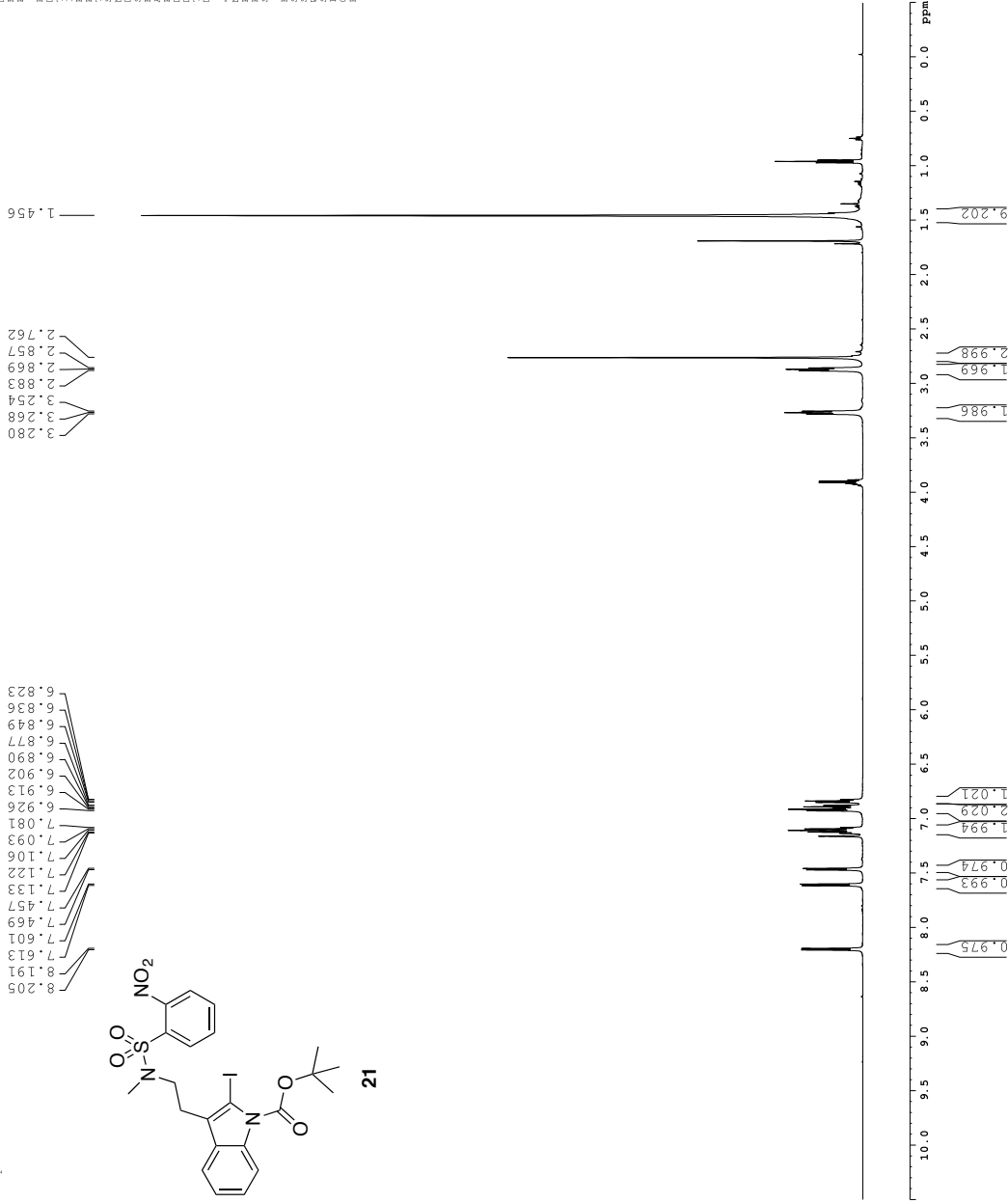
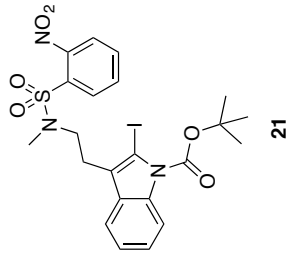
1H spectrum

Current Data Parameters
NAME: 21-19-1
EXPNO: 1
PROCNO: 1
F2 - Acquisition Parameters
Time: 20.16.52.9
INSTRUM: av600
PULPROG: zgpg30
SOLVENT: CDCl3
NS: 16
DSH: 9615.385 Hz
FIDRES: 0.098042 Hz
RG: 5.092666
AQ: 22.1666
DM: 52.000 usec
TE: 298.3 K
DE: 0.10000000 sec
----- CHANNEL f1 -----
NUC1: 13C
P1: 8.00 usec
PL1: 23.01441926 W
SFO1: 60.1342000 MHz
F2 - Processing Parameters
SI: 32768
SF: 600.1299653 MHz
WDW: EM
SSB: 0
LB: 0.30 Hz
GB: 0
PC: 1.00

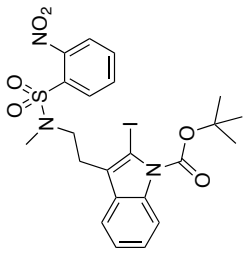
8.205
8.191
7.613
7.601
7.469
7.457
7.133
7.122
7.106
7.093
7.081
6.926
6.913
6.902
6.890
6.877
6.849
6.836
6.823

3.280
3.268
3.254
3.244
3.234
3.224
3.214
3.204
3.194
3.184
3.174
3.164
3.154
3.144
3.134
3.124
3.114
3.104
3.094
3.084
3.074
3.064
3.054
3.044
3.034
3.024
3.014
3.004
2.994
2.984
2.974
2.964
2.954
2.944
2.934
2.924
2.914
2.904
2.894
2.884
2.874
2.864
2.854
2.844
2.834
2.824
2.814
2.804
2.794
2.784
2.774
2.764
2.754
2.744
2.734
2.724
2.714
2.704
2.694
2.684
2.674
2.664
2.654
2.644
2.634
2.624
2.614
2.604
2.594
2.584
2.574
2.564
2.554
2.544
2.534
2.524
2.514
2.504
2.494
2.484
2.474
2.464
2.454
2.444
2.434
2.424
2.414
2.404
2.394
2.384
2.374
2.364
2.354
2.344
2.334
2.324
2.314
2.304
2.294
2.284
2.274
2.264
2.254
2.244
2.234
2.224
2.214
2.204
2.194
2.184
2.174
2.164
2.154
2.144
2.134
2.124
2.114
2.104
2.094
2.084
2.074
2.064
2.054
2.044
2.034
2.024
2.014
2.004
1.994
1.984
1.974
1.964
1.954
1.944
1.934
1.924
1.914
1.904
1.894
1.884
1.874
1.864
1.854
1.844
1.834
1.824
1.814
1.804
1.794
1.784
1.774
1.764
1.754
1.744
1.734
1.724
1.714
1.704
1.694
1.684
1.674
1.664
1.654
1.644
1.634
1.624
1.614
1.604
1.594
1.584
1.574
1.564
1.554
1.544
1.534
1.524
1.514
1.504
1.494
1.484
1.474
1.464
1.454
1.444
1.434
1.424
1.414
1.404
1.394
1.384
1.374
1.364
1.354
1.344
1.334
1.324
1.314
1.304
1.294
1.284
1.274
1.264
1.254
1.244
1.234
1.224
1.214
1.204
1.194
1.184
1.174
1.164
1.154
1.144
1.134
1.124
1.114
1.104
1.094
1.084
1.074
1.064
1.054
1.044
1.034
1.024
1.014
1.004
0.994
0.984
0.974
0.964
0.954
0.944
0.934
0.924
0.914
0.904
0.894
0.884
0.874
0.864
0.854
0.844
0.834
0.824
0.814
0.804
0.794
0.784
0.774
0.764
0.754
0.744
0.734
0.724
0.714
0.704
0.694
0.684
0.674
0.664
0.654
0.644
0.634
0.624
0.614
0.604
0.594
0.584
0.574
0.564
0.554
0.544
0.534
0.524
0.514
0.504
0.494
0.484
0.474
0.464
0.454
0.444
0.434
0.424
0.414
0.404
0.394
0.384
0.374
0.364
0.354
0.344
0.334
0.324
0.314
0.304
0.294
0.284
0.274
0.264
0.254
0.244
0.234
0.224
0.214
0.204
0.194
0.184
0.174
0.164
0.154
0.144
0.134
0.124
0.114
0.104
0.094
0.084
0.074
0.064
0.054
0.044
0.034
0.024
0.014
0.004

1.456



¹³C spectrum with ¹H decoupling



21

```

Current Data Parameters
NAME      CRA-11-187Pr1
EXPNO     2
PROCNO    1

F2 - Acquisition Parameters
Date_     20120709
Time      16.57
INSTRUM   av600
PROBHD    5 mm TBI zgpg30
PULPROG   zgpg30
TD         65536
SOLVENT   CDCl3
DS         2
SS        24.0
SRH        36231.883
FIDRES     0.552855
AQ         0.9049456
RG         13.800
DN         13.800
DE         6.00
TE         300.2
D1         0.40000001
D11        0.033000000

===== CHANNEL f1 =====
NUC1       13C
P1         15.00
PLM1      107.15190125
SFO1      150.9194080

===== CHANNEL f2 =====
NUC2       13C
P2         15.00
PLM2      107.15190125
SFO2      150.9194080

===== CHANNEL f3 =====
NUC3       13C
P3         15.00
PLM3      107.15190125
SFO3      150.9194080

===== CHANNEL f4 =====
NUC4       13C
P4         15.00
PLM4      107.15190125
SFO4      150.9194080

===== CHANNEL f5 =====
NUC5       13C
P5         15.00
PLM5      107.15190125
SFO5      150.9194080

===== CHANNEL f6 =====
NUC6       13C
P6         15.00
PLM6      107.15190125
SFO6      150.9194080

===== CHANNEL f7 =====
NUC7       13C
P7         15.00
PLM7      107.15190125
SFO7      150.9194080

===== CHANNEL f8 =====
NUC8       13C
P8         15.00
PLM8      107.15190125
SFO8      150.9194080

===== CHANNEL f9 =====
NUC9       13C
P9         15.00
PLM9      107.15190125
SFO9      150.9194080

===== CHANNEL f10 =====
NUC10      13C
P10        15.00
PLM10     107.15190125
SFO10     150.9194080

===== CHANNEL f11 =====
NUC11     13C
P11        15.00
PLM11     107.15190125
SFO11     150.9194080

===== CHANNEL f12 =====
NUC12     13C
P12        15.00
PLM12     107.15190125
SFO12     150.9194080

===== CHANNEL f13 =====
NUC13     13C
P13        15.00
PLM13     107.15190125
SFO13     150.9194080

===== CHANNEL f14 =====
NUC14     13C
P14        15.00
PLM14     107.15190125
SFO14     150.9194080

===== CHANNEL f15 =====
NUC15     13C
P15        15.00
PLM15     107.15190125
SFO15     150.9194080

===== CHANNEL f16 =====
NUC16     13C
P16        15.00
PLM16     107.15190125
SFO16     150.9194080

===== CHANNEL f17 =====
NUC17     13C
P17        15.00
PLM17     107.15190125
SFO17     150.9194080

===== CHANNEL f18 =====
NUC18     13C
P18        15.00
PLM18     107.15190125
SFO18     150.9194080

===== CHANNEL f19 =====
NUC19     13C
P19        15.00
PLM19     107.15190125
SFO19     150.9194080

===== CHANNEL f20 =====
NUC20     13C
P20        15.00
PLM20     107.15190125
SFO20     150.9194080

===== CHANNEL f21 =====
NUC21     13C
P21        15.00
PLM21     107.15190125
SFO21     150.9194080

===== CHANNEL f22 =====
NUC22     13C
P22        15.00
PLM22     107.15190125
SFO22     150.9194080

===== CHANNEL f23 =====
NUC23     13C
P23        15.00
PLM23     107.15190125
SFO23     150.9194080

===== CHANNEL f24 =====
NUC24     13C
P24        15.00
PLM24     107.15190125
SFO24     150.9194080

===== CHANNEL f25 =====
NUC25     13C
P25        15.00
PLM25     107.15190125
SFO25     150.9194080

===== CHANNEL f26 =====
NUC26     13C
P26        15.00
PLM26     107.15190125
SFO26     150.9194080

===== CHANNEL f27 =====
NUC27     13C
P27        15.00
PLM27     107.15190125
SFO27     150.9194080

===== CHANNEL f28 =====
NUC28     13C
P28        15.00
PLM28     107.15190125
SFO28     150.9194080

===== CHANNEL f29 =====
NUC29     13C
P29        15.00
PLM29     107.15190125
SFO29     150.9194080

===== CHANNEL f30 =====
NUC30     13C
P30        15.00
PLM30     107.15190125
SFO30     150.9194080

===== CHANNEL f31 =====
NUC31     13C
P31        15.00
PLM31     107.15190125
SFO31     150.9194080

===== CHANNEL f32 =====
NUC32     13C
P32        15.00
PLM32     107.15190125
SFO32     150.9194080

===== CHANNEL f33 =====
NUC33     13C
P33        15.00
PLM33     107.15190125
SFO33     150.9194080

===== CHANNEL f34 =====
NUC34     13C
P34        15.00
PLM34     107.15190125
SFO34     150.9194080

===== CHANNEL f35 =====
NUC35     13C
P35        15.00
PLM35     107.15190125
SFO35     150.9194080

===== CHANNEL f36 =====
NUC36     13C
P36        15.00
PLM36     107.15190125
SFO36     150.9194080

===== CHANNEL f37 =====
NUC37     13C
P37        15.00
PLM37     107.15190125
SFO37     150.9194080

===== CHANNEL f38 =====
NUC38     13C
P38        15.00
PLM38     107.15190125
SFO38     150.9194080

===== CHANNEL f39 =====
NUC39     13C
P39        15.00
PLM39     107.15190125
SFO39     150.9194080

===== CHANNEL f40 =====
NUC40     13C
P40        15.00
PLM40     107.15190125
SFO40     150.9194080

===== CHANNEL f41 =====
NUC41     13C
P41        15.00
PLM41     107.15190125
SFO41     150.9194080

===== CHANNEL f42 =====
NUC42     13C
P42        15.00
PLM42     107.15190125
SFO42     150.9194080

===== CHANNEL f43 =====
NUC43     13C
P43        15.00
PLM43     107.15190125
SFO43     150.9194080

===== CHANNEL f44 =====
NUC44     13C
P44        15.00
PLM44     107.15190125
SFO44     150.9194080

===== CHANNEL f45 =====
NUC45     13C
P45        15.00
PLM45     107.15190125
SFO45     150.9194080

===== CHANNEL f46 =====
NUC46     13C
P46        15.00
PLM46     107.15190125
SFO46     150.9194080

===== CHANNEL f47 =====
NUC47     13C
P47        15.00
PLM47     107.15190125
SFO47     150.9194080

===== CHANNEL f48 =====
NUC48     13C
P48        15.00
PLM48     107.15190125
SFO48     150.9194080

===== CHANNEL f49 =====
NUC49     13C
P49        15.00
PLM49     107.15190125
SFO49     150.9194080

===== CHANNEL f50 =====
NUC50     13C
P50        15.00
PLM50     107.15190125
SFO50     150.9194080

===== CHANNEL f51 =====
NUC51     13C
P51        15.00
PLM51     107.15190125
SFO51     150.9194080

===== CHANNEL f52 =====
NUC52     13C
P52        15.00
PLM52     107.15190125
SFO52     150.9194080

===== CHANNEL f53 =====
NUC53     13C
P53        15.00
PLM53     107.15190125
SFO53     150.9194080

===== CHANNEL f54 =====
NUC54     13C
P54        15.00
PLM54     107.15190125
SFO54     150.9194080

===== CHANNEL f55 =====
NUC55     13C
P55        15.00
PLM55     107.15190125
SFO55     150.9194080

===== CHANNEL f56 =====
NUC56     13C
P56        15.00
PLM56     107.15190125
SFO56     150.9194080

===== CHANNEL f57 =====
NUC57     13C
P57        15.00
PLM57     107.15190125
SFO57     150.9194080

===== CHANNEL f58 =====
NUC58     13C
P58        15.00
PLM58     107.15190125
SFO58     150.9194080

===== CHANNEL f59 =====
NUC59     13C
P59        15.00
PLM59     107.15190125
SFO59     150.9194080

===== CHANNEL f60 =====
NUC60     13C
P60        15.00
PLM60     107.15190125
SFO60     150.9194080

===== CHANNEL f61 =====
NUC61     13C
P61        15.00
PLM61     107.15190125
SFO61     150.9194080

===== CHANNEL f62 =====
NUC62     13C
P62        15.00
PLM62     107.15190125
SFO62     150.9194080

===== CHANNEL f63 =====
NUC63     13C
P63        15.00
PLM63     107.15190125
SFO63     150.9194080

===== CHANNEL f64 =====
NUC64     13C
P64        15.00
PLM64     107.15190125
SFO64     150.9194080

===== CHANNEL f65 =====
NUC65     13C
P65        15.00
PLM65     107.15190125
SFO65     150.9194080

===== CHANNEL f66 =====
NUC66     13C
P66        15.00
PLM66     107.15190125
SFO66     150.9194080

===== CHANNEL f67 =====
NUC67     13C
P67        15.00
PLM67     107.15190125
SFO67     150.9194080

===== CHANNEL f68 =====
NUC68     13C
P68        15.00
PLM68     107.15190125
SFO68     150.9194080

===== CHANNEL f69 =====
NUC69     13C
P69        15.00
PLM69     107.15190125
SFO69     150.9194080

===== CHANNEL f70 =====
NUC70     13C
P70        15.00
PLM70     107.15190125
SFO70     150.9194080

===== CHANNEL f71 =====
NUC71     13C
P71        15.00
PLM71     107.15190125
SFO71     150.9194080

===== CHANNEL f72 =====
NUC72     13C
P72        15.00
PLM72     107.15190125
SFO72     150.9194080

===== CHANNEL f73 =====
NUC73     13C
P73        15.00
PLM73     107.15190125
SFO73     150.9194080

===== CHANNEL f74 =====
NUC74     13C
P74        15.00
PLM74     107.15190125
SFO74     150.9194080

===== CHANNEL f75 =====
NUC75     13C
P75        15.00
PLM75     107.15190125
SFO75     150.9194080

===== CHANNEL f76 =====
NUC76     13C
P76        15.00
PLM76     107.15190125
SFO76     150.9194080

===== CHANNEL f77 =====
NUC77     13C
P77        15.00
PLM77     107.15190125
SFO77     150.9194080

===== CHANNEL f78 =====
NUC78     13C
P78        15.00
PLM78     107.15190125
SFO78     150.9194080

===== CHANNEL f79 =====
NUC79     13C
P79        15.00
PLM79     107.15190125
SFO79     150.9194080

===== CHANNEL f80 =====
NUC80     13C
P80        15.00
PLM80     107.15190125
SFO80     150.9194080

===== CHANNEL f81 =====
NUC81     13C
P81        15.00
PLM81     107.15190125
SFO81     150.9194080

===== CHANNEL f82 =====
NUC82     13C
P82        15.00
PLM82     107.15190125
SFO82     150.9194080

===== CHANNEL f83 =====
NUC83     13C
P83        15.00
PLM83     107.15190125
SFO83     150.9194080

===== CHANNEL f84 =====
NUC84     13C
P84        15.00
PLM84     107.15190125
SFO84     150.9194080

===== CHANNEL f85 =====
NUC85     13C
P85        15.00
PLM85     107.15190125
SFO85     150.9194080

===== CHANNEL f86 =====
NUC86     13C
P86        15.00
PLM86     107.15190125
SFO86     150.9194080

===== CHANNEL f87 =====
NUC87     13C
P87        15.00
PLM87     107.15190125
SFO87     150.9194080

===== CHANNEL f88 =====
NUC88     13C
P88        15.00
PLM88     107.15190125
SFO88     150.9194080

===== CHANNEL f89 =====
NUC89     13C
P89        15.00
PLM89     107.15190125
SFO89     150.9194080

===== CHANNEL f90 =====
NUC90     13C
P90        15.00
PLM90     107.15190125
SFO90     150.9194080

===== CHANNEL f91 =====
NUC91     13C
P91        15.00
PLM91     107.15190125
SFO91     150.9194080

===== CHANNEL f92 =====
NUC92     13C
P92        15.00
PLM92     107.15190125
SFO92     150.9194080

===== CHANNEL f93 =====
NUC93     13C
P93        15.00
PLM93     107.15190125
SFO93     150.9194080

===== CHANNEL f94 =====
NUC94     13C
P94        15.00
PLM94     107.15190125
SFO94     150.9194080

===== CHANNEL f95 =====
NUC95     13C
P95        15.00
PLM95     107.15190125
SFO95     150.9194080

===== CHANNEL f96 =====
NUC96     13C
P96        15.00
PLM96     107.15190125
SFO96     150.9194080

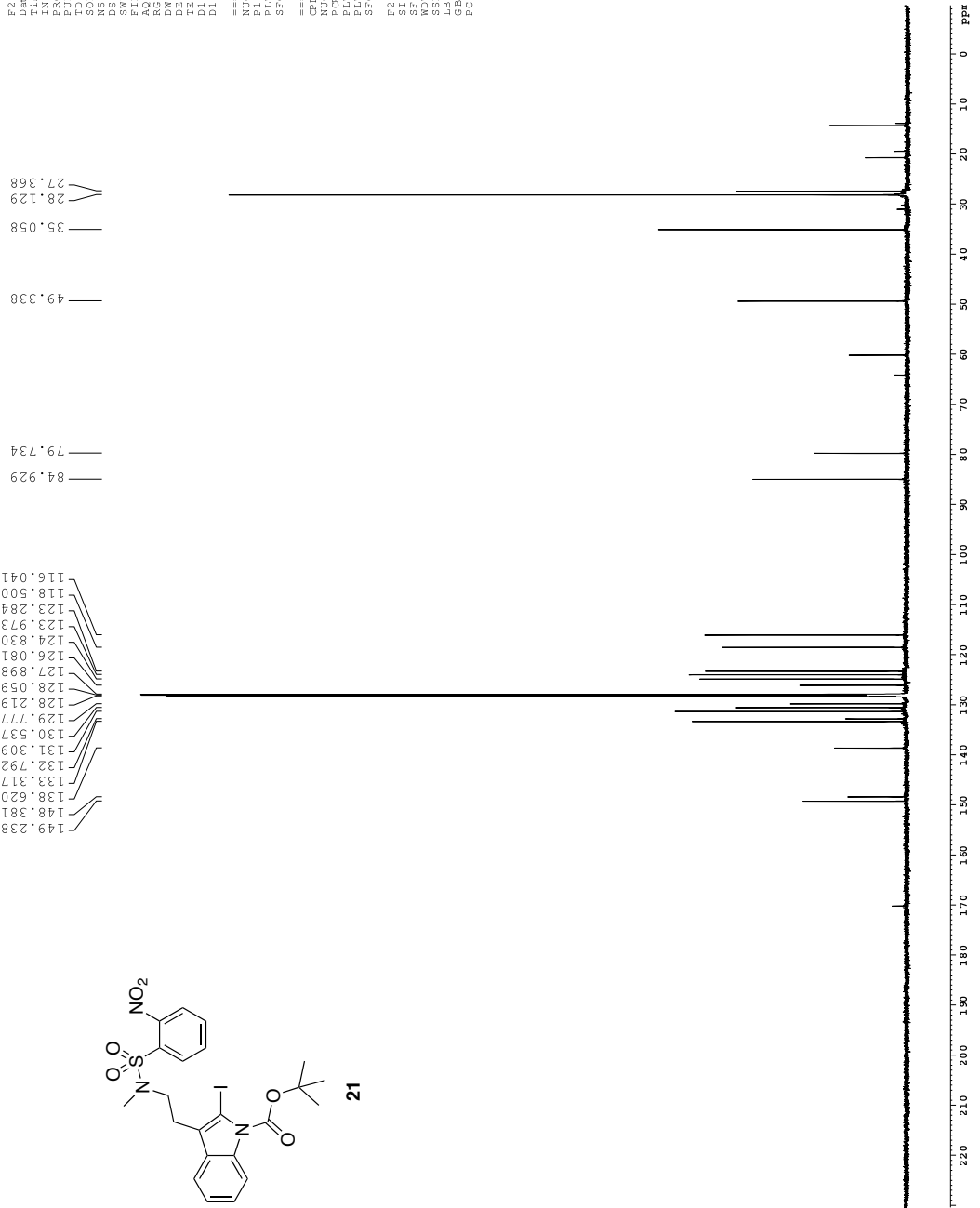
===== CHANNEL f97 =====
NUC97     13C
P97        15.00
PLM97     107.15190125
SFO97     150.9194080

===== CHANNEL f98 =====
NUC98     13C
P98        15.00
PLM98     107.15190125
SFO98     150.9194080

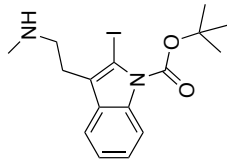
===== CHANNEL f99 =====
NUC99     13C
P99        15.00
PLM99     107.15190125
SFO99     150.9194080

===== CHANNEL f100 =====
NUC100    13C
P100       15.00
PLM100    107.15190125
SFO100    150.9194080
    
```

116.041
 118.500
 123.284
 123.973
 124.830
 126.081
 127.898
 128.059
 128.219
 129.777
 130.537
 131.309
 132.792
 133.317
 138.620
 148.381
 149.238

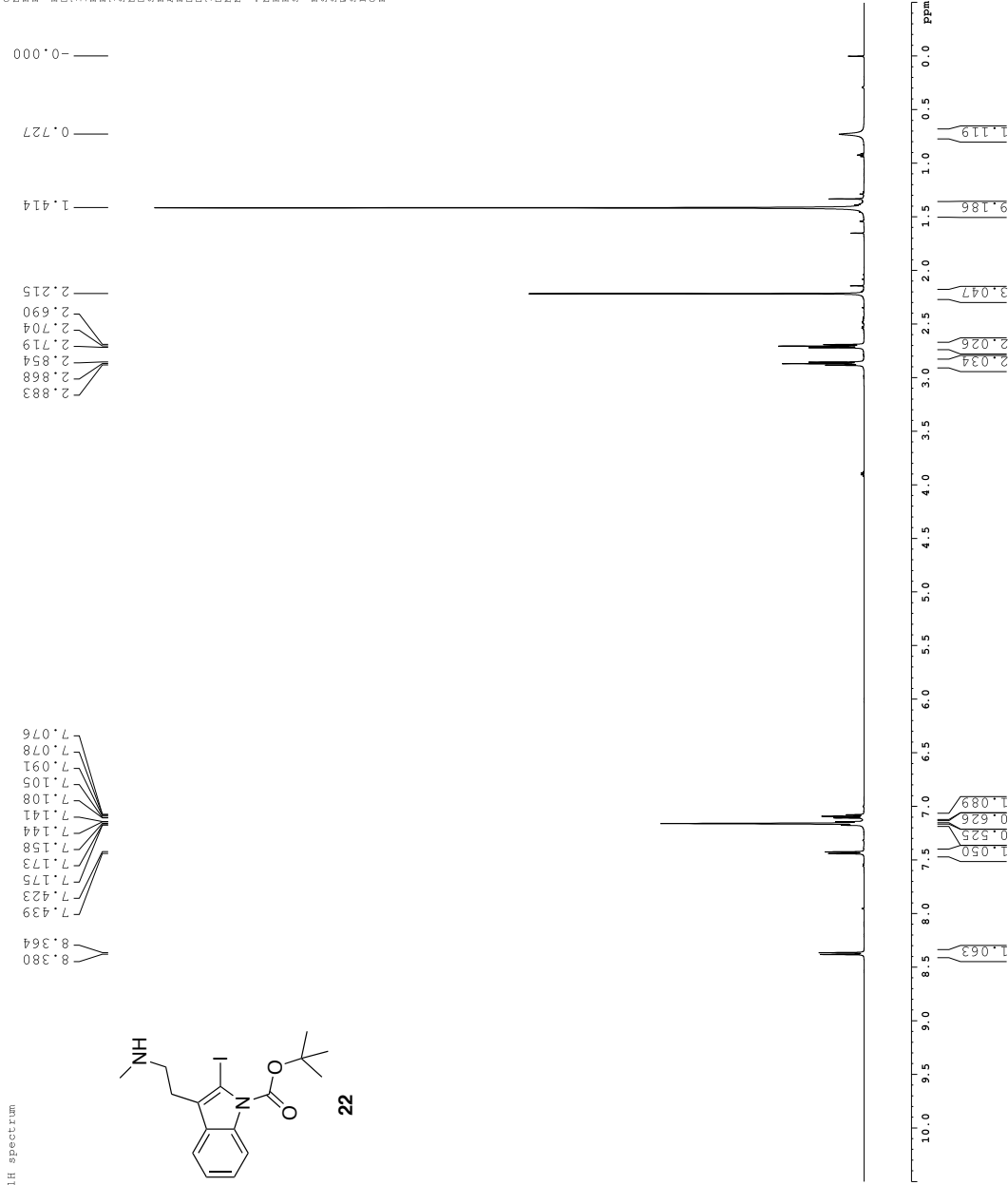


1H spectrum

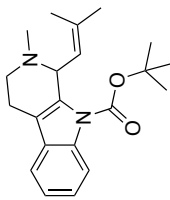


22

Current Data Parameters
NAME: 941124001-24-27
EXPNO: 1
PROCNO: 1
F2 - Acquisition Parameters
Time: 20.11447
INSTRUM: spect
PULPROG: zgpg30
SOLVENT: DMSO-d6
NS: 8
DSH: 8012.820 Hz
FIDRES: 0.098043 Hz
RG: 5.039971 ssec
AQ: 62.400 usec
DM: 0.2980 K
TE: 0.10000000 sec
MCNRF2: 0.01500000 sec
MCNRF1: 0.01500000 sec
----- CHANNEL f1 -----
NUC1: 1H
P1: 7.160 usec
PL1: 1.60 dB
SFO1: 500.2235015 MHz
F2 - Processing parameters
SI: 32768
SF: 500.2200000 MHz
WDW: EM
SSB: 0
GB: 0
PC: 4.00



Z-restored spin-echo 13C spectrum with 1H decoupling

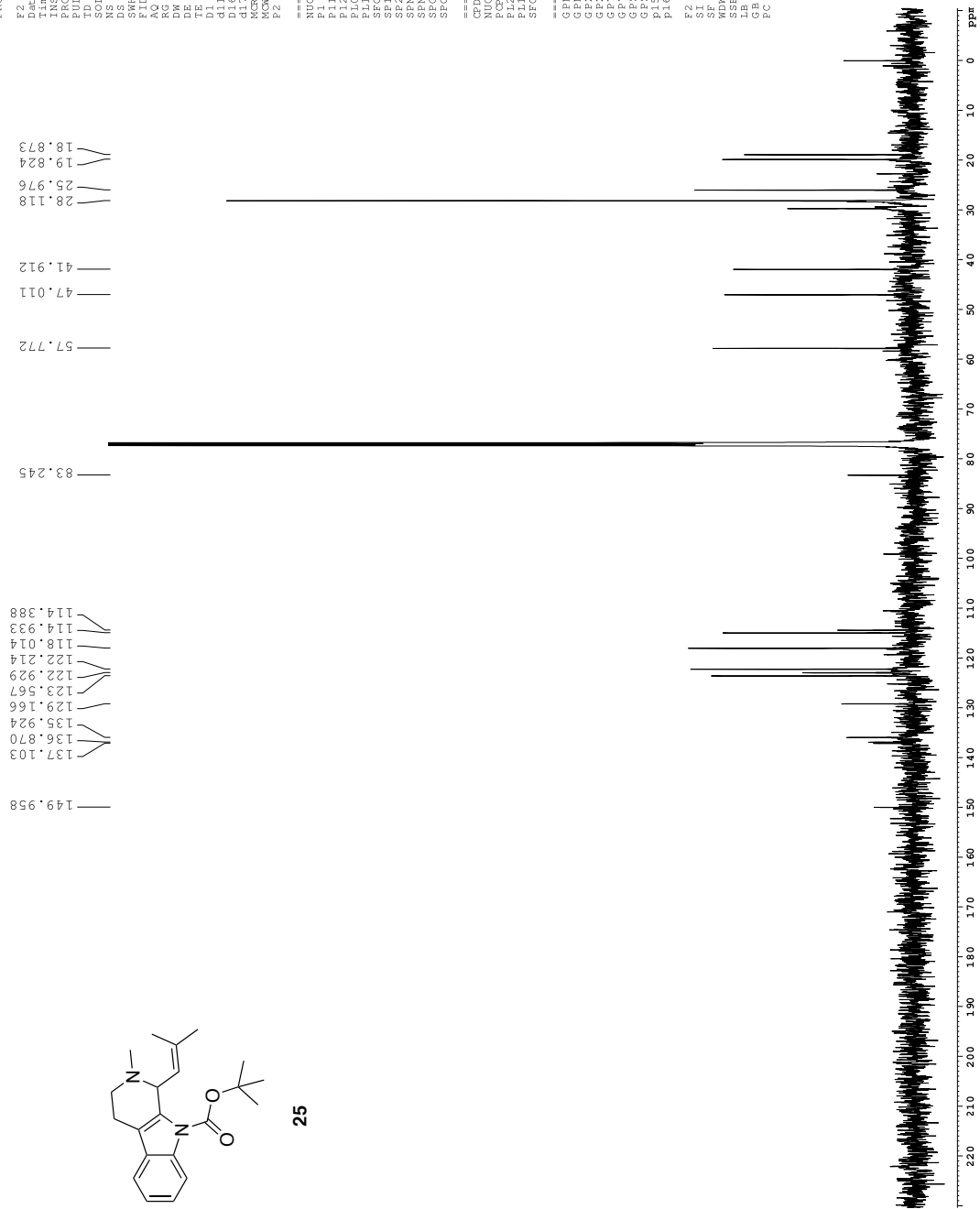


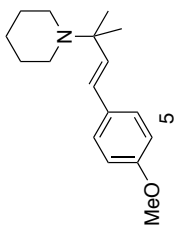
25

```

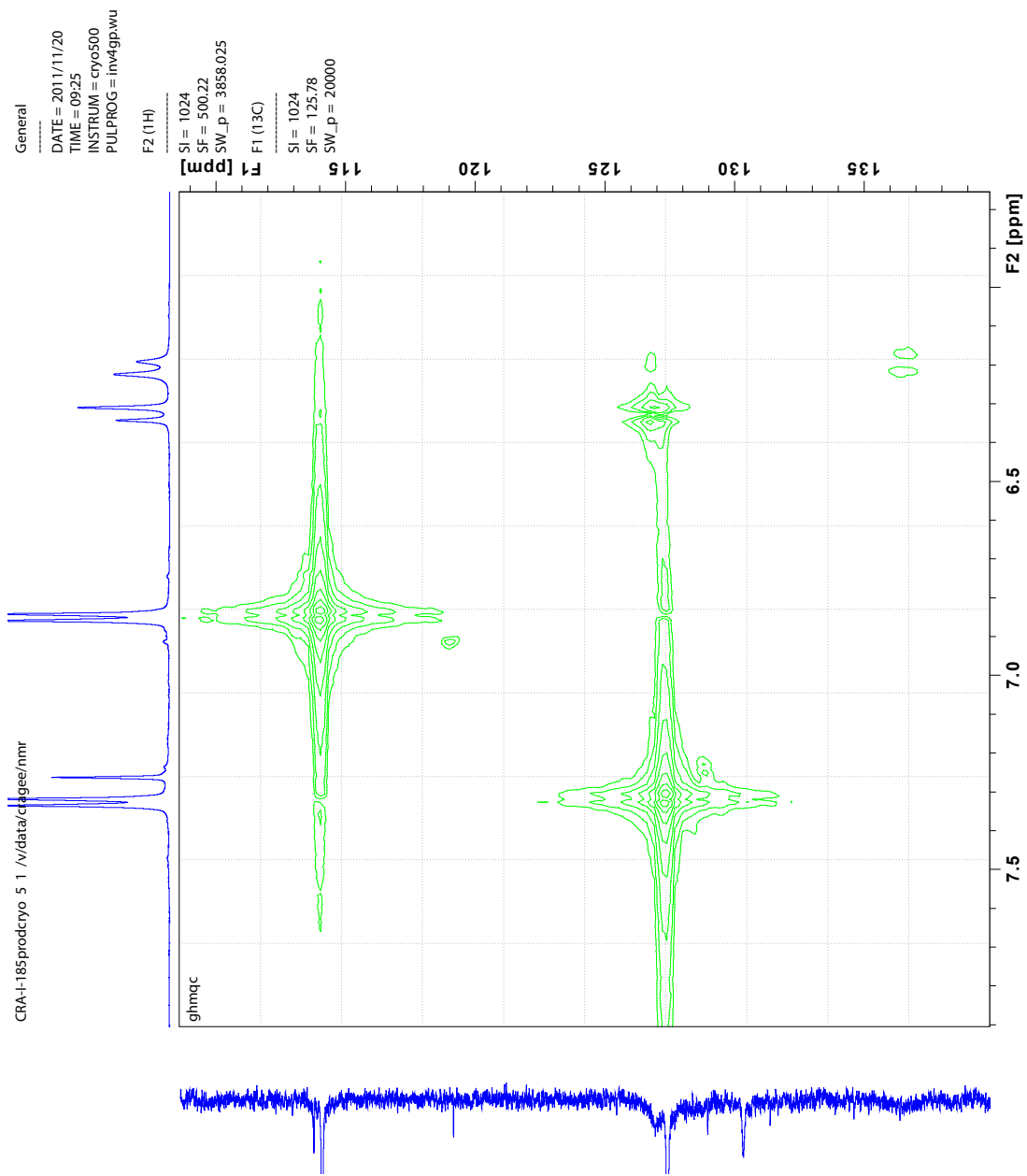
Current Data Parameters
NAME   CEA-II-231co12-
EXPNO  3
PROCNO 1
F2 - Acquisition Parameters
Date_  20121029
Time   11.23
PROBHD 5 mm CPYCI 1H-
PULPROG SpinEcho309p.
TD      65536
SFOF1   125.760256
NS       838
DS       16
SR      3030.031
AQ       1.0813440
RG       11585.2
DM       16.500
TE       298.0
D1       0.25000000
d11      0.03000000
d12      0.00200000
d13      0.00200000
d14      0.00200000
d15      0.00200000
d16      0.00200000
d17      0.00200000
d18      0.00200000
d19      0.00200000
d20      0.00200000
d21      0.00200000
d22      0.00200000
d23      0.00200000
d24      0.00200000
d25      0.00200000
d26      0.00200000
d27      0.00200000
d28      0.00200000
d29      0.00200000
d30      0.00200000
d31      0.00200000
d32      0.00200000
d33      0.00200000
d34      0.00200000
d35      0.00200000
d36      0.00200000
d37      0.00200000
d38      0.00200000
d39      0.00200000
d40      0.00200000
d41      0.00200000
d42      0.00200000
d43      0.00200000
d44      0.00200000
d45      0.00200000
d46      0.00200000
d47      0.00200000
d48      0.00200000
d49      0.00200000
d50      0.00200000
d51      0.00200000
d52      0.00200000
d53      0.00200000
d54      0.00200000
d55      0.00200000
d56      0.00200000
d57      0.00200000
d58      0.00200000
d59      0.00200000
d60      0.00200000
d61      0.00200000
d62      0.00200000
d63      0.00200000
d64      0.00200000
d65      0.00200000
d66      0.00200000
d67      0.00200000
d68      0.00200000
d69      0.00200000
d70      0.00200000
d71      0.00200000
d72      0.00200000
d73      0.00200000
d74      0.00200000
d75      0.00200000
d76      0.00200000
d77      0.00200000
d78      0.00200000
d79      0.00200000
d80      0.00200000
d81      0.00200000
d82      0.00200000
d83      0.00200000
d84      0.00200000
d85      0.00200000
d86      0.00200000
d87      0.00200000
d88      0.00200000
d89      0.00200000
d90      0.00200000
d91      0.00200000
d92      0.00200000
d93      0.00200000
d94      0.00200000
d95      0.00200000
d96      0.00200000
d97      0.00200000
d98      0.00200000
d99      0.00200000
d100     0.00200000
MCWRRK 0.01500000
P2       31.00
===== CHANNEL F1 =====
NUC1     13C
P1       1.13C
P2       1.13C
P3       1.13C
P4       1.13C
P5       1.13C
P6       1.13C
P7       1.13C
P8       1.13C
P9       1.13C
P10      1.13C
P11      1.13C
P12      1.13C
P13      1.13C
P14      1.13C
P15      1.13C
P16      1.13C
P17      1.13C
P18      1.13C
P19      1.13C
P20      1.13C
P21      1.13C
P22      1.13C
P23      1.13C
P24      1.13C
P25      1.13C
P26      1.13C
P27      1.13C
P28      1.13C
P29      1.13C
P30      1.13C
P31      1.13C
P32      1.13C
P33      1.13C
P34      1.13C
P35      1.13C
P36      1.13C
P37      1.13C
P38      1.13C
P39      1.13C
P40      1.13C
P41      1.13C
P42      1.13C
P43      1.13C
P44      1.13C
P45      1.13C
P46      1.13C
P47      1.13C
P48      1.13C
P49      1.13C
P50      1.13C
P51      1.13C
P52      1.13C
P53      1.13C
P54      1.13C
P55      1.13C
P56      1.13C
P57      1.13C
P58      1.13C
P59      1.13C
P60      1.13C
P61      1.13C
P62      1.13C
P63      1.13C
P64      1.13C
P65      1.13C
P66      1.13C
P67      1.13C
P68      1.13C
P69      1.13C
P70      1.13C
P71      1.13C
P72      1.13C
P73      1.13C
P74      1.13C
P75      1.13C
P76      1.13C
P77      1.13C
P78      1.13C
P79      1.13C
P80      1.13C
P81      1.13C
P82      1.13C
P83      1.13C
P84      1.13C
P85      1.13C
P86      1.13C
P87      1.13C
P88      1.13C
P89      1.13C
P90      1.13C
P91      1.13C
P92      1.13C
P93      1.13C
P94      1.13C
P95      1.13C
P96      1.13C
P97      1.13C
P98      1.13C
P99      1.13C
P100     1.13C
===== CHANNEL F2 =====
CPDPRG12 waltz16
NUC2     13C
P1       1.13C
P2       1.13C
P3       1.13C
P4       1.13C
P5       1.13C
P6       1.13C
P7       1.13C
P8       1.13C
P9       1.13C
P10      1.13C
P11      1.13C
P12      1.13C
P13      1.13C
P14      1.13C
P15      1.13C
P16      1.13C
P17      1.13C
P18      1.13C
P19      1.13C
P20      1.13C
P21      1.13C
P22      1.13C
P23      1.13C
P24      1.13C
P25      1.13C
P26      1.13C
P27      1.13C
P28      1.13C
P29      1.13C
P30      1.13C
P31      1.13C
P32      1.13C
P33      1.13C
P34      1.13C
P35      1.13C
P36      1.13C
P37      1.13C
P38      1.13C
P39      1.13C
P40      1.13C
P41      1.13C
P42      1.13C
P43      1.13C
P44      1.13C
P45      1.13C
P46      1.13C
P47      1.13C
P48      1.13C
P49      1.13C
P50      1.13C
P51      1.13C
P52      1.13C
P53      1.13C
P54      1.13C
P55      1.13C
P56      1.13C
P57      1.13C
P58      1.13C
P59      1.13C
P60      1.13C
P61      1.13C
P62      1.13C
P63      1.13C
P64      1.13C
P65      1.13C
P66      1.13C
P67      1.13C
P68      1.13C
P69      1.13C
P70      1.13C
P71      1.13C
P72      1.13C
P73      1.13C
P74      1.13C
P75      1.13C
P76      1.13C
P77      1.13C
P78      1.13C
P79      1.13C
P80      1.13C
P81      1.13C
P82      1.13C
P83      1.13C
P84      1.13C
P85      1.13C
P86      1.13C
P87      1.13C
P88      1.13C
P89      1.13C
P90      1.13C
P91      1.13C
P92      1.13C
P93      1.13C
P94      1.13C
P95      1.13C
P96      1.13C
P97      1.13C
P98      1.13C
P99      1.13C
P100     1.13C
===== GRADIENT CHANNEL =====
GPM1[1] 0 %
GPM1[2] 0 %
GPM2[1] 0 %
GPM2[2] 0 %
GPM3[1] 0 %
GPM3[2] 0 %
GPM4[1] 0 %
GPM4[2] 0 %
GPM5[1] 0 %
GPM5[2] 0 %
GPM6[1] 0 %
GPM6[2] 0 %
GPM7[1] 0 %
GPM7[2] 0 %
GPM8[1] 0 %
GPM8[2] 0 %
GPM9[1] 0 %
GPM9[2] 0 %
GPM10[1] 0 %
GPM10[2] 0 %
GPM11[1] 0 %
GPM11[2] 0 %
GPM12[1] 0 %
GPM12[2] 0 %
GPM13[1] 0 %
GPM13[2] 0 %
GPM14[1] 0 %
GPM14[2] 0 %
GPM15[1] 0 %
GPM15[2] 0 %
GPM16[1] 0 %
GPM16[2] 0 %
GPM17[1] 0 %
GPM17[2] 0 %
GPM18[1] 0 %
GPM18[2] 0 %
GPM19[1] 0 %
GPM19[2] 0 %
GPM20[1] 0 %
GPM20[2] 0 %
GPM21[1] 0 %
GPM21[2] 0 %
GPM22[1] 0 %
GPM22[2] 0 %
GPM23[1] 0 %
GPM23[2] 0 %
GPM24[1] 0 %
GPM24[2] 0 %
GPM25[1] 0 %
GPM25[2] 0 %
GPM26[1] 0 %
GPM26[2] 0 %
GPM27[1] 0 %
GPM27[2] 0 %
GPM28[1] 0 %
GPM28[2] 0 %
GPM29[1] 0 %
GPM29[2] 0 %
GPM30[1] 0 %
GPM30[2] 0 %
GPM31[1] 0 %
GPM31[2] 0 %
GPM32[1] 0 %
GPM32[2] 0 %
GPM33[1] 0 %
GPM33[2] 0 %
GPM34[1] 0 %
GPM34[2] 0 %
GPM35[1] 0 %
GPM35[2] 0 %
GPM36[1] 0 %
GPM36[2] 0 %
GPM37[1] 0 %
GPM37[2] 0 %
GPM38[1] 0 %
GPM38[2] 0 %
GPM39[1] 0 %
GPM39[2] 0 %
GPM40[1] 0 %
GPM40[2] 0 %
GPM41[1] 0 %
GPM41[2] 0 %
GPM42[1] 0 %
GPM42[2] 0 %
GPM43[1] 0 %
GPM43[2] 0 %
GPM44[1] 0 %
GPM44[2] 0 %
GPM45[1] 0 %
GPM45[2] 0 %
GPM46[1] 0 %
GPM46[2] 0 %
GPM47[1] 0 %
GPM47[2] 0 %
GPM48[1] 0 %
GPM48[2] 0 %
GPM49[1] 0 %
GPM49[2] 0 %
GPM50[1] 0 %
GPM50[2] 0 %
GPM51[1] 0 %
GPM51[2] 0 %
GPM52[1] 0 %
GPM52[2] 0 %
GPM53[1] 0 %
GPM53[2] 0 %
GPM54[1] 0 %
GPM54[2] 0 %
GPM55[1] 0 %
GPM55[2] 0 %
GPM56[1] 0 %
GPM56[2] 0 %
GPM57[1] 0 %
GPM57[2] 0 %
GPM58[1] 0 %
GPM58[2] 0 %
GPM59[1] 0 %
GPM59[2] 0 %
GPM60[1] 0 %
GPM60[2] 0 %
GPM61[1] 0 %
GPM61[2] 0 %
GPM62[1] 0 %
GPM62[2] 0 %
GPM63[1] 0 %
GPM63[2] 0 %
GPM64[1] 0 %
GPM64[2] 0 %
GPM65[1] 0 %
GPM65[2] 0 %
GPM66[1] 0 %
GPM66[2] 0 %
GPM67[1] 0 %
GPM67[2] 0 %
GPM68[1] 0 %
GPM68[2] 0 %
GPM69[1] 0 %
GPM69[2] 0 %
GPM70[1] 0 %
GPM70[2] 0 %
GPM71[1] 0 %
GPM71[2] 0 %
GPM72[1] 0 %
GPM72[2] 0 %
GPM73[1] 0 %
GPM73[2] 0 %
GPM74[1] 0 %
GPM74[2] 0 %
GPM75[1] 0 %
GPM75[2] 0 %
GPM76[1] 0 %
GPM76[2] 0 %
GPM77[1] 0 %
GPM77[2] 0 %
GPM78[1] 0 %
GPM78[2] 0 %
GPM79[1] 0 %
GPM79[2] 0 %
GPM80[1] 0 %
GPM80[2] 0 %
GPM81[1] 0 %
GPM81[2] 0 %
GPM82[1] 0 %
GPM82[2] 0 %
GPM83[1] 0 %
GPM83[2] 0 %
GPM84[1] 0 %
GPM84[2] 0 %
GPM85[1] 0 %
GPM85[2] 0 %
GPM86[1] 0 %
GPM86[2] 0 %
GPM87[1] 0 %
GPM87[2] 0 %
GPM88[1] 0 %
GPM88[2] 0 %
GPM89[1] 0 %
GPM89[2] 0 %
GPM90[1] 0 %
GPM90[2] 0 %
GPM91[1] 0 %
GPM91[2] 0 %
GPM92[1] 0 %
GPM92[2] 0 %
GPM93[1] 0 %
GPM93[2] 0 %
GPM94[1] 0 %
GPM94[2] 0 %
GPM95[1] 0 %
GPM95[2] 0 %
GPM96[1] 0 %
GPM96[2] 0 %
GPM97[1] 0 %
GPM97[2] 0 %
GPM98[1] 0 %
GPM98[2] 0 %
GPM99[1] 0 %
GPM99[2] 0 %
GPM100[1] 0 %
GPM100[2] 0 %
===== Processing Parameters =====
SI        32768
SF        125.760256
WDW       0
SSB       0
GB        0
PC        1.00

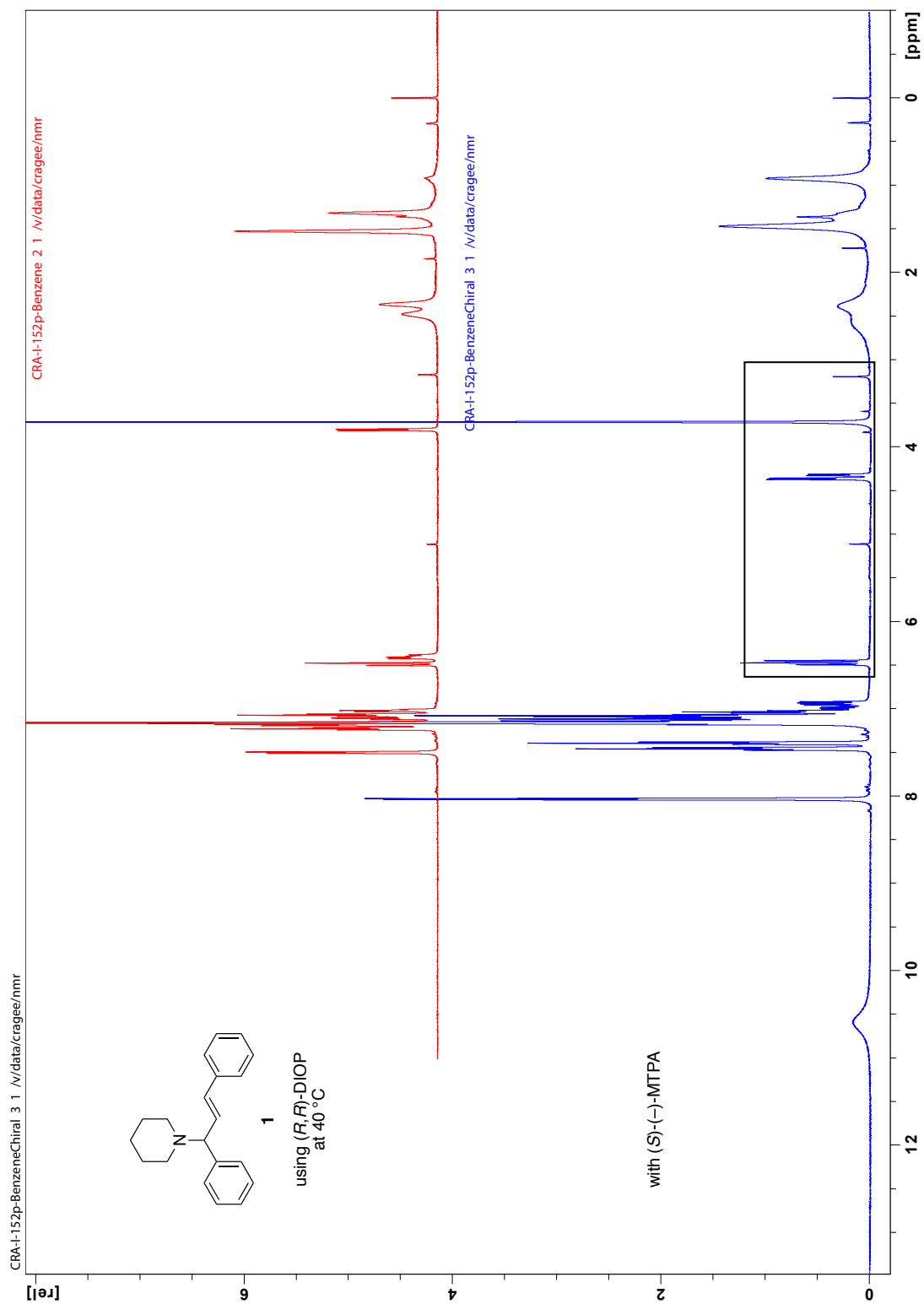
```





HMQC
Zoom on
alkene protons





CRA-I-152p-BenzeneChiral 3 1 \v\data\cra\ee/nmr

General

DATE = 2011/12/14
TIME = 22:28
INSTRUM = av600
PULPROG = zg30
F1 (1H)
SI = 65536
SF = 600.13
SWH_p = 8680.556

